Operation Simulation and Control of a Hybrid Vehicle Based on a Dual Clutch Configuration

by

Walid M. Elzaghir

A dissertation submitted in partial fulfillment
of the requirements for the degree of
Doctor of Philosophy
(Information Systems Engineering)
in The University of Michigan-Dearborn
2018

Doctoral Committee:

Professor Chris Mi, Co-Chair, San Diego State University
Professor Yi Zhang, Co-Chair
Professor Selim Awad
Associate Professor Hafiz Malik
Associate Professor Frank Massey
Associate Professor Narasimhamurthi Natarajan (Deceased)

Walid M. Elzaghir

wmel@umich.edu

ORCID iD: 0000-0002-2082-3595

ACKNOWLEDGEMENTS

First and foremost, I would like to thank my advisors: professors Yi Zhang and Chris Mi. They provided the finest possible support to me throughout this process and are the main reason I was able to complete this degree. They pushed me countless times over the years and put a specific plan in place to ensure a successful and timely completion of this work. Their dedication to the success of students is something that all academic professionals should aspire to have. It is something that I truly appreciate and will never forget. It wouldn't have been possible for me to have completed this thesis work without the motivating discussions and valuable guidance.

Second, I would like to specifically thank Dr. Hafiz Malik, Dr. Frank Massey and Dr. Salim Awad for agreeing to serve on my committee, who were more than generous with their expertise and precious time. I truly appreciate the time they spent mentoring me throughout the entire process. Special thanks to Dr. Malik for his assistance in finalizing the paper published in IEEE journal of vehicular technology.

My special thanks to the late committee member N. Natarajan for all his support. Dr. Natarajan helped me take the first step in the correct path and direction. It wouldn't have been possible for me to have developed the control strategies in the research work without his invaluable guidance and support. I cannot say in words how much I appreciate his contributions and guidance. He is truly a control expert with higher caliber and someone I aspire to emulate in my career.

Last but not the least, I would also like to dedicate this work to my wife, family and parents for supporting me, and my children Hadi and Mohammad as they are the reasons for which I am doing this work.

TABLE OF CONTENTS

LIST OF TABLES

LIST OF FIGURES

LIST OF APPENDICES

ABSTRACT

Today, the world thrives on making more fuel-efficient vehicles that consume less energy, emit fewer emissions and have enhanced overall performance. Hybrid Electric Vehicles (HEVs) offer the advantages of improved fuel economy and emissions without sacrificing vehicle performance factors such as safety, reliability and other features. The durability and performance enhancements of HEVs have encouraged researchers to develop various hybrid power-train configurations and improve associated issues, such as component sizing and control strategies.

HEVs with dual clutch transmissions (HDCT) are used in operation modes to improve fuel efficiency and dynamic performance for both diesel engines and high-speed gas engines. Dual clutch transmissions (DCTs) are proved to be the first automatic transmission type to provide better efficiency than manual transmissions. DCTs also provide reduced shift shocks and shift time that result in better driving experience. In addition, advanced software allows more simplistic approaches and tunable launch strategies in HDCT development. In this dissertation, an innovative approach to develop a desired mode controller for a HDCT configuration is proposed. This mode controller allows the driver to select the desired driving style of the vehicle. The proposed controller was developed based on adaptive control theory for the overall HDCT system.

The proposed Model Reference Adaptive Control (MRAC) was applied to a parallel hybrid electric vehicle with dual clutch transmission (HDCT), and yielded good performance under different conditions. This implies that the MRAC is adaptive to different torque distribution strategies. The current study, which was performed on adaptive control applications, revealed that the Lyapunov method was effective and yielded good performance. The MRAC method was also applied to the mode transition of an HDCT bus. The simulation results confirmed that the MRAC outperformed the conventional operation method for an HDCT with reduced vehicle jerk and the torque interruption for the driveline and with improved fuel efficiency.

Keywords: HEV: Hybrid Electric Vehicle
PHEV: Parallel Hybrid Electric Vehicle
DCT: Dual Clutch Transmission
HDCT: Hybrid Dual Clutch Transmission
MRAC: Model-Reference Adaptive Control
MIT: Massachusetts Institute of Technology

CHAPTER I: Introduction

Background

Today, the world thrives on making more fuel-efficient vehicles that consume less power, emit fewer emissions and have enhanced overall performance. Hybrid Electric Vehicles (HEVs) offer the advantages of improved fuel economy and emissions without sacrificing vehicle performance factors such as safety, reliability and other features. The durability and performance enhancements of HEVs have encouraged researchers to develop modern hybrid power-train configurations and improve associated issues, such as component sizing and control strategies.

Increasing customer demand and emission regulations have kept the automotive industry on a constant mission to find cost-effective technologies for vehicles that offers both fuel efficiency and dynamic performance. The key benefit of hybridization is to lower fuel consumption, which can be achieved through:

- Recouping kinetic energy during deceleration and coasting
- Turning off the engine during standstill
- Engine downsizing
- Utilizing the on-board stored electric energy from the grid, which is cheaper and has lower CO2 emissions than ordinary fuel combustion
- Optimizing of engine operations

The other benefits of hybridization are improved acceleration performance and lower emission. Considering the cost and development of the battery technology, employing all of these features, while simultaneously satisfying customer demand, will result in a very high cost per vehicle. Therefore, most vehicle manufacturers employ some of the features mentioned above, such as recouping kinetic energy during braking, and turning off the engine when the vehicle is at

standstill and using the battery for startup. This approach maintains a characteristics-to-cost ratio equivalent to that of a conventional power train.

This leads to a couple of hybrid categories: mild hybrids and full hybrids. Hybrid vehicles employing just some of the above-mentioned features, such as recuperation of kinetic energy and using electric energy for startup are normally referred to as mild hybrids. Hybrid vehicles employing all of the above features are usually referred to as full hybrids, Toyota Prius is a typical example. Depending on the architecture of the power-train, hybrid vehicles can be classified into series, parallel and series-parallel hybrid architectures, each having its own advantages and disadvantages for specific classes of vehicles and specific patterns of driving cycles. Hybrid vehicles that employ series architectures are usually beneficial for fuel economy in urban driving environments. Hybrid vehicles that employ a parallel architecture have good performance and are more fuel efficient than hybrid vehicles employing a series architecture. Hybrid vehicles employing series-parallel hybrid architecture have good fuel economy, but usually come with an increase in the number and size of prime movers when compared to hybrid vehicles employing a parallel architecture.

It is clear from hybrid vehicles on the market that the two major companies in the automotive industry, General Motors (GM) and Toyota, prefer the series-parallel hybrid architecture with electro-mechanical continuously variable transmission (ECVT) over the other architectures to achieve better fuel consumption.

The cost of the vehicle increases dramatically with mass and overall complexity of the power-train. Some inherent and expected power losses in the series-parallel architecture itself decrease the fuel efficiency benefit of ECVT. On the other hand, parallel hybrid architecture has the benefit of using a high-performance transmission. By smartly incorporating the electric prime movers, all of the required functionalities of a series-parallel architecture can be accomplished with a low cost per vehicle.

The reduced price and high efficiency battery technology have resulted in more demand on HEVs and a slow transition from them to plug-in hybrid electric vehicles (PHEV). The PHEV

has a bigger battery that can be charged through a charging cable which can be plugged into a household or industrial outlet.

Motivation

Studies on new fuel-saving technologies that make the environment cleaner and free of emissions have been popular in recent years because of decreasing global crude oil supplies and growing environmental concerns. As can be seen in Figure 1 (InflationData.com), the average price of crude oil during the past decade (about $70 / barrel) has been approximately three times the average price during the period 1978-2004 (about $25/ barrel), and future progression is likely to continue. To reduce oil consumption by ground vehicles, the Corporate Average Fuel Economy (CAFE) was enacted by the US Congress in 1975.

The CAFE legislation is overseen by the National Highway Traffic Safety Administration (NHTSA), which sets fuel economy standards for cars and light trucks (trucks, vans, and sport utility vehicles) sold in the US. While the CAFE standards have remained relatively constant for the last twenty years, the discussion of increasing the standards has been significant in the past fifteen years due to shrinking oil supplies and increasing oil demands (Figure 2). One of the growing goals of CAFE is to decimate emissions from Tier 2 types of vehicles and form standards for the automotive industries to face major challenges. Thus, the main challenge is to consume less energy, produce fewer emissions and have enhanced overall performance.

Oil is the ideal source to provide energy and power to the vehicle powertrain systems. In this case, we need to set standards and regulations to assess what is being used in the vehicle and optimize it to a higher impact solution. The Environmental Protection Agency (EPA) is the federal authority that sets the regulations of the environmental standards. These standards focus on limiting the production of harmful tailpipe pollutants.

Various engine-based technologies—such as variable valve timing, turbo charger application, and cylinder deactivation—have only limited impact on fuel economy. The continuously variable transmission is promising, but its in-field performance has not been satisfactory [1]. Limited

success has been achieved by new technologies of diesel-fueled vehicles. Low-sulfur (15ppm) diesel is a consistent fuel and has been proven successful for light-duty diesel vehicles.

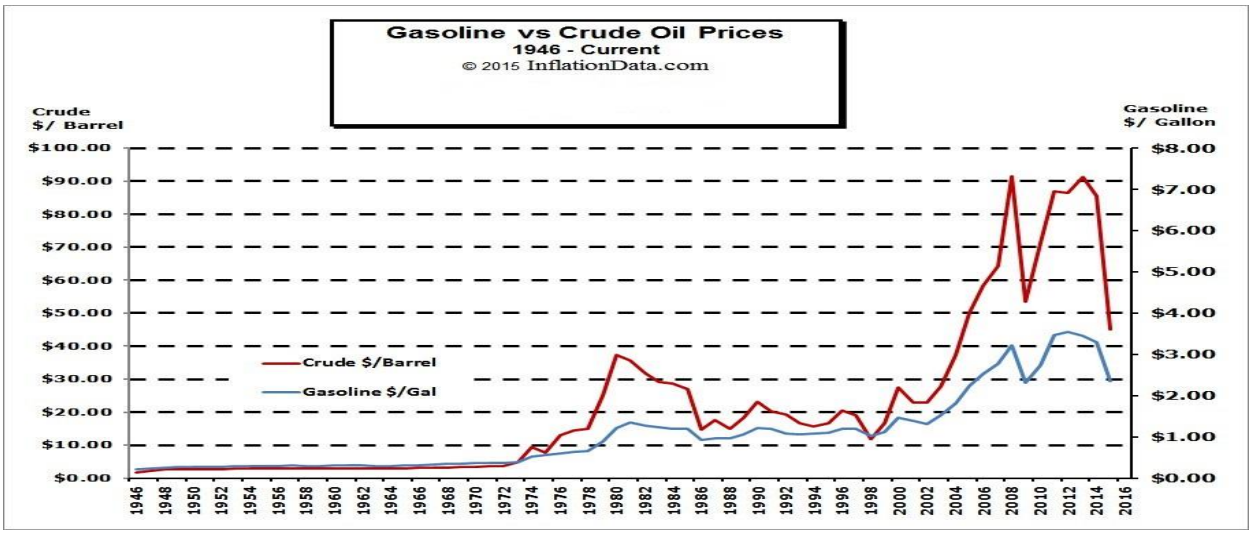

Figure 1: World crude oil prices have increased over 400% since 1998

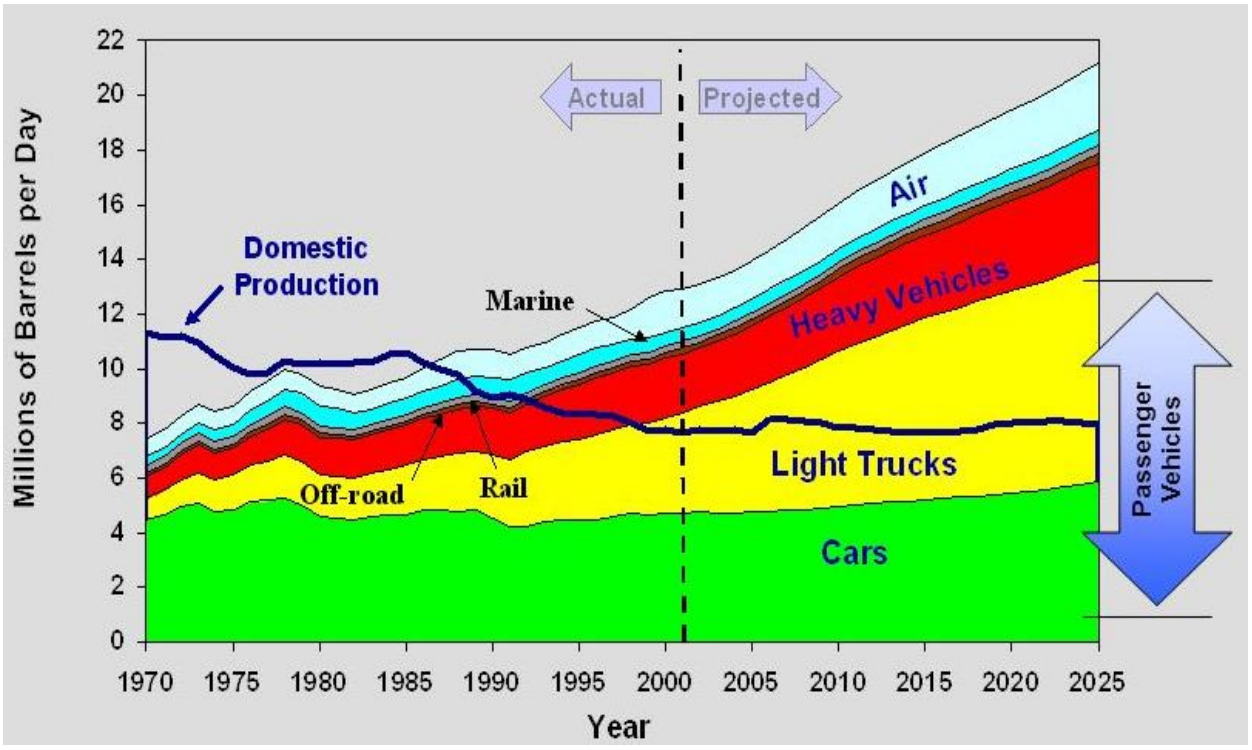

Figure 2: United States petroleum production and consumption. "EIA Annual energy outlook, Jan 2003"

Objective of this research

The objective of this thesis work “Control of a Hybrid Vehicle with a Dual Clutch Configuration" is to develop novel model-based methods for optimal control. The key to achieve this objective is to build a motor controller for the hybrid dual clutch transmission (HDCT) topology so that the motor torque covers the torque lost by the engine during gear shifting, speed changes or mode transitions. In this respect, the controller design will minimize fuel consumption, reduce torque interruption and vehicle jerk due to shifting. The speed of the vehicle should track the desired performance of the adaptive control system specified by a reference model [2]. In this project, a standard first-order response was chosen as the reference model [3]. The controller should be able to operate under the following conditions:

- Vehicle is operating under constant speed and the fuel injected into the Internal Combustion Engine (ICE) undergoes a step change. This requires the ability of the motor controller to adapt to the torque output of the ICE.
- Throttle is fixed but there is a step change in the desired speed. This is to study the ability of a motor controller to take over when the driver desires a rapid change in speed.
- Throttle and speed are both fixed, but the transmission gear changes. The motor controller should be able to mimic the typical behavior of a manual transmission (sport shifting mode) or mimic the typical behavior of an automatic transmission (comfortable mode).
- The performance of the motor controller is under various mode transitions, such as mode transitions between motor only, engine alone, combined mode or between other available modes.

Moreover, this type of system controller should be able to select the desired driver mode, control the selected mode and switch from one to another, if applicable. The two available modes that we have in this project are: sport shifting mode and comfortable mode.

- Sport shifting mode: this mode allows the driver to feel the transmission shifting from one gear to another and sense the manual transmission experience.

- Comfortable mode: this mode provides smooth shifting and no sense of any gear change.

Assumptions

The following assumptions were made to reduce the overall complexity of the system. They were necessary to avoid having an overly complex model which required an excessive amount of execution time to simulate. The main focus was on designing the controller and proving its stability and performance for the HDCT power train. The assumptions and ground rules include the following:

- The gear shift dynamics involved in the power-train were not considered.
- The efficiency of meshing gears was assumed to be 97% and that of the differential was assumed to be 95%.
- The dynamic losses in the HDCT gear box, such as clutch slipping and gear shifting, were assumed to be very low and ignored.
- Losses in hydraulics due to controlling the pre-selection of the gear in HDCT design were ignored.
- The power losses due to the control of the speed of the electric machines were considered to be low and ignored.
- The electric motor will operate as a generator.
- The cooling requirements of the power-train were not considered.

Dissertation Outline

This dissertation work is divided into 8 chapters. After the introduction in Chapter 1, different types of hybrid power-train architectures are discussed in Chapter 2. Then a brief discussion is made on transmission technology in Chapter 3, followed by a literature review of current hybrid powertrain and control technology in Chapter 4. In Chapter 5, the modeling of HDCTs is discussed. Chapter 6 presents the design of control strategy and methodology of the HDCT power-train using Matlab and Simulink. Chapter 7 presents the results and discussion, and Chapter 8 presents the conclusions.

CHAPTER II: Hybrid Models

Hybrid Power-train Architectures

For HEVs, there is a consistent implementation that will add an electric power path to the original design of the powertrain. This implementation will help improve the fuel economy by engine down-sizing. The purpose of this method is to obtain better fuel efficiency by allowing the system to achieve performance requirements with reduced peak power and by using the electric machine to meet the power demands.

We can then focus on launching performance that leads to the enhancement of the HEVs with balancing the overall ratio of the power. Load balancing can also be achieved through the electrical path. When establishing an optimal set of regions with the electric drive assistance, the engine can be controlled to operate in an optimal region, regardless of the road load. The last expectation is that when a vehicle is reducing speed, part of the vehicle's kinetic energy can be recouped through an electric machine, which is then used to charge the battery state for optimal balance.

Based on the degree of hybridization, the HEVs can be divided into several categories: mild hybrid, power-assist hybrid, full hybrid and plug-in hybrid.

- A mild hybrid is the conventional vehicle with an oversized starter motor; the engine will turn off if the car is coasting, braking, or stopped, and will restart quickly.
- A power-assist hybrid has the electric motor placed between the engine and transmission. The engine is the main power of the vehicle and the motor operates on two conditions:
    I. When the engine is off.
    II. When the driver accelerates and steps on the gas pedal so the vehicle requires more power.

- A full hybrid, sometimes called a strong hybrid, can run on one source of power if necessary: the engine, the battery, or a combination of both. A large battery pack is needed for the battery-only operation.
- A plug-in hybrid or full hybrid is able to run in electric-only mode, with a larger battery mounted that can be used as an external power for long trips. The advantages of these models are that they can be gasoline-independent for daily commuting and have the ability to recharge from the electric power station.

Based on the powertrain system design, HEVs models can be divided into three categories: parallel hybrid, series hybrid or power-split hybrid (parallel/series hybrid). The definition and characteristics of each type are described in the following sections:

Parallel Hybrid Electric Vehicle:

The design of this configuration consists of two separate power sources that propel the vehicle: the engine transmission powertrain and motor/generator (MG) power assist as shown in Figure 3. Most of the time, the alternative power source (MG) is supplied by a battery or ultra-capacitor. When the MG is relatively small (e.g. mild hybrids or power-assist hybrids), it cannot fully drive the vehicle by itself without engine power. When the secondary power source is relatively large (e.g. full hybrids), the engine and MG can drive the vehicle individually or simultaneously.

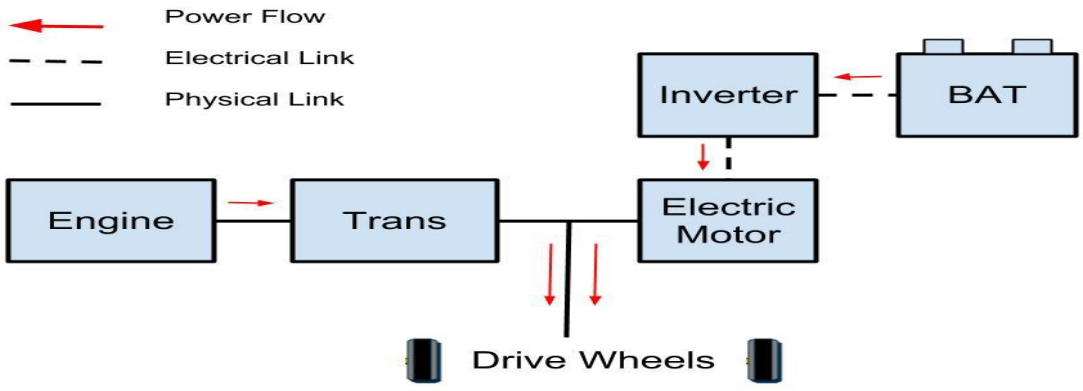

Figure 3: Parallel HEV Configuration

The basic function of the motor/generator is to support the engine power when needed, and control and capture regenerative braking energy. The power assistance has to be controlled to avoid draining the battery because MG is a single-mode operator. It can either charge the battery or assist the engine, but not both simultaneously. This is why most parallel HEVs do not have remarkable city fuel-efficiency, as the engine has to produce power in its low-efficiency range to cover the demand of the frequent stop-and-go traffic that occurs in the city.

Series Hybrid Electric Vehicle:

The series configuration consists of a battery and a generator (transforming the mechanical power from the engine into electric power), or the combination of both, to supply the motor that works alone to drive the wheels, with a split ratio determined by the power management controller (shown in Figure 4). The engine operation is controlled to drive the system in or near the optimal condition most of the time because the mechanical power transition path is eliminated. The energy loss due to the torque converter and the transmission is avoided. The control strategy of the series configuration is relatively simple [4] and [5], because the power-flow analysis for series HEVs is straightforward and the engine is controlled separately from the vehicle operation. Many prototype hybrid buses and trucks use the series hybrid configuration [6]. The problem with the series configuration is that they rely on the electrical devices and machines for the power path rather than mechanical components, which leads to a lower

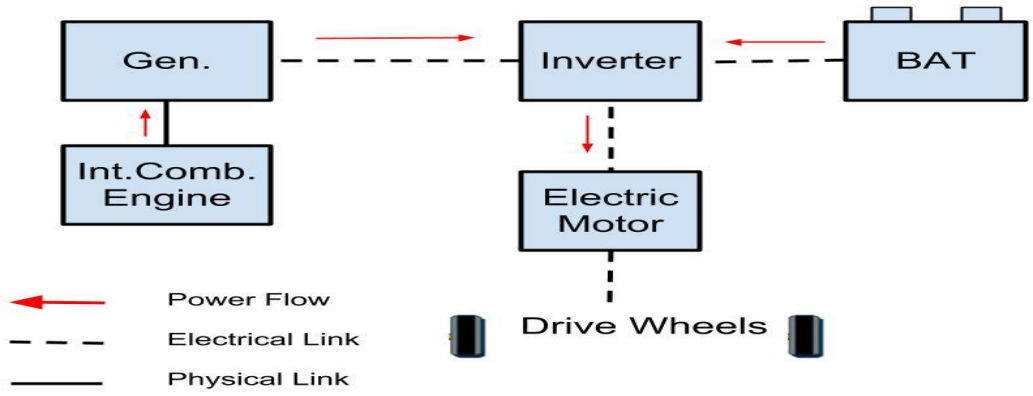

Figure 4: Series HEV Configuration

efficiency and reduces the overall performance of the system.

Disadvantages include the additional magnetic electric field transformation and the heat loss of the electrical accessories. Since the driving power of a series hybrid vehicle flows through the electrical path all the time, it becomes relatively inefficient when the vehicle reaches the driving range that could be more efficiently driven by the engine directly. This is true especially when the vehicle is running on the highway.

Power-Split Hybrid Electric Vehicle (Parallel/Series Hybrid):

The powertrain configuration of the power-split hybrid system, also known as parallel/series hybrid or combined hybrid, is different than the previous two models. However, it can be designed to take advantage of both parallel and series types and avoid their problems (shown in Figure 5).

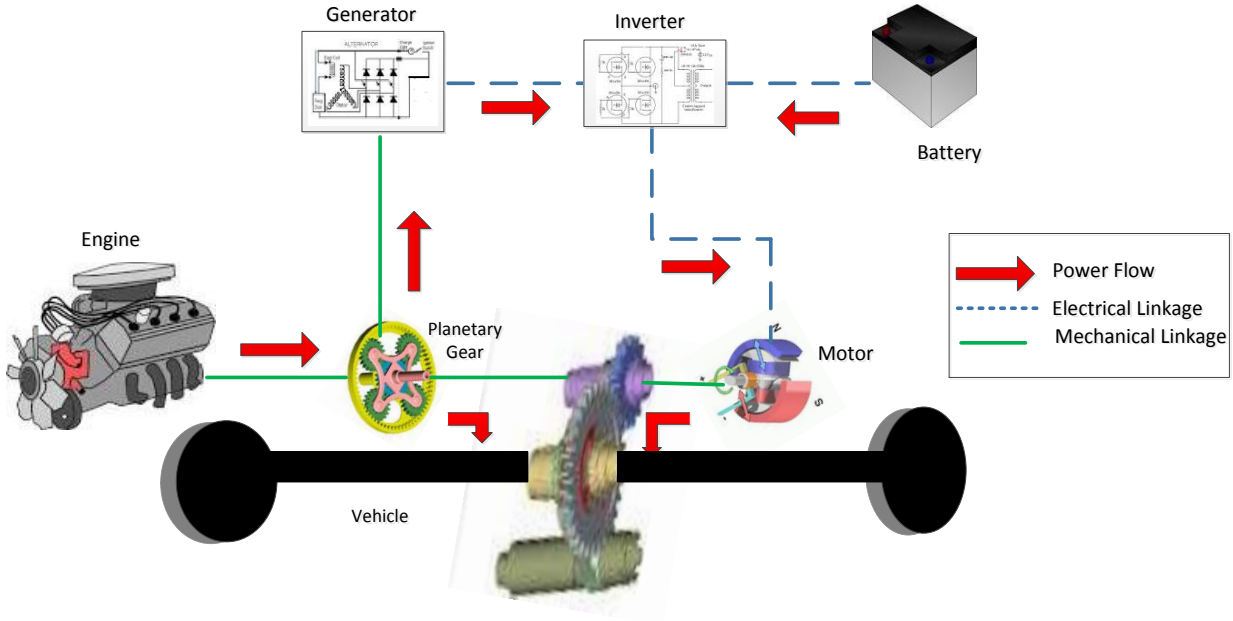

Figure 5: Power-split HEV Configuration

The power-split configuration combines the parallel and series powertrains. It is comparable to the parallel configuration from the design portion of the power-flow. It has the separate engine

power-flow path and battery-motor power-flow path, in addition to a power-split planetary gear set that replace the transmission in order to link the engine with the final drive.
On the other hand, it is also comparable to the series configuration from the power-flow; the engine drives a generator to either charge the battery or supply power to the motor. The parallel/series hybrid can operate like both a series and parallel hybrid. It has the series configuration when the vehicle is driving at low speed to avoid the drawback of parallel hybrid, and can switch to the parallel hybrid when running at high speed to avoid the drawback of series hybrid. Because it has more energy flow paths and operating modes compared to other configurations, the power management control becomes more complicated [7].

1. The Single-Mode Power-Split Hybrid system (Figure 6) is built using a single planetary gear set that serves as a power-split device that transfers the engine power to the vehicle through two paths: a mechanical path and an electrical path. Most of the power will be delivered from the engine to the final drive of the vehicle through the mechanical path. The remaining power transforms into electricity in motor/generator 1 (MG1) to be sent to motor/generator 2 (MG2) by a controlled power bus or stored in the battery for later usage. This operation may improve the overall efficiency of the vehicle since the engine power going through the electrical path is less efficient than the mechanical path.

   In this powertrain design, the carrier gear connected to the engine is the input node. The ring gear connected to the final drive is the output node. MG is connected to the third node of the planetary gear set. This setup is called an input-split system because the engine torque is split into two paths from the input node; the split power then goes to the output node without any further split ratio. And since this is the only operating mode, it is called a single-mode system [7].

2. The Dual-Mode Power-Split Hybrid system (Figure 7) handles the engine power in the same way as the single-mode. The engine power flows into the gear trains and splits into a mechanical power and an electric power path, but the configuration design is different; the dual-mode system has extra planetary gear set and two clutches in its powertrain design compared to the single-mode system.

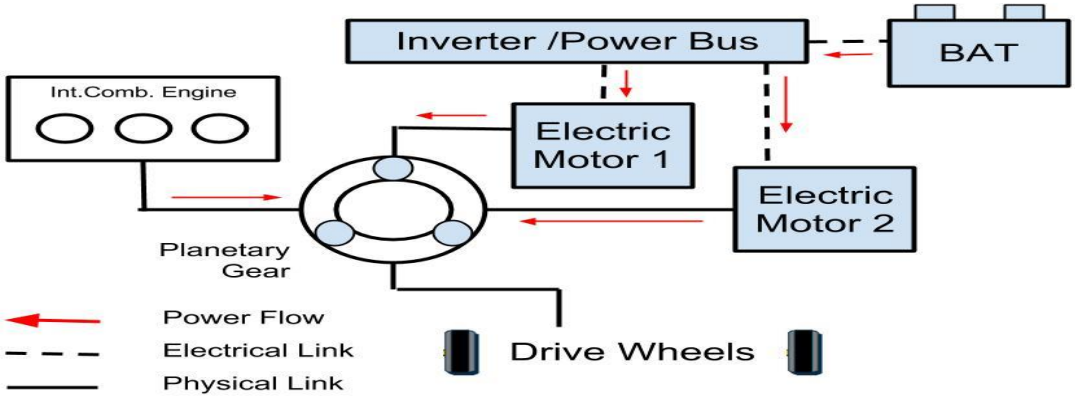

Figure 6: Powertrain Configuration of a Single-mode Hybrid System

The dual-mode consists of two different power-split modes and can be switched from one to another by coordinately engaging and disengaging the two clutches. As is shown in Figure 7, the powertrain design can either work as a single-mode (same as the previous design) or as a dual-mode system. Identified as an operated power-split system, the engine torque is then set by two different paths to the final drive with another split ratio. Although the system appears more complex, such dual-split modes prove to provide higher flexibility [8] [9].

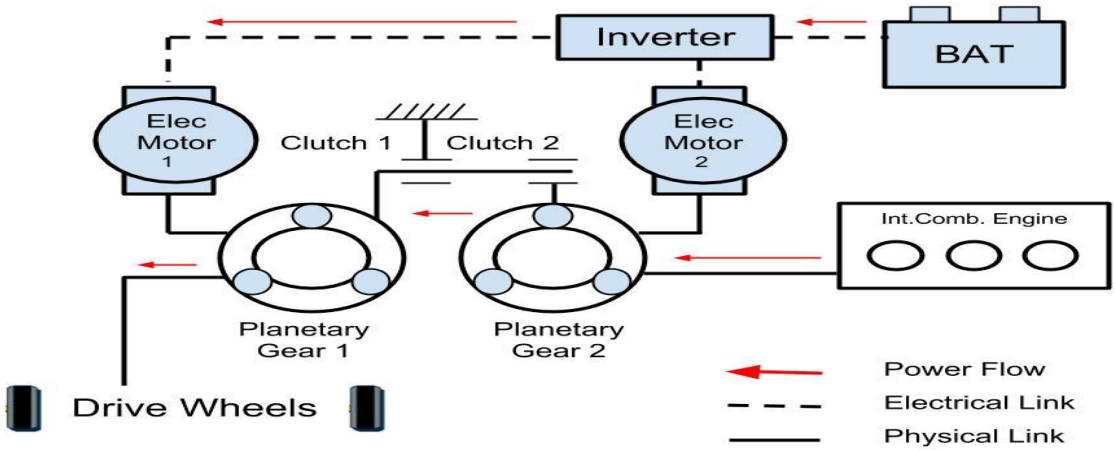

Figure 7: Powertrain Configuration of a Dual-mode Hybrid System

CHAPTER III: Transmission Technologies

Basics of Transmission Technologies

It is important to understand how efficiency can be implemented through the major components. Engine power and speed are transmitted to the wheels through the transmission, per driver demand. The transmission capability to allow sufficient amount of power, along with minimum loss, has always been considered one of the major challenges. The key drivers for automotive transmission development are [10]

• Fuel Economy

• Emissions

• Cost

Table I shows the various pros and cons of automatic and manual transmissions [11].

Table I: Qualitative Comparison of Automatic and Manual Transmission

Aspects	Automatic Transmission	Manual Transmission	Desired Transmission
Cost	Expensive	Lower	Low
Efficiency	Moderate	High	High
Ease of use	Easy	Hard	Easy
Comfort	Good	Poor	Good

Market Research and Global Trends

Every region has strong points to offer their consumers. The consumers in Japan are more influenced by enhancing their fuel economy and comfort through technological breakthroughs.
In Europe, in contrast, there is a seeming indifference to driver convenience, with an emphasis on maximizing fuel economy, and hence manual transmissions dominate [12]. The European market remains unique in that over 75% of the cars sold there are equipped with manual transmissions. However, advances in electronics and a need for compliance with strict environmental and legislative requirements have provided an impetus to automated transmissions such as automated manual transmissions (AMT), dual clutch transmissions (DCT) and continuously variable transmissions (CVT). A closer look at the market shows that depending on the market (North America, Europe, or Japan), each of these technologies have their own penetration levels [13].

Fundamentals of Dual Clutch Transmissions

Successful developments of AMTs depend on reliable by-wire technologies. An AMT (Figure 8) typically contains a dry clutch and a multi-speed gearbox. Clutch and gear shifters are controlled by electro-mechanical or electro-hydraulic actuators. Advantages of the AMT are lower weight and higher efficiency. In addition, the AMT is essentially derived from the manual transmissions by integrating servo actuators that are compliant in existing systems, not to mention that they also lower production costs [14].

A dual-clutch transmission (DCT), as shown in Figure 9, offers the function of two manual gearboxes in one set. The two gear boxes respond depending upon how the driver attempts to establish contact with the system based on the single clutch, which allows the system to respond as if it was built for one single clutch. There is a clutch pedal that allows the vehicle to be shifted into another gear as the driver desires, depending upon driving conditions. A DCT combines the convenience of an automatic transmission with the fuel efficiency of a manual transmission. To

ensure smooth shifting and optimal efficiency, DCTs require advanced controllers capable of preselecting the next gear and engaging the appropriate clutch precisely when required.

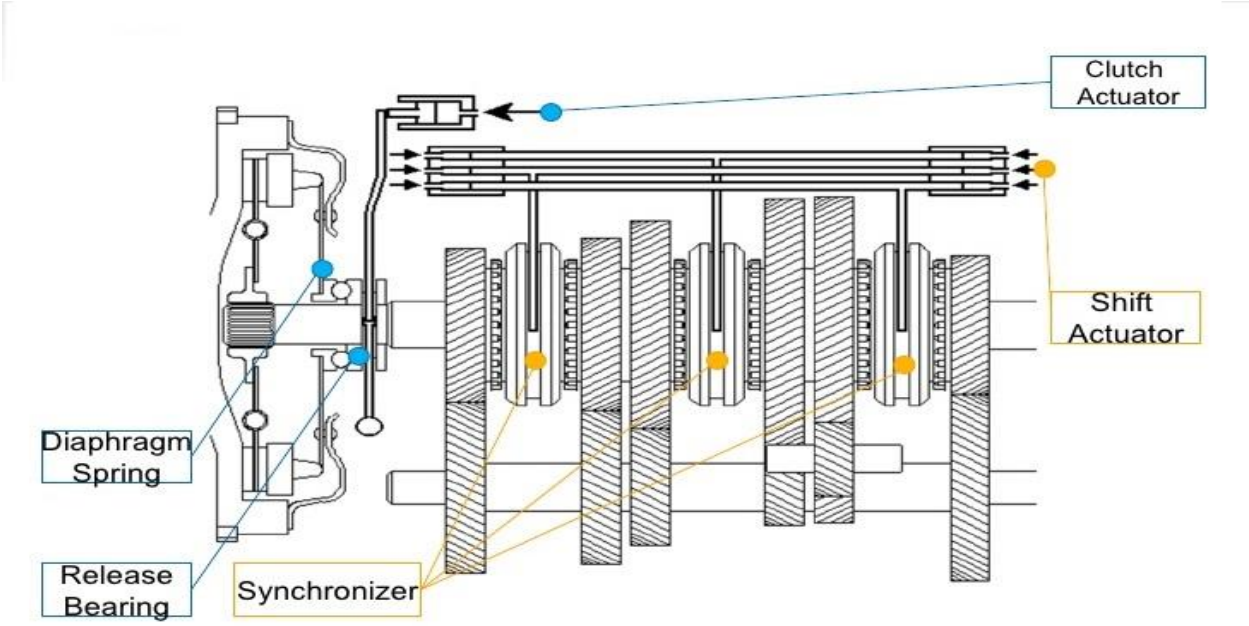

Figure 8: Automated Manual Transmission (AMT). TC-CDA.com

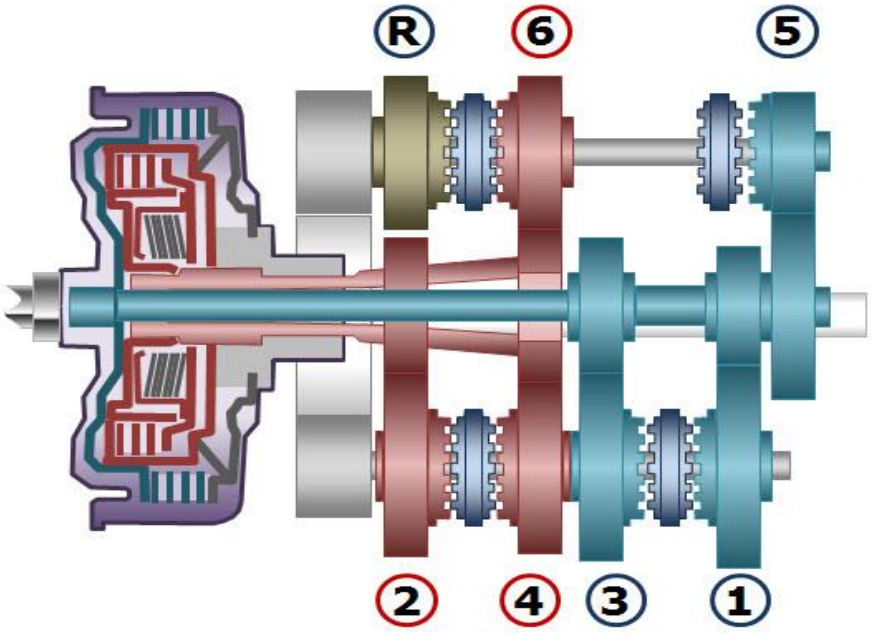

Figure 9: Dual Clutch Transmission (DCT). Matlab toolbox

Devices that allow the gear to move from one shift mode to another are called synchronizers. The synchronizers allow the new gear to be engaged as the clutch pedal is released, allowing the engine to be connected and power to be transmitted to the wheels. This establishes better performance, in addition to resulting in no grinding of the gear box.

A dual-clutch gearbox has many different lay-outs. For example, it uses a construction of two clutches, but has no clutch pedal. There are many complex components and structures that stipulate the control of the clutches. The control is accomplished through the electronics and the hydraulics that lead to an accomplished systematic approach for clutch controls. The DCT allows the clutch to operate in an independent functionality. Specifically targeting one clutch for the odd gears and one for the even gears, the establishment of dual functionality allows the clutch to lead into multi-functionality without the loss of power, and prevent power interruptions from the source (engine).

In a DCT system, the two clutches are connected to two separate sets of gears. The odd gear set (clutches: 1, 3, 5) is connected to one of the clutches and the even set (clutches: 2, 4, 6, R) to the other clutch. It is necessary to preselect the gears to realize the benefits of the DCT system. Accordingly, the off-going clutch is released simultaneously as the on-coming clutch is engaged, as shown in Figure 10. This gives the uninterrupted torque supply to the driveline during the shifting process. This pre-selection of gears can be implemented using complicated controllers such as fuzzy logic, or simple ones such as selections, based on the next anticipated vehicle speed.

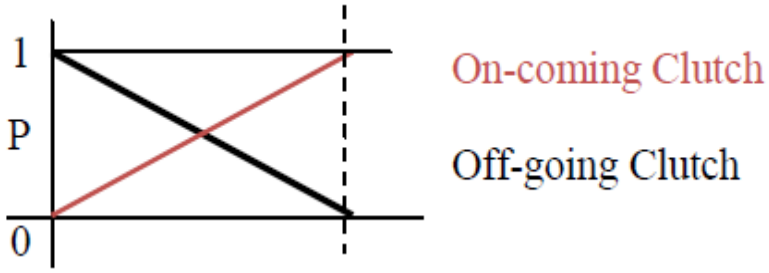

Figure 10: Dual Clutch Pressure Profiles

The DCT, with its refinement, efficiency, low cost and driving satisfaction is the probable market winner. Conservative estimates show DCT technology to be around 10% of the global market by 2021. The European Union (EU) is poised to undergo the change from manual transmissions to DCTs. It reports the expected DCT penetration in the EU to rise from 7% (2012 level) to around 11% in 2020. Also, most EU OEMs, except Renault, are expected to favor the DCT. [15]

DCTs are well structured for higher-torque efficiency in diesel engines and high revving gas engines alike. The DCT is recognized among the other transmissions based on the system through software tenability, which allows them to be handpicked among all the other powertrain engineers in the global market. Because of its characteristics and attributes, Getrag (the world's largest supplier of transmission systems for passenger cars and commercial vehicle) expects emissions reductions of up to 30% for the hybrid dual clutch transmissions compared to the traditional and conventional drive train systems [16].

CHAPTER IV: Literature Review

Modeling of HEVs with DCT

Modeling and simulation tools are very essential in the early stages of design. HEVs have multiple configurations and components and numerous control strategies that need to be optimized and evaluated in order to select the best design. One of the most popular HEV simulation model packages is the ADvanced VehIcle SimulatOR (ADVISOR), developed by the National Renewable Energy Laboratory (2007). ADVISOR is an empirical, map-based simulation tool that combines the vehicle dynamics model with the efficiency map of each component to predict system performance. It calculates the powertrain operation backward from a given driving schedule, based on a quasi-static assumption that inverts the physical causality [17].

Another popular HEV simulation model is the PNGV System Analysis Toolkit (PSAT) which was developed by the Argonne National Laboratory (ANL). The experimental data is applied to validate and improve the simulation model [18]. In contrast to ADVISOR, PSAT is a forward-looking model that calculates the powertrain states, based on driver input. It is suitable for investigating the dynamic response of individual components, as well as designing the control strategy for hybrid vehicles, although forward models are computationally more intensive than backward models. Besides these two simulators, Matlab/Simulink can also be used for developing a vehicle simulation model. It was applied by many researchers and used to prove various unified power flow concepts and to define general structures for a vehicle sub-system.
Building HEVs models and the study of their powertrain systems have attracted industry wide interest. Control of a hybrid vehicle based on a dual clutch configuration is a new idea and the topic has garnered a lot of attention in past few years. The current research on hybrid electric vehicles with dual clutch transmissions is focused on two parts:

- Improve fuel economy of the vehicle and attempt to minimize emissions.

- Implement an optimal control for the powertrain components to satisfy the driver's power demand and ensure a smooth power transfer.

Configuration Design of HEVs

The powertrain of a HEV is more complex than the conventional powertrain. It can be varied based on different components: engine-to-gear connections, motor-to-gear connections or clutch-to-gear connections. In addition, the size of the engine battery and electric units can be varied according to the target vehicle's specifications. The performance of the HEV depends on the optimal selections of engine, battery, motor and other electric units, as well as optimized transmission design.

The Toyota Hybrid System is a single-mode power-split design. It has been modified with different gear linkage to achieve motor torque multiplication for heavier vehicles in recent years [19]. GM introduced the concept of multi-modes on a power-split system based on the conventional transmission design. Although the planetary gear with electric machines provides CVT type of operation, having multi-gear modes for different driving scenarios can be beneficial.

Toyota introduced the Prius Gen 3 (Full hybrid - HEV) in 2011; the design configuration is based on parallel hybrid/power-split. Simultaneously, GM launched its first Plug-in Range Extender EV Chevrolet Volt (PHEVs powertrain) based on series hybrid design configuration.

The Toyota Prius powertrain system (Figure 11, right) has both an electric and a gas motor. The relationship between both motors is alternating and depends on power needed and battery state of charge. In some cases, the combustion engine is dominant and the use of the electric power is to provide an extra boost, if needed. In others, the electric motor provides most of the power. Both motors feed power through a single transmission. Parallel hybrids can be categorized depending on how balanced the different portions are at providing more power. Since the two motors are operating in parallel, this setup is known as a Parallel Hybrid Electric Vehicle.

On the other hand, the GM Volt Extended Range Electric Vehicle (EREV) is a Series Hybrid Vehicle (Figure 11, left "GM-Volt.com"). This powertrain system has an internal combustion

engine that drives an electric generator in which the electrical output is connected to an electric bus connected to the battery pack and the electric motor controller instead of directly driving the wheels. The motor produces power from both the batteries and the generator to supply the amount of power required. Since the two motors are operating in series, this setup is known as a Series Hybrid Vehicle .

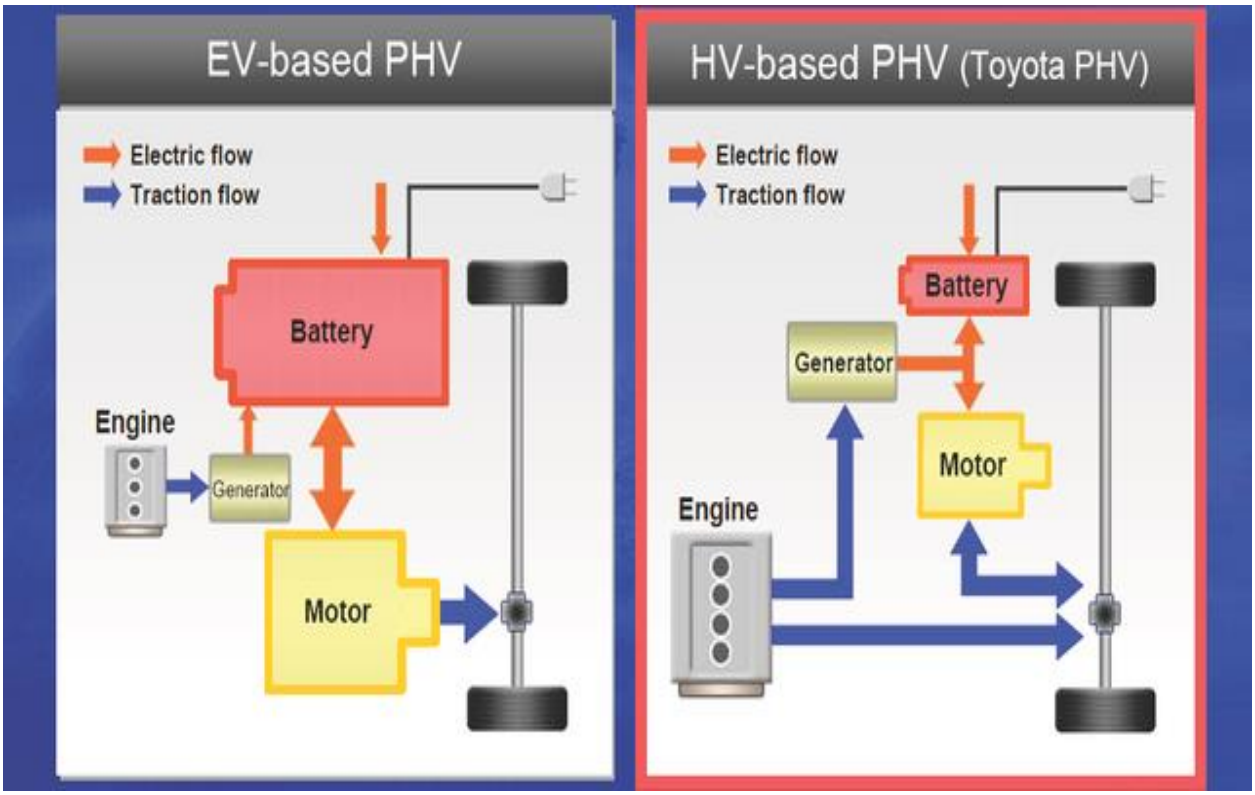

Figure 11: Chevrolet Volt vs. Toyota Prius

Within the series architecture, the battery tends to be larger (Volt = 16 kWh, 40-mile range, 90% <> 40% state of charge (SOC)). The electric motor also tends to be larger (Volt = peak power 140kW, 180HP) and the ICE tends to be smaller (Volt = 1.4L, 53kW, 71 HP), as shown in Figure 12 (www.greencarcongress.com). Within the parallel and series-parallel architecture the battery is smaller (Prius gen 3 = 4kWh, 9-mile range, 90% <>30% SOC), the electric motor is smaller (Prius gen 3 = peak power 50kW, 67HP) and the ICE tends to be larger (Prius gen 3 = 1.8L, 70kW, 94HP) [20].

The different architectures have major implications for the modes of operation of the vehicle, the overall energy efficiency of the vehicle and how much fuel is consumed. The Toyota Prius will

be a plug-in hybrid with initial EV operation, all electric range (AER) of about 9 miles. The Chevrolet Volt will be an extended range electric vehicle with an AER of 40 miles [20].

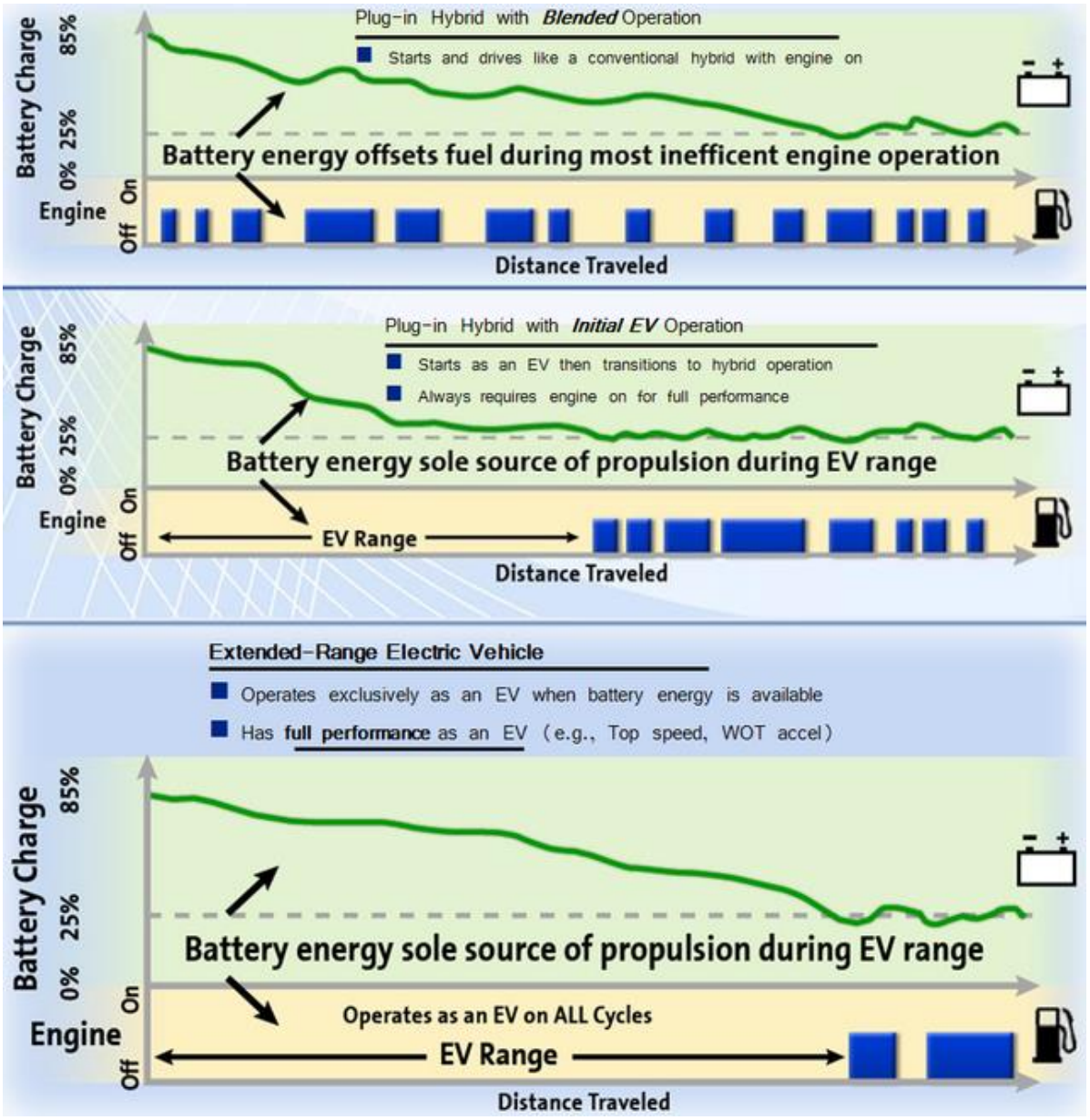

Figure 12: PHEV Modes of Operation Strategies

Control of HEVs

The control of hybrid electric vehicles uses a two-level hierarchical architecture. The lower level includes all sub-systems in the vehicle, such as the engine, motor and battery. Each one of those sub-systems is equipped with sensors, actuators and a control system to regulate its behavior. The higher level is a supervisory powertrain control that determines the desired output and sends order to the sub-systems for operation to satisfy the best selection.
The supervisory control strategies of hybrid electric vehicles in the existing literature can be classified into three categories.

- The first approach is a rules/fuzzy logic for control algorithm development. The control strategy is based on threshold values; the concept attempts to operate the ICE to work at its most efficient and preserve the rest of the energy in the storage device (e.g., battery or Ultra capacitor) [21]. Many research papers adopt the fuzzy logic technique to implement load-leveling concept and charge strategy [22], [23] and [24].

- The second approach is based on instantaneous optimization methods; this method is used to minimize the cost function of the energy. Equivalent consumption minimization strategy (ECMS) is a typical example of the instantaneous optimization. In this strategy, electric power is translated into an equivalent (steady-state) fuel rate to calculate the overall fuel cost [25]. A new method has been developed and called the adaptive-ECMS technique [26]. It periodically refreshes the converting factor according to the current road load to sustain the battery SOC [27].

- The third approach is based on optimization methods; dynamic programming (DP) is the famous method used in this application. It calculates the optimal control signals over a given driving schedule. On the other hand, it attempts to optimize a cost function over a time horizon to achieve a global optimal strategy. The stochastic dynamic programming (SDP) method was proposed in 2004 to solve the problem from DP. It targets the general driving cycle rather than a specified one with known power demand probabilities, but this optimization method is computationally expensive and requires a lot of calculation. This approach is also computationally complex. To avoid these issues, researchers suggested

using a near-optimal controller inspired by SDP and quantized the state space and solved a shortest path SDP by using a combination of linear programming and interpolation [28].

Developing a control strategy for a hybrid vehicle based on a dual clutch configuration to select the desired driving mode is a hot topic. The development of such a controller for hybrid vehicles systems is still worth investigating because the powertrain system of HEV offers more control inputs and more flexible operating options than other vehicle systems, and the optimal control strategy involves many different techniques for development and some of them are still facing a lot of challenges. Lastly, to our knowledge there has not been any optimal control strategy that has considered any desired mode selection of HDCT systems. This dissertation will address our work on these areas.

CHAPTER V: Dual Clutch Powertrain Modeling

Dual Clutch Transmission

The dual clutch transmission is modeled in Matlab. It consists of gears, synchronizers and each of the two clutches which are modeled as shown in Figure 13 [42].

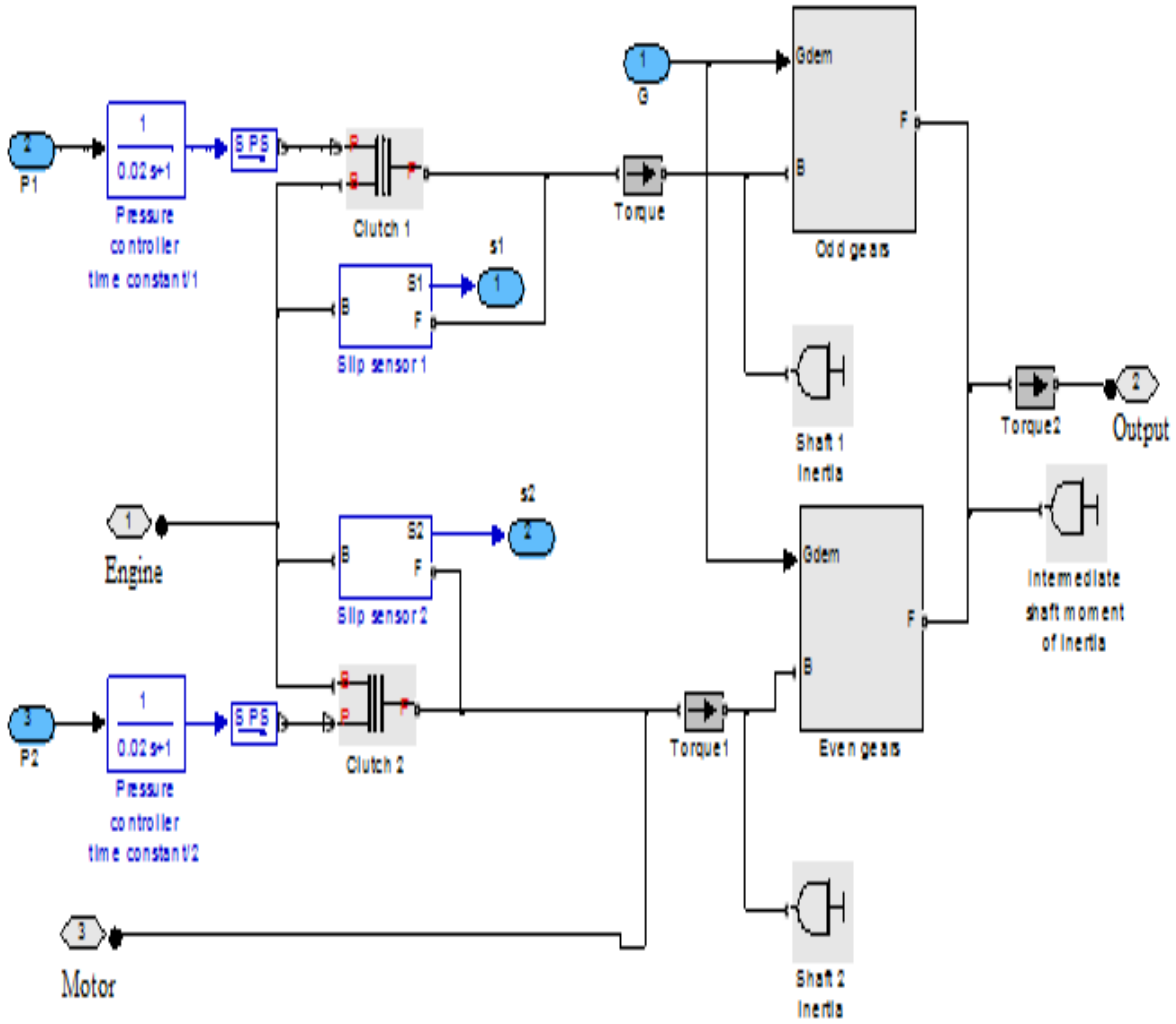

Figure 13: DCT Model modeled in Matlab Toolbox

Transmission Shifter Controller

The transmission controller converts the pedal deflection into a demanded torque. The pedal deflection and the vehicle speed are also used by the transmission controller to determine when the gear shifts should occur (Figure 14) [42]. Gear shifts are implemented via the two clutches, one clutch pressure being ramped up as the other clutch pressure is ramped down. Gear pre-selection via dog clutches ensures that the correct gear is fully selected before the on-going clutch is enabled. This controller intelligently preselects the higher or the lower gear depending on the input signals: pedal, rpm, speed (mph) and slip sensors (S1and S2).

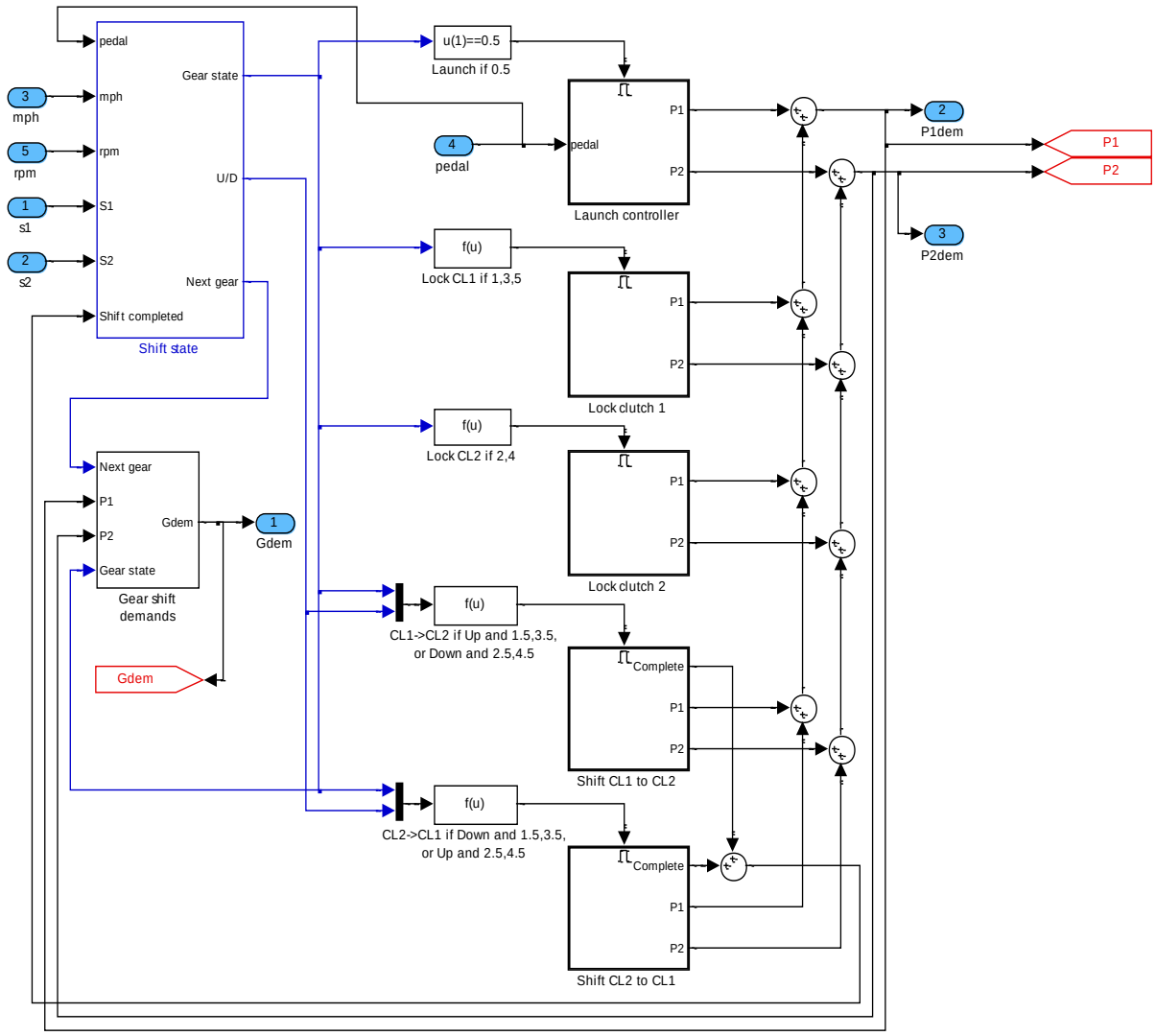

Figure 14 Transmission Controller Design modeled in Matlab Toolbox

Gear Ratios

A gear imposes a single constraint, specified by the fixed gear ratio, on the motion and torques of base to follower axes. The gear ratio:

$$i_{fb} = \frac{\mathrm{T_f}}{\mathrm{T_b}} = \frac{\omega_\mathrm{b}}{\omega_\mathrm{f}}, \text{ always } i_{fb} > 0 \qquad (5.1)$$

Clutch

The clutch is a friction clutch which transfers torque between the two driveline axes, when actuated above threshold pressure, by coupling them with friction. It includes both kinetic and static friction as shown in Figure 15 [42]. The clutch has three operating states.

- Unengaged or (open), $T_{transfered} = 0$
- Engaged but slipping, $T_{transfered} = C_\mu(\Delta\omega)P$
- Locked or (close), $T_{transfered} = T$

Where T is the torque determined by the system dynamics.

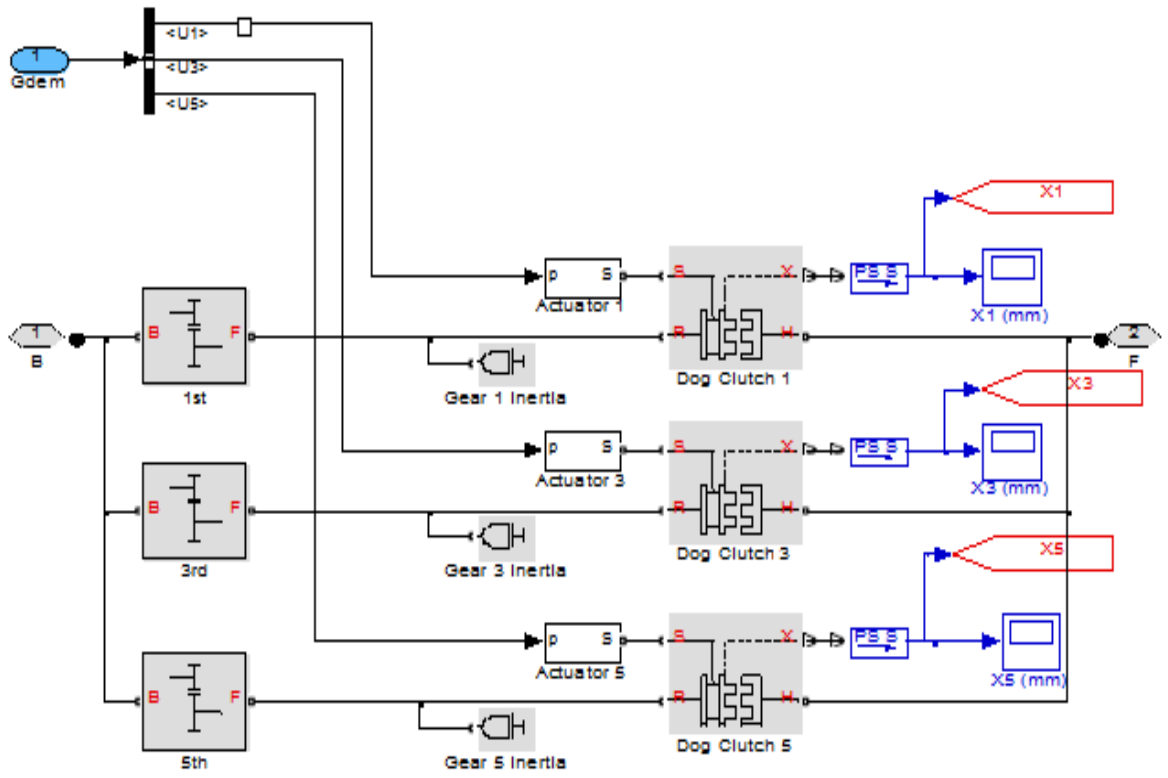

Figure 15: DCT Clutch and Gears Design modeled in Matlab Toolbox

Dynamic Equations

The baseline hybrid electric vehicle studied in this work is a parallel one which typically consists of an internal combustion engine, an electric motor and a Ni-H battery pack with a conventional drive train, as shown in Figure 16. As for simulation, a corresponding model "parallel HEV" has been built in Matlab.

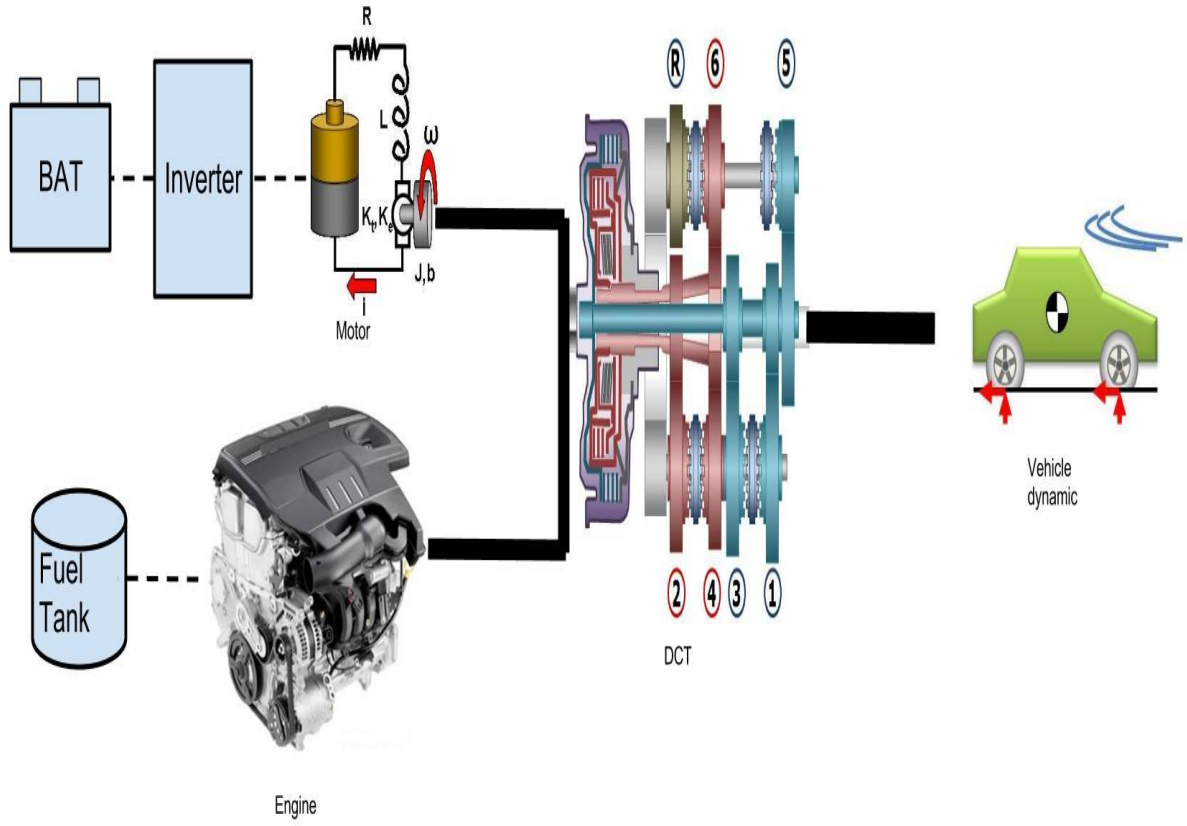

Figure 16: Configuration of Parallel Hybrid Electric Vehicle

Electric Motor

A common actuator in control systems is the DC motor. It directly provides rotary motion and, coupled with wheels or drums and cables, can provide translational motion. Motors used in hybrid electric vehicles can work in either motoring or generating mode. The DC motor is modeled for simplicity as shown in Figure 17. The voltage and torque characteristics are similar to those of typical brushless DC motors and vector controlled induction motors. The speed command and the voltage command are provided by the motor controllers.

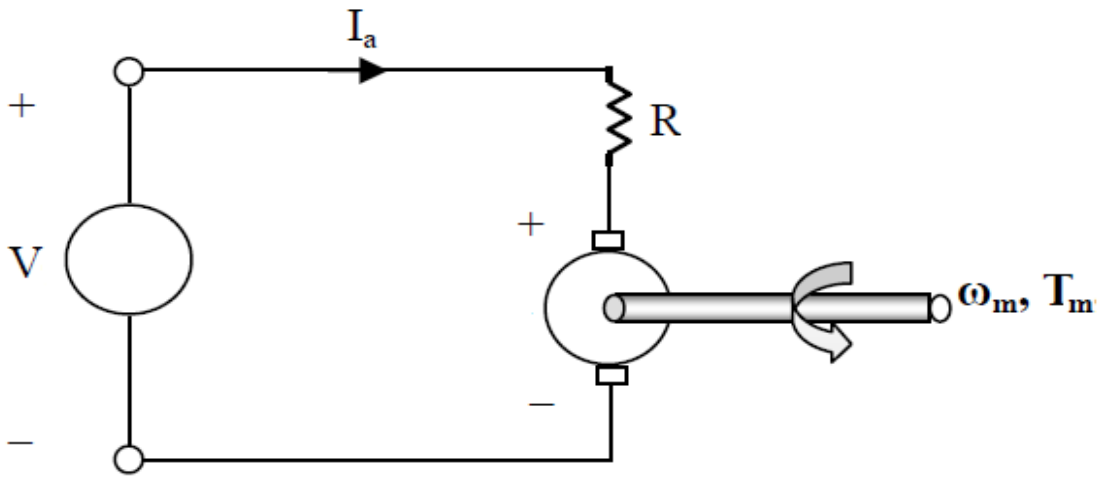

Figure 17: Electric Motor Model

For this model, we will assume that the input of the system is the voltage source (V) applied to the motor's armature, while the output is the rotational speed of the shaft ω_m. The rotor and shaft are assumed to be rigid. We further assume a viscous friction model, that is, the friction torque is proportional to shaft angular velocity.

This system will be modeled by summing the torques acting on the rotor inertia and integrating the acceleration to give velocity. Also, Kirchhoff's law will be applied to the armature circuit. First, we will model the integrals of the rotational acceleration and of the rate of change of the armature current. Next, we will apply Newton's law and Kirchhoff's law to the motor system.

Applying Kirchhoff's law to the armature circuit one has

$$R\,I_a \;+\; K\omega_m \;=\; V \tag{5.2}$$

Where

R = resistance in armature circuit = 1 Ω

$K = K_e$ = electromotive force constant = 0.01 V/rad/sec

V = voltage of voltage source

I_a = current in armature circuit

$\omega = \omega_m$ = speed of motor

Solving (5.2) for I_a gives

$$I_a \;=\; \frac{\mathrm{V}}{\mathrm{R}} \;-\; \frac{\mathrm{K}\omega}{\mathrm{R}} \tag{5.3}$$

Applying Newton's law to the motor one has

$$J_M \frac{\mathrm{d}\omega}{\mathrm{dt}} \;+\; b\omega \;+\; T_M \;=\; T_m \tag{5.4}$$

Where

J_M = moment of inertia of motor = 0.01 kg-m

b = motor friction constant = 0.1 N-m-s

T_M = torque delivered to the drive train by the motor

T_m = torque produced by motor

One has

$$T_m \;=\; K\,I_a \tag{5.5}$$

Where

$K = K_T$ = motor torque constant = K_e = 0.01 N-m/amp

Combining (5.3), (5.4) and (5.5) gives

$$J_M \frac{\mathrm{d}\omega}{\mathrm{dt}} + b\omega + T_M = K I_a = K\left(\frac{\mathrm{V}}{\mathrm{R}} - \frac{\mathrm{K}\omega}{\mathrm{R}}\right) = \frac{\mathrm{KV}}{\mathrm{R}} - \frac{K^2}{R}\omega \quad (5.6)$$

Or

$$J_M \frac{\mathrm{d}\omega}{\mathrm{dt}} + (b + \frac{K^2}{R})\omega + T_M = \frac{\mathrm{KV}}{\mathrm{R}} \quad (5.7)$$

The transmission equations are the following

$$\omega_o = \frac{\omega}{i_{Mg}} \quad (5.8)$$

$$T_o = i_{Mg} T_M \quad (5.9)$$

Where

i_{Mg} = gear ratio of transmission

ω_o = output speed of the wheel

T_o = output torque of the wheel

The wheel equations are the following

$$v = r\omega_o \quad (5.10)$$

Where

r = tire radius

v = speed of vehicle

Combining (5.10) with (5.8) gives

$$\omega = i_{Mg}\omega_o = \frac{i_{Mg} v}{r} \quad (5.11)$$

Substituting into (5.7) gives

$$\boldsymbol{J_M \frac{dv}{dt} + \left(b + \frac{K^2}{R}\right)v + \frac{rT_M}{i_{Mg}} = \frac{rKV}{i_{Mg}R}} \quad \textbf{(5.12)}$$

Internal Combustion Engine

The characteristics of the internal combustion engine can be represented by a nonlinear static map. The torque generated by the engine depends on the amount of fueling u_f and the engine speed ω_e. The engine torque is modeled as a function of the current throttle input from the driver pedal (fuel) and the engine speed (Figure 18) using the following equations.

$$T_e = f_e(u_f, \omega_e) \tag{5.13}$$

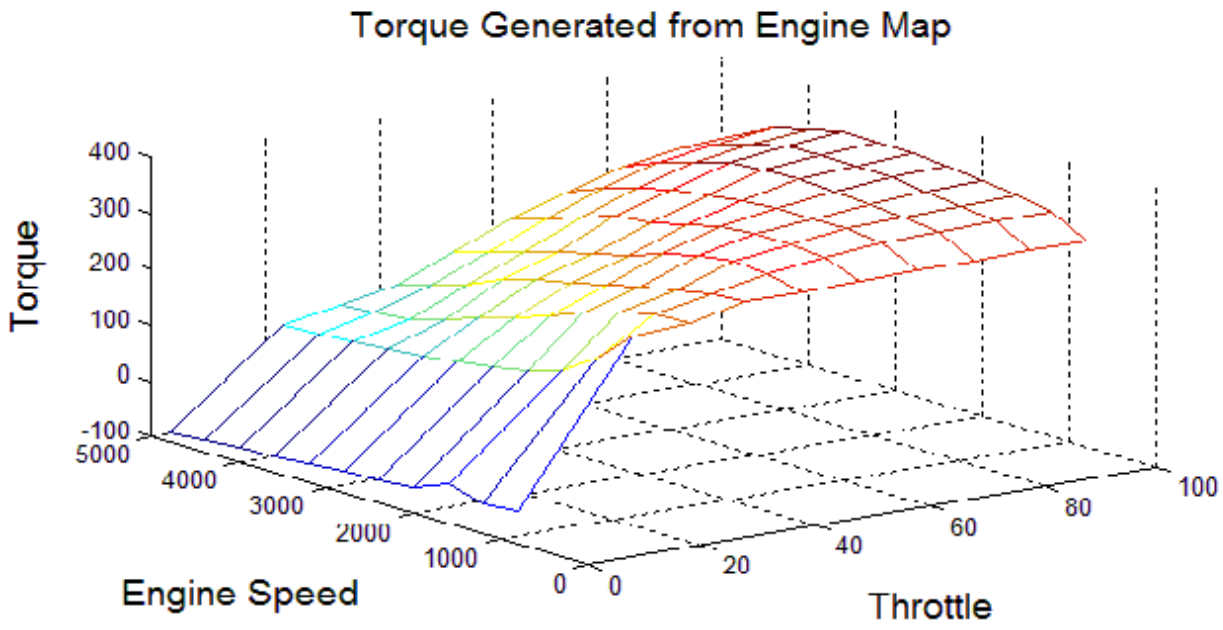

Figure 18: Engine Fuel Map as a Function of Throttle and Engine Speed

Given a torque request from the driver, the engine controller will supply a certain amount of fuel to produce the torque to respond to the speed request at a given engine speed. The amount of fuel required to make that torque depends on the engine's efficiency at that torque and speed.

Applying Newton's law to the engine one has

$$J_E \frac{d\omega}{dt} + T_i = T_e \tag{5.14}$$

Where

J_E = moment of inertia of engine

$\omega = \omega_E$ = speed of engine

T_i = torque delivered to the drive train by the engine

= impeller torque

T_e = torque produced by engine

Engine torque is modelled as a function of throttle (u_f) and engine speed (ω_e). The second-order quadratic model is used to determine the torque value. The quadratic model contains a squared term (ω^2), a linear term (ω), and a constant term (c), which have coefficients of (c_{ij}) as shown in equation (5.15).

Consider

$$T_e = f_e(u_f, \omega_e)$$
$$= (c_{11}\omega^2 + c_{12}\omega + c_{13})u_f{}^2 + (c_{21}\omega^2 + c_{22}\omega + c_{23})\,u_f + (c_{31}\omega^2 + c_{32}\omega + c_{33}) \quad (5.15)$$

Where

u_f = fuel input to engine = throttle input to engine

c_{ij} = (for i, j=1,2,3) are constant values derived for the approximation of the quadratic function of the fuel map using the Maxima tool. Figure 59 quantify the percentage change for fuel engine map and its approximation from quadratic function.

Combining (5.14) and (5.15) gives

$$J_E\frac{d\omega}{dt} + T_i = (c_{11}\omega^2 + c_{12}\omega + c_{13})\,u_f{}^2 + (c_{21}\omega^2 + c_{22}\omega + c_{23})\,u_f + (c_{31}\omega^2 + c_{32}\omega + c_{33}) \quad (5.16)$$

The transmission equations are the following

$$\omega_o = \frac{\omega}{i_{Eg}} \quad (5.17)$$

$$T_o = i_{Eg}T_i \quad (5.18)$$

Where

i_{Eg} = gear ratio of transmission

ω_o = output speed of the wheel; T_o = output torque of the wheel

The wheel equations are the following

$$v = r\omega_o \tag{5.19}$$

Where

r = tire radius; v = speed of vehicle

Combining (5.17) with (5.19) gives

$$\omega = i_{Eg}\omega_o = \frac{i_{Eg}v}{r} \tag{5.20}$$

Substituting into (5.16) gives

$$J_E\frac{dv}{dt} + \frac{rT_i}{i_{Eg}} = \frac{r}{i_{Eg}}[(C_{11}(\frac{i_{Eg}v}{r})^2 + C_{12}(\frac{i_{Eg}v}{r}) + C_{13})u_f{}^2 + (C_{21}(\frac{i_{Eg}v}{r})^2 + C_{22}(\frac{i_{Eg}v}{r}) + C_{23})u_f + (C_{31}(\frac{i_{Eg}v}{r})^2 + C_{32}(\frac{i_{Eg}v}{r}) + C_{33})] \tag{5.21}$$

Or

$$\boldsymbol{T_i = (d_{11}v^2 + d_{12}v + d_{13})\, u_f{}^2 + (d_{21}v^2 + d_{22}v + d_{23})\, u_f + (d_{31}v^2 + d_{32}v + d_{33}) - \frac{i_{Eg}J_E}{r}\frac{dv}{dt}} \tag{5.22}$$

Where

$$d_{i1} = \frac{i_{Eg}{}^2 c_{i1}}{r^2} \qquad i = 1, 2, 3$$

$$d_{i2} = \frac{i_{Eg}c_{i2}}{r} \qquad i = 1, 2, 3$$

$$d_{i3} = c_{i3} \qquad i = 1, 2, 3$$

The longitudinal vehicle dynamics are

$$\frac{\eta i_{Eg}T_i}{r} = mg(f_0 + f_1 v) + mg\sin\theta + \frac{C_D A}{21.15}v^2 + (m + \frac{\delta}{r^2})\frac{dv}{dt} \tag{5.23}$$

Where

η = transmission efficiency; m = mass of vehicle

f_0 = rolling resistance force constant

f_1 = speed dependent rolling resistance force constant

θ = slope angle; C_D = air drag coefficient constant

δ = wheel inertia; A = frontal surface area of vehicle

Combining (5.22) and (5.23) gives

$$J_E \frac{dv}{dt} + \frac{r^2}{\eta\, i_{Eg}{}^2}\left(mg\,(f_0 + f_1 v) + mg\sin\theta + \frac{C_D A}{21.15}v^2 + \left(m + \frac{\delta}{r^2}\right)\frac{dv}{dt}\right)$$
$$= \frac{r}{i_{Eg}}\left[(d_{11}v^2 + d_{12}v + d_{13})\,u_f{}^2 + (d_{21}v^2 + d_{22}v + d_{23})\,u_f + (d_{31}v^2 + d_{32}v + d_{33})\right] \quad (5.24)$$

Simplifying gives the following plant equation for the ICE

$$\boldsymbol{\alpha \frac{dv}{dt}} = \boldsymbol{(g_{11}v^2 + g_{12}v + g_{13})\,u_f{}^2 + (g_{21}v^2 + g_{22}v + g_{23})\,u_f + (g_{31}v^2 + g_{32}v + g_{33})} \quad \textbf{(5.25)}$$

Where

$$\alpha = J_E + \frac{r^2\, m + \delta}{\eta\, i_{Eg}{}^2}$$

$$g_{1j} = \frac{r}{i_{Eg}} d_{1j} \qquad \text{for } j = 1, 2, 3$$

$$g_{2j} = \frac{r}{i_{Eg}} d_{2j} \qquad \text{for } j = 1, 2, 3$$

$$g_{31} = \frac{r}{i_{Eg}} d_{31} - \frac{r^2\, C_D A}{21.15\,\eta\, i_{Eg}{}^2}$$

$$g_{32} = \frac{r}{i_{Eg}} d_{32} - \frac{r^2\, mg\, f_1}{\eta\, i_{Eg}{}^2}$$

$$g_{33} = \frac{r}{i_{Eg}} d_{33} - \frac{r^2\, mg}{\eta\, i_{Eg}{}^2}(f_0 + \sin\theta)$$

Hybrid System: Motor and Engine

Both the engine and the motor provide the required power to the drive shaft depending on the vehicle speed. The vehicle torque output can be expressed as,

$$T_o = i_M T_M + i_E T_i \tag{5.26}$$

Where, i_M ,i_E are proportion of torques from the power sources contributed to the wheel, T_M is the torque delivered to the drive train by the motor, and T_i is the torque delivered to the drive train by the engine.

The longitudinal vehicle dynamics are:

$$\frac{T_o i_g \eta}{r} = mg(f_0 + f_1 v) + mg \sin\theta + \frac{C_D A}{21.15} v^2 + (m + \frac{\delta}{r^2}) \frac{dv}{dt} \tag{5.27}$$

Or

$$T_o = \frac{r}{i_g \eta} [mg(f_0 + f_1 v) + mg \sin\theta + \frac{C_D A}{21.15} v^2 + (m + \frac{\delta}{r^2}) \frac{dv}{dt}] \tag{5.28}$$

Where

η = transmission efficiency; m = mass of vehicle

f_0 = rolling resistance force constant; θ = slope angle

f_1 = speed dependent rolling resistance force constant

i_g = final drive gear ratio; C_D = air drag coefficient constant

δ = wheel inertia; A = frontal surface area of vehicle

One has

$$T_o = i_M T_M + i_E T_i$$

Substituting (5.12) and (5.22) gives

$$\boldsymbol{T_0} = i_M \left[\frac{KV}{R} - \frac{i_{Mg} J_M}{r} \frac{dv}{dt} - \frac{i_{Mg}}{r} \left(b + \frac{K^2}{R}\right) v \right] + i_E \left[(d_{11} v^2 + d_{12} v + d_{13}) u_f^2 + (d_{21} v^2 + d_{22} v + d_{23}) u_f + (d_{31} v^2 + d_{32} v + d_{33}) - \frac{i_{Eg} J_E}{r} \frac{dv}{dt} \right] \quad (5.29)$$

Combining with (5.28) gives

$$\frac{r}{i_g \eta} \left[mg (f_0 + f_1 v) + mg \sin\theta + \frac{C_D A}{21.15} v^2 + \left(m + \frac{\delta}{r^2}\right) \frac{dv}{dt} \right] = i_M \left[\frac{KV}{R} - \frac{i_{Mg} J_M}{r} \frac{dv}{dt} - \frac{i_{Mg}}{r} \left(b + \frac{K^2}{R}\right) v \right] + i_E \left[(d_{11} v^2 + d_{12} v + d_{13}) u_f^2 + (d_{21} v^2 + d_{22} v + d_{23}) u_f + (d_{31} v^2 + d_{32} v + d_{33}) - \frac{i_{Eg} J_E}{r} \frac{dv}{dt} \right] \quad (5.30)$$

Or

$$\alpha \frac{dv}{dt} = (g_{11} v^2 + g_{12} v + g_{13}) u_f^2 + (g_{21} v^2 + g_{22} v + g_{23}) u_f + g_{31} v^2 + g_{32} v + g_{33} + \frac{i_M KV}{R} \quad (5.31)$$

Where

$$\alpha = \frac{i_M \, i_{Mg} \, J_M}{r} + \frac{i_E i_{Eg} J_E}{r} + \frac{r \left(m + \frac{\delta}{r^2}\right)}{i_g \eta}$$

$$g_{1j} = i_E d_{1j} \qquad \text{for } j = 1, 2, 3$$

$$g_{2j} = i_E d_{2j} \qquad \text{for } j = 1, 2, 3$$

$$g_{31} = i_E d_{31} - \frac{r \, C_D A}{21.15 \, i_g \eta}$$

$$g_{32} = i_E d_{32} - \frac{i_M \, i_{Mg}}{r} \left(b + \frac{K^2}{R}\right) - \frac{r \, mg \, f_1}{i_g \eta}$$

$$g_{33} = i_E d_{33} - \frac{r \, mg}{i_g \eta} (f_0 + \sin\theta)$$

And the hybrid plant equation can be written as,

$$\boldsymbol{\frac{dv}{dt} = C_0 + C_1 v + C_2 v^2 + B V_{dc}} \quad \textbf{(5.32)}$$

Assume that $\eta = 1$.Therefore, C_0, C_1, C_2 and B can be expressed as:

$$C_0 = \frac{r\,(d_{13} i_E u^2{}_f i_g \; + \; d_{23} i_E u_f i_g \; + d_{33} i_E i_g \; - mg \sin\theta\, r - mg f_0 r)}{I_T}$$

$$C_1 = -\frac{i_{Mg}\mathrm{BK} i_g - \; r d_{12} i_E u^2{}_f i_g - r d_{22} i_E u_f i_g - d_{32} i_E i_g + f_1 mg\, r^3 + rb i_M \; i_{Mg}\, i_g)}{I_T r i_g}$$

$$C_2 = -\frac{\frac{1}{2}\,\rho\, C_D r^2 \mathrm{A} - \; r d_{11} i_E u^2{}_f i_g - r d_{21} i_E u_f i_g - r d_{31} i_E i_g}{I_T i_g}$$

$$B = \frac{i_M r\, K}{I_T\, R}; \quad V = \quad V_{dc}$$

$$I_T = \frac{(m\, r^2 + \delta) + r i_g i_E i_{Eg} J_E + r i_g i_M \; i_{Mg}\, J_M}{i_g}$$

The following assumptions are made for Eq. (5.32):

- The slope of the road is assumed to be negligible.
- When the throttle is constant: C_0, C_1, C_2 and B are always constant parameters.
- When the throttle is varying, the parameters will vary slowly and the switching from one value to another occurs at low frequencies. In the throttle change case, there should be enough time between changes so that θ_t can guarantee closed loop stability and the adaptive law has time to "learn" about the change in the parameters. The same approach as above can be used to show that the error will be bounded, provided the switching frequency is sufficiently small, as shown in Figure 26.

The system described by (5.32) can be easily converted to a first order linear system using feedback linearization. We are primarily interested in systems where v tracks a desired speed profile v_d and it is slightly more intuitive to write the control law as,

$$\boldsymbol{V_{dc} = \theta_1 v_d + \theta_2 (v_d - v) + \theta_3 + \theta_4 v^2} \qquad \textbf{(5.33)}$$

Note that the feedback law given in equation (5.33) can be written in a concise form as,

$$\boldsymbol{V_{dc}} = [\boldsymbol{\theta_1}\ \ \boldsymbol{\theta_2}\ \ \boldsymbol{\theta_3}\ \boldsymbol{\theta_4}] \begin{bmatrix} \boldsymbol{v_d} \\ \boldsymbol{v_d - v} \\ \boldsymbol{1} \\ \boldsymbol{v^2} \end{bmatrix} = \boldsymbol{\theta\phi} \qquad \textbf{(5.34)}$$

The choice of the symbols θ and ϕ is to be consistent with the generally accepted notation used in MRAC, and θ is a vector of gains to be determined. The gains θ_i can be expressed as

$$\boldsymbol{\theta_1} = \frac{(-C_1 - a_m + b_m)}{B}\ ;\quad \boldsymbol{\theta_2} = \frac{(C_1 + a_m)}{B}$$

$$\boldsymbol{\theta_3} = \frac{-C_0}{B}\ ;\quad \boldsymbol{\theta_4} = \frac{-C_2}{B}.$$

The above choice of gains will result in the following closed loop system

$$\frac{dv}{dt} = -a_m v + b_m v_d \qquad (5.35)$$

This shows that by proper choice of the gains, we can obtain any first order linear system behavior. In section 6.4, we will briefly introduce the key results concerning model reference adaptive control (MRAC) to show how we can design an adaptive controller so that the gains can be tuned in real time to achieve any first order linear system behavior.

Hybrid Dual Clutch Transmission for HEV

The DCTs have two input shafts. Therefore, by connecting an electric machine on one of the shafts, a hybrid dual clutch transmission can be obtained. One motor-generator can be made to work both as a generator and motor thereby obtaining full hybrid functionality. In addition, a set of gear ratios are available for the electric mode; thus the size of the motor-generator unit can be made a little smaller. The system architecture of our hybrid dual clutch transmission is of parallel hybrid type architecture.

A similar design has been patented by GM with two electric machines (one as generator), but was never developed as a product [29]. Our system is equipped with one motor that can serve as a generator as well, which makes the proposed design less expensive and the torque range of the EM does not need to be high since the EM torque can be multiplied by the DCT. Shown in Figure 19 are some similar designs equipped with one motor only [29]. The first configuration (EM connected before transmission) and the third configuration (EM connected after transmission) are similar to the power-train of the 'Audi A3-etron' and 'P1-McLaren' respectively, exhibited at the March 2013 Geneva Motor Show. The second configuration (EM connected within transmission) is our design studied in this research. The proposed design is different from the existing state of the art on controllers.

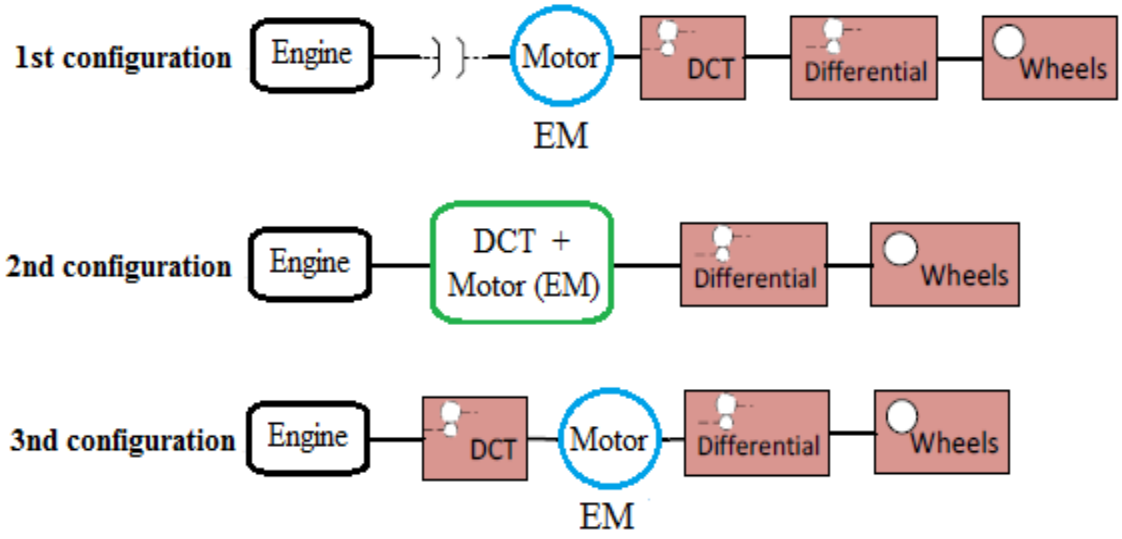

Figure 19: Different Design of Parallel Hybrid Architecture

Unlike in ECVT operated hybrid vehicle, where the engine speed is independent of the vehicle speed, in a HDCT the engine speed is dependent on the vehicle speed. The power-train consists of only one electric machine which can be made to operate both as generator and motor depending on the requirement. Clutch 1 is used for odd gears and clutch 2 is used for even gears. The electric machine is connected to one of the input shafts and can use gears: 2, 4, 6 and reverse gear whereas the engine can use all the gears including the reverse gears. A schematic of the HDCT is shown in Figure 20 [29].

For example, consider a driving scenario where the vehicle is accelerating from standing still. When the vehicle is standing still, second gear is preselected and the motor is ready to drive the wheels by drawing power from the battery thus making the vehicle operate in electric mode. While the vehicle is still in second gear, any odd gear on the other shaft can be preselected. Let's assume third gear is preselected. When clutch 1 is closed both motor and engine will drive the vehicle without any power loss during shifting unlike in the conventional manual and automatic transmissions.

When the vehicle is standing still, clutch 2 can be activated without selecting any gears on the output shaft, thus charging the battery using the electric machine as a generator.

The engine can be used to charge the battery while the vehicle is moving via two paths. The first path is when the engine is using odd gears to drive the vehicle. Some part of the engine output via the odd gears can be transmitted through the final drive to the motor-generator via one of the even gears. The second path is when the engine is using odd gears to drive the vehicle and some part of the engine output is directly transmitted.

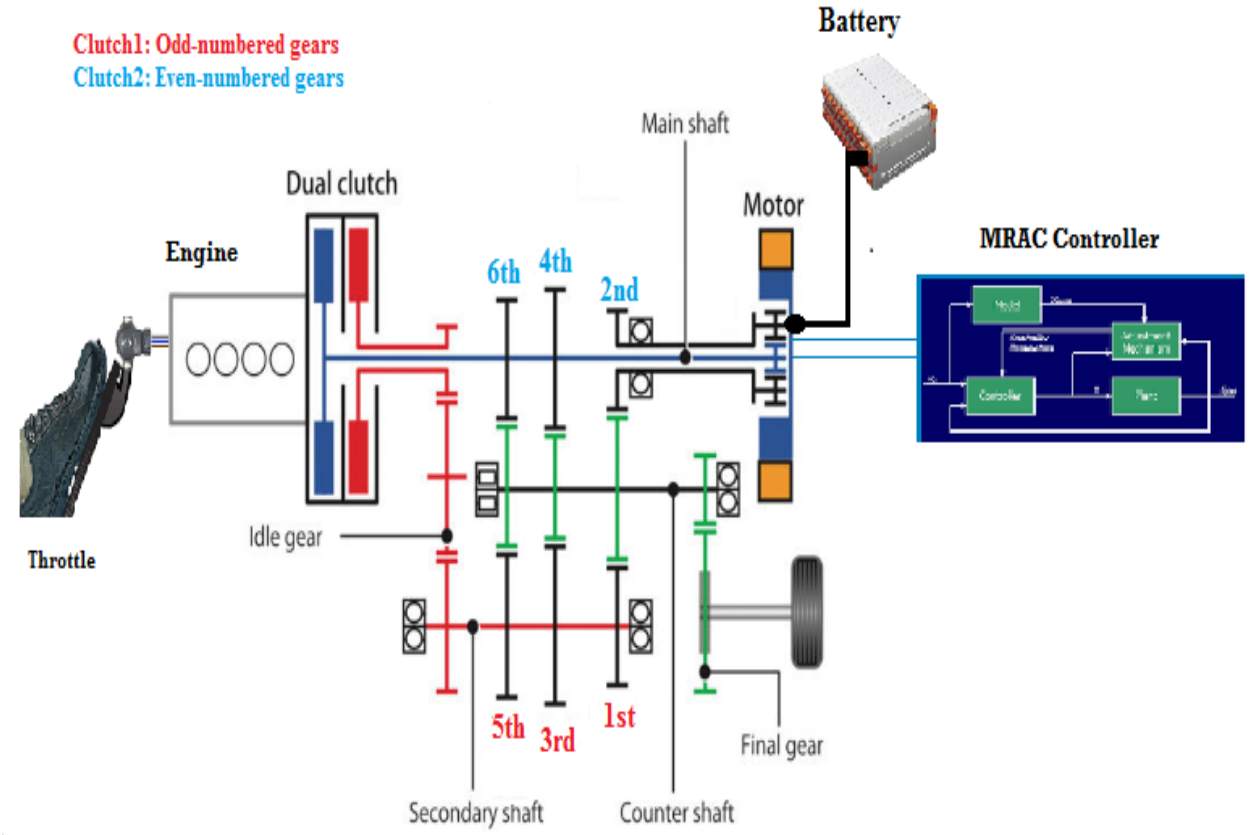

Figure 20: Vehicle Architecture of HDCT

HDCT Power Equation Model

A hybrid dual clutch transmission is modelled as two simple manual transmissions in one, with even and odd gears on two different shafts. The power loss during shifting is attributed only to clutch losses during its engagement which is assumed to be very small and is not taken into consideration in this thesis work. The efficiency of each meshing gear is assumed to be 97% and the efficiency of the differential is assumed to be 95%.

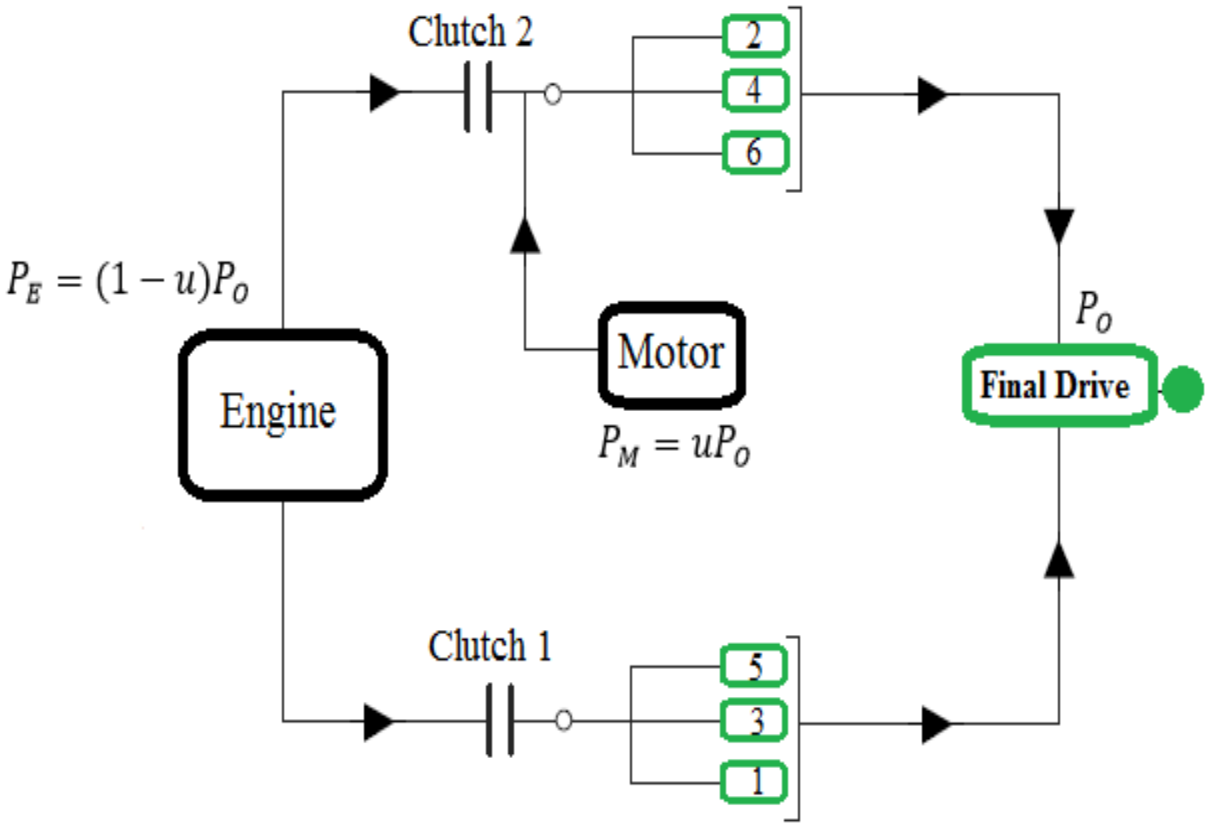

Figure 21: Schematic of Hybrid Dual Clutch Transmission

To ensure smooth shifting and optimal efficiency, DCTs need sophisticated controllers capable of preselecting the next gear and engaging the appropriate clutch precisely when required.

The torque transmitted through DCT can be expressed as,

$$I_{DCT}\ \frac{d_{\omega_{DCT}}}{dt} =\ T_i - T_{DCT} \tag{5.36}$$

Where T_{DCT} is the torque carried by DCT, ω_{DCT} and I_{DCT} are the speed and the mass moments of inertia of the flywheel respectively.

For the sake of simplicity, the following assumptions are made in the design of the controller: $\omega_E = \omega_{DCT}, \omega_M = \omega_E \left(\frac{i_M}{i_E}\right)$ and the gear imposes a single constraint, specified by the fixed gear ratio. Consequently the DCT equation is embedded into the HDCT plant equation. Then the HDCT simplified model is shown in Figure 21[29].

The power split ratio *u* for the HDCT design is defined as the power request to the motor (P_M) divided by the total power request at the wheels (P_O), which can be expressed as,

$$u = \frac{P_M}{P_O} \tag{5.37}$$

Therefore, engine torque and power are given by,

$$T_i = \frac{(1-u)}{i_E} T_O,\ \ P_E = (1-u)P_O \tag{5.38}$$

Motor torque and power are given by,

$$T_M = \frac{u}{i_M} T_O,\ \ P_M = uP_O \tag{5.39}$$

CHAPTER VI: Adaptive Control

Design of Control Strategy and Methodology

The hybrid electric system that was studied in this dissertation was intended to provide the mode selection strategy for electric vehicle integration. This design of the hybrid electric vehicle is based on a dual clutch configuration and involves building a controller to make the desired selection mode based on defined inputs. The development of such a system according to the normative aspects of functional safety is a reality in key industries, particularly in the automotive industry.

This dissertation focuses on the process of HEV modeling, design and control optimization. A HDCT simulation model was established with a Matlab simulation to emulate powertrain configurations. Using this model, a combined configuration design and control optimization strategy was proposed for HEVs.

- Improving shifting quality of the HEV by selecting the desired mode that fits the input variables requirement of the dual-clutch.

- Achieving fast and accurate tracking of the desired engine and dual-clutch speed trajectories. Furthermore, the controller should also be robust for disturbances and be able to achieve better performance.

- Creating a math-based model format to present HEV designs. This model format presents the powertrain dynamics regardless of the various connections of engine-to-gear, motor-to-gear and clutch-to-gear. With such a model format, a technique will quickly and automatically connect to the control system in order to make the best selection possible with the addition of the other inputs.

- Generating the system equation of the HEV model and systematically exploring possible configuration designs with the help of Matlab/Simulink and other math tools. A design screening process was developed based on various design requirements including feasibility, drivability, power source component sizing, transmission efficiency and desired mode shifting.

- Adopting an optimal control design procedure based on Model Reference Adaptive Control (MRAC) in the desired mode selection. MRAC was employed to find the optimum mode of operation based on driver selection and achieve the benchmarks for different powertrain configurations.

Control Strategy for HDCT

The control strategy in the hybrid electric vehicle system involves translating driver and other command inputs into power to master the powertrain components. Common objectives include minimizing fuel consumption and emissions, while maintaining safety and improving performance and drivability.

Minimizing power losses implies higher efficiency and less fuel consumption. This is accomplished through optimizing powertrain design and control. Powertrain optimal design is composed of configuration design and component design. Not only the drivetrain architecture and each component need to be power efficient, but these components need to be matching in type and size to obtain high overall efficiency [30].

The general control strategy for a HEV can be summarized as follows:

1. When the speed of the vehicle is small, the ICE stops and the electric motor provides the required driving power, which avoids higher fuel consumption and emissions. It is assumed that SOC is sufficient.

2. When the speed of the vehicle is high enough, the electric motor stops, ICE starts and gives the required driving power. Currently, ICE works along the optimum curve, depending on the cost function.
3. If the power required is greater than the output of the ICE, the ICE and the electric motor work together and the electric motor takes additional required power from the battery. It is assumed that SOC is sufficient.
4. If SOC of the battery drops under the safe level, ICE supplies both the energy required for traveling and extra power to charge the battery through the electric motor, whereby the electric motor is in generator mode.
5. In the braking state, energy floats from the vehicle body to the drive train. The electric motor works as a generator and transforms braking energy to electricity to charge the battery.

Desired Mode Selection Controller for HDCT Design

For the most practical HEV, the control strategies adopted are rules based on threshold values, which restrict the engine to work at its most efficient while preserving a required state of charge. When the torque demand is lower than the threshold value, the engine is off and only the electric motor is used to power the vehicle [31]. When the torque demand is higher than the threshold value, both the electric motor and engine are used together, otherwise the engine is used for driving the vehicle and the electric motor for generating charge, depending on the battery state. However, there are many factors which affect engine start/stop: downtime, coolant temperature, catalytic converter temperature, speeds of the engine, battery SOC, required power, overall fuel economy and emissions performance [32].

In our design, the control objectives will be determined by ensuring that the engine and dual-clutch speeds track the desired reference signals. The input signals for the desired mode controller include the vehicle speed to control the throttle of the engine and the voltage of the electric motor, in addition to another controller to control the engine torque to deliver optimum value based on efficiency. There is no consideration of the influence of the catalytic converter's temperature and coolant temperature on the engine.

In this dissertation, the controller will be designed based on Model Reference Adaptive Control (MRAC) using the MIT Rule. MRAC was originally proposed to solve the problem in which the design specifications are given by a reference model, and the parameters of the controller are adjusted by an adaptation mechanism/law, such that the closed-loop dynamics of the system are the same as the reference model, which gives the desired response to a command signal. In solving this class of problem, the Lyapunov equation plays a very important role in choosing the Lyapunov function and deriving the feedback control and adaptation mechanism. In fact, the construction of Lyapunov functions is systematic and straightforward for the class of systems which can be transformed into two parts:

- A stable linear portion so that linear stability results can be directly applied, and
- A matched nonlinear portion which can be handled using different techniques, such as adaptive or robust control techniques in different situations [29].

Basic Concepts in Adaptive Control

In this section, we address a few basic questions, namely, why we need adaptive control, what the basic structures of adaptive control systems are, and how to go about designing adaptive control systems.

Why Adaptive Control?

In some control tasks, such as those in hybrid and electric manipulation, the systems to be controlled have parameter uncertainty at the beginning of the control operation. Unless such parameter uncertainty is gradually reduced on-line by an adaptation or estimation mechanism, it may cause inaccuracy or instability for the control systems. In many other tasks, such as those in power systems, the system dynamics may have well known dynamics at the beginning, but experience unpredictable parameter variations as the control operation goes on. Without continuous "redesign" of the controller, the initially appropriate controller design may not be able to control the changing plant well. Generally, the basic objective of adaptive control is to maintain consistent performance of a system in the presence of uncertainty or unknown variation

in plant parameters. Since such parameter uncertainty or variation occurs in many practical problems, adaptive control is useful in many industrial contexts [33]. These include:

Ship steering: On long courses, ships are usually put under automatic steering. However, the dynamic characteristics of a ship strongly depend on many uncertain parameters, such as water depth, ship loading, and wind and wave conditions. Adaptive control can be used to achieve good control performance under varying operating conditions, as well as to avoid energy loss due to excessive rudder motion.

• **Aircraft control**: The dynamic behavior of an aircraft depends on its altitude, speed, and configuration. The ratio of variations of some parameters can lie between 10 and 50 in a given flight. As mentioned earlier, adaptive control was originally developed to achieve consistent aircraft performance over a large flight envelope.

• **Process control**: Models for metallurgical and chemical processes are usually complex and also hard to obtain. The parameters characterizing the processes vary from batch to batch. Furthermore, the working conditions are usually time-varying (e.g., reactor characteristics vary during the reactor's life, the raw materials entering the process are never exactly the same, atmospheric and climatic conditions also tend to -change). In fact, process control is one of the most important and active application areas of adaptive control.

Adaptive control has also been applied to other areas, such as power systems and biomedical engineering. Most adaptive control applications are aimed at handling inevitable parameter variation or parameter uncertainty. However, in some applications, particularly in process control, where hundreds of control loops may be present in a given system, adaptive control is also used to reduce the number of design parameters to be manually tuned, thus yielding an increase in engineering efficiency and practicality.

Model Reference Adaptive Control (MRAC)

An adaptive controller differs from an ordinary controller in that the controller parameters are variable, and there is a mechanism for adjusting these parameters online based on signals in the system. The main approaches for constructing adaptive controllers by using the model reference adaptive control method.

Generally, a model-reference adaptive control system can be schematically represented by Figure 22. It is composed of four parts: a plant containing unknown parameters, a reference model for compactly specifying the desired output of the control system, a feedback control law containing adjustable parameters, and an adaptation mechanism for updating the adjustable parameters.

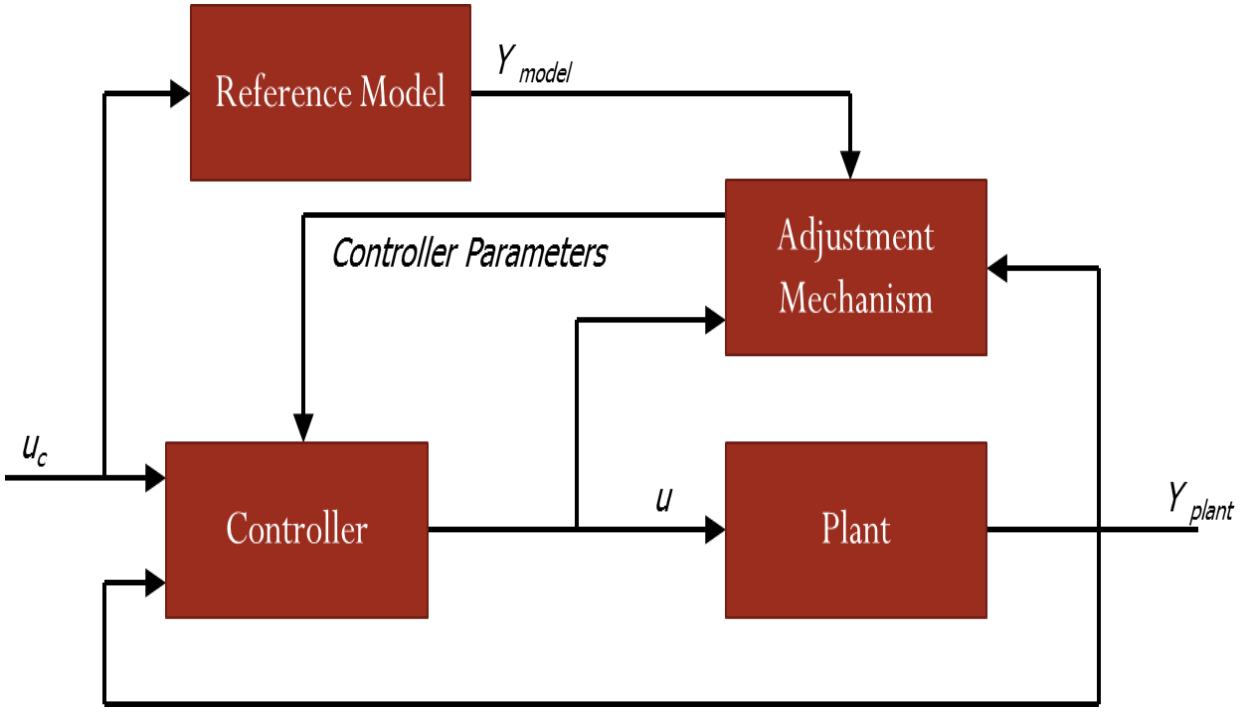

Figure 22: Model Reference Adaptive Control

- The ***plant*** is assumed to have a known structure, although the parameters are unknown.

1. For linear plants, this means that the number of poles and the number of zeros are assumed to be known, but that the locations of these poles and zeros are not.
2. For nonlinear plants, this implies that the structure of the dynamic equations is known, but that some parameters are not.

- A ***reference model*** is used to specify the ideal response of the adaptive control system to the external command. Intuitively, it provides the ideal plant response which the adaptation mechanism should seek in adjusting the parameters.
- The ***controller*** is usually parameterized by a number of adjustable parameters. The controller should have perfect tracking capacity in order to allow the possibility of tracking convergence. That is, when the plant parameters are exactly known, the corresponding controller parameters should make the plant output identical to that of the reference model. When the plant parameters are not known, the adaptation mechanism will adjust the controller parameters so that perfect tracking is asymptotically achieved

- The ***adaptation*** mechanism is used to adjust the parameters in the control law. In MRAC systems, the adaptation law searches for parameters such that the response of the plant under adaptive control becomes the same as that of the reference model, *i.e.*, the objective of the adaptation is to make the tracking error converge to zero. Although the application of one formalism may be more convenient than that of another, the results are often equivalent. In this chapter, we shall mostly use Lyapunov theory.

The MRAC controller has been well established for many nonlinear problems, such as the Shunt active power-filter system [34], the Piezo-positioning system [35], the Three-phase three level boost rectifier [36], Controlling water level of boiler system [37], DC electric drive alone [38], and Control and Real- Time Optimization of Dry Dual Clutch Transmission during the Vehicle's Launch [39]. In addition, a model reference control law is proposed to coordinate the motor torque, engine torque, and clutch torque to manage transitions to Series- Parallel Hybrid electric vehicles (SPHEVs) [40].

Design Adaptive Controller for HDCT

The design of an adaptive controller usually involves the following three steps:

• choose a control law containing variable parameters
• choose an adaptation law for adjusting those parameters
• analyze the convergence properties of the resulting control system.

The MRAC Architecture

The MRAC architecture (as shown in Figure. 23) contains a reference model that is built to match the desired powertrain dynamics of the driving mode. An output feedback MRAC algorithm will be proposed, the conditions for closed-loop system stability will be derived, and the methods for selecting input combinations and controller parameters will be discussed. The discussions and experimental results presented will establish the effectiveness of the proposed MRAC.

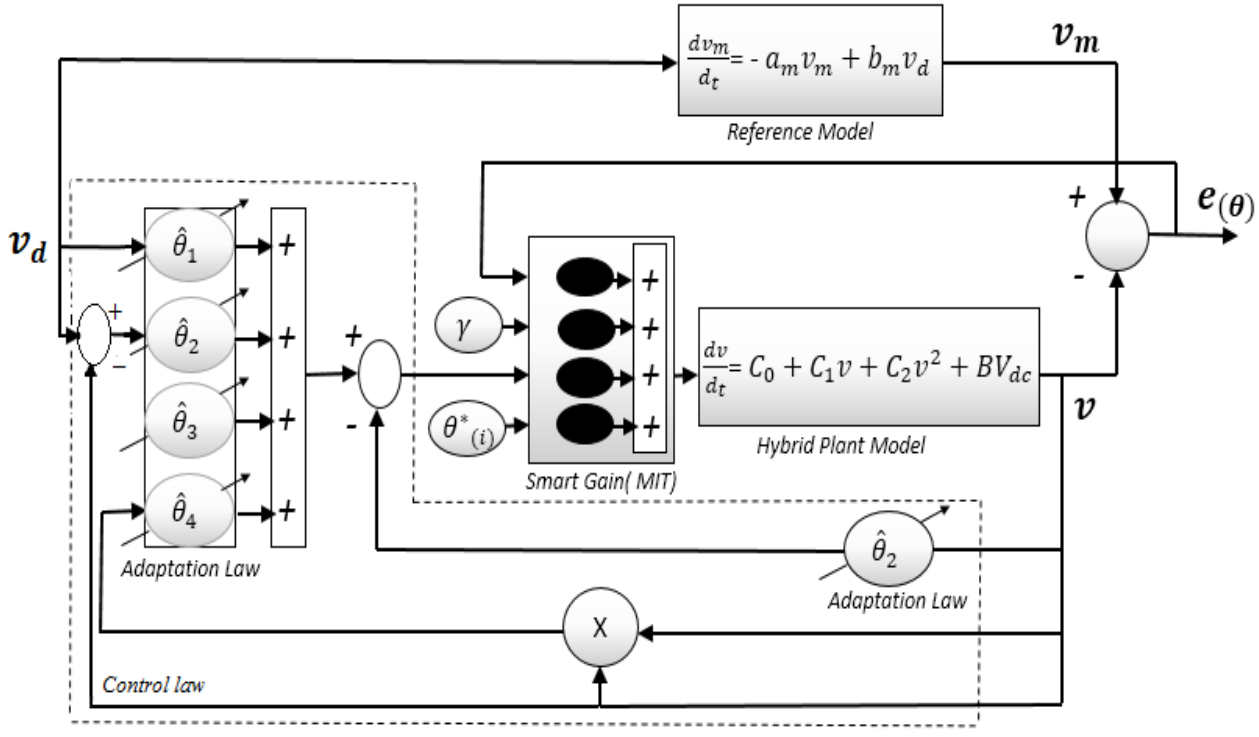

Figure 23: The MRAC Architecture for HDCT

MIT Rule

The gradient method, also referred as the MIT rule, was developed by the Instrumentation Laboratory at the Massachusetts Institute of Technology (MIT) [41]. It will be assumed that in the closed loop system, the controller has one adjustable parameter θ. The parameter $e\ (\theta\ )$ represents the error between the output of the plant $y_{plant}\ (\theta)$ and the output of the model reference $y_{model}\ (\theta)$. The goal here is to adjust θ to minimize the cost function $J_{(\theta)} = \frac{1}{2}\ e^2(\theta)$

- Tracking error:

$$e(\theta) = y_{plant}\ (\theta) - y_{model}\ (\theta) \tag{6.1}$$

- Form cost function:

$$J_{(\theta)} = \frac{1}{2}\ e^2(\theta) \tag{6.2}$$

- Update rule:

$$\frac{d\theta}{dt} = -\gamma \frac{\delta J}{d\theta} = \ -\gamma e \frac{\delta e}{d\theta} \tag{6.3}$$

Change in θ is proportional to negative gradient of $J\ (\theta)$.

Adaptive Control Law

The adaptive control law is very general. Here, we focus on a special case of a first order system where the model is a stable linear system. The adaptation is a set of feedback gains, and the control signal given in (5.34) for the MIT rule can be expressed as,

$$\dot{\theta} = -\gamma\ \emptyset^T e \tag{6.4}$$

In terms of each gain, the above formula is decoupled and can be written as,

$$\dot{\theta_1} = -\gamma v_d e;\ \ \dot{\theta_2} = -\gamma(v_d - v);\quad \dot{\theta_3} = -\gamma 1 e;\qquad \dot{\theta_4} = -\gamma v^2 e \tag{6.5}$$

This control law has been implemented successfully in our design and proven to be effective as shown in Figures 24 and 25.

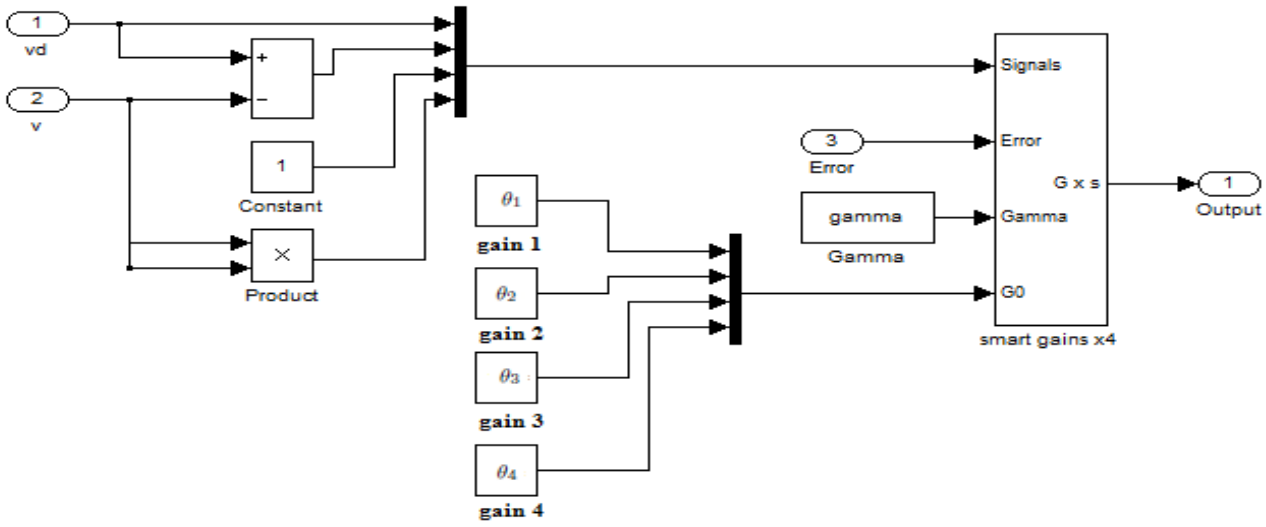

Figure 24: Block Diagram of Adaptive Control Law in Matlab

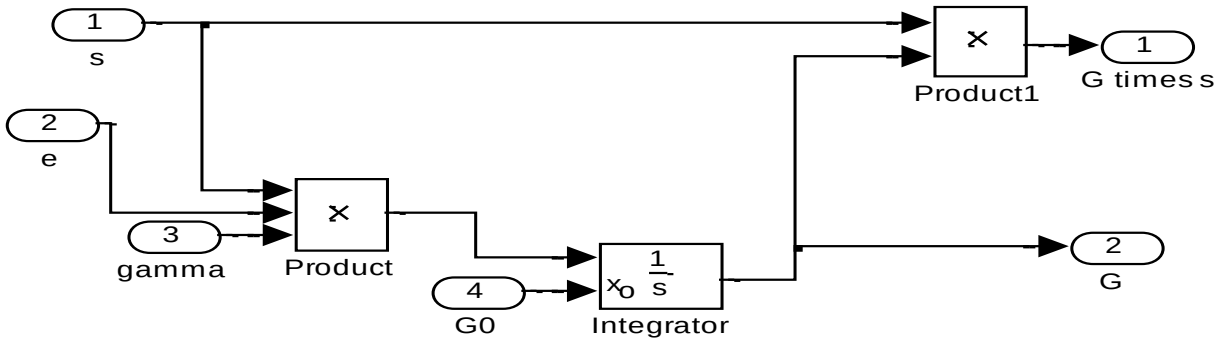

Figure 25: Block diagram of Smart Gain in Matlab

Proving the Control Law and Stability Using Lyapunov's Method

The adaptive control of non-linear plants using the MRAC method is discussed next. The hybrid vehicle system can be represented by using the following first-order differential equation based on Newton's second law:

$$\frac{dv}{dt} = C_0 + C_1 v + C_2 v^2 + BV_{dc} \qquad (6.6)$$

Where, v *and* V_{dc} represent plant output and input, respectively, and v^2 denote the quadratic term.

1) Problem Specification:

Let the desired performance of the adaptive control system be specified by a first-order reference model

$$\frac{dv_m}{dt} = -a_m v_m + b_m v_d \tag{6.7}$$

Where a_m *and* b_m are constant parameters, and v_d is a bounded external reference signal. The parameter a_m is required to be strictly positive, so that the reference model is stable, and b_m is chosen strictly positive without loss of generality [33].

The motivation behind using the adaptive control design is to formulate a control law, and an adaptation law, such that the resulting model following error $v - v_m$ asymptotically converges to zero.

2) Choice of Control Law

As the first step in the adaptive controller design, let us choose the control law to be:

$$V_{dc} = \hat{\theta}_1 v_d + \hat{\theta}_2 (v_d - v) + \hat{\theta}_3 + \hat{\theta}_4 v^2 \tag{6.8}$$

Where $\hat{\theta}_1$, $\hat{\theta}_2$, $\hat{\theta}_3$ *and* $\hat{\theta}_4$ are variable feedback gains. With this control law, the closed-loop dynamics are:

$$\frac{dv}{dt} = \left(C_1 - B\hat{\theta}_2\right)v + \left(B\hat{\theta}_1 + B\hat{\theta}_2\right)v_d + B\hat{\theta}_3 + C_0 + (B\hat{\theta}_4 \quad + C_2)v^2 \tag{6.9}$$

If the plant parameters were *known*, the values of control parameters (initial value) would be:

$$\theta_1^* = \frac{(-C_1 - a_m + b_m)}{B}\ ; \quad \theta_2^* = \frac{(C_1 + a_m)}{B}; \quad \theta_3^* = \frac{-C_0}{B}\ ; \quad \theta_4^* = \frac{-C_2}{B} \tag{6.10}$$

This would lead to the closed-loop dynamics identical to the reference model dynamics, and yields zero tracking error. In this case, the first term in (6.8) would result in the right DC gain,

while the second term in the control law Eq. (6.8) would achieve the dual objectives of canceling the term $C_1 v$ in Eq. (6.6) and imposing the desired pole $a_m v_m$.

In the adaptive control problem, since C_0, C_1, C_2 and B are unknown, the control input will achieve these objectives adaptively, i.e., the adaptation law will continuously search for the right gains, based on the tracking error $v - v_m$, so as to make *v* tend to v_m, asymptotically.

3) Choice of Adaptation Law

The adaptation law for the parameters $\hat{\theta}_1,\ \hat{\theta}_2,\ \hat{\theta}_3\ and\ \hat{\theta}_4$ can be chosen as follows:

Let, $$e = v - v_m,$$

be the tracking error. The parameter errors are defined as the difference between the controller parameter provided by the adaptation law and the ideal parameters, *i.e.*,

$$\tilde{\boldsymbol{\theta}}(t) = \begin{bmatrix} \tilde{\theta}_1 \\ \tilde{\theta}_2 \\ \tilde{\theta}_3 \\ \tilde{\theta}_4 \end{bmatrix} = \begin{bmatrix} \hat{\theta}_1 - \theta_1^* \\ \hat{\theta}_2 - \theta_2^* \\ \hat{\theta}_3 - \theta_3^* \\ \hat{\theta}_4 - \theta_4^* \end{bmatrix} \tag{6.11}$$

The dynamics of tracking error can be found by subtracting (6.9) from (6.7) result in,

$$\frac{de}{dt} = \frac{dv}{dt} - \frac{dv_m}{dt}$$

$$\begin{aligned} \frac{\boldsymbol{de}}{\boldsymbol{dt}} = \left(\boldsymbol{C_1} - \boldsymbol{B\hat{\theta}_2}\right)\boldsymbol{v} + \left(\boldsymbol{B\hat{\theta}_1} + \boldsymbol{B\hat{\theta}_2}\right)\boldsymbol{v_d} + \boldsymbol{B\hat{\theta}_3} + \boldsymbol{C_0} \\ + \left(\boldsymbol{B\hat{\theta}_4} + \boldsymbol{C_2}\right)\boldsymbol{v^2} + \boldsymbol{a_m v_m} - \boldsymbol{b_m v_d} \end{aligned} \tag{6.12}$$

Thus, the adaptation law can be expressed as,

$$\dot{\hat{\boldsymbol{\theta}}}_1 = -\gamma e v_d;\ \ \dot{\hat{\boldsymbol{\theta}}}_2 = -\gamma e\ (v_d - v);\quad \dot{\hat{\boldsymbol{\theta}}}_3 = -\gamma e;\qquad \dot{\hat{\boldsymbol{\theta}}}_4 = -\gamma e\ v^2$$

4) Tracking Convergence Analysis

With the control law and adaptation law chosen above, we can now analyze the system's stability and convergence behavior using Lyapunov theory. The Lyapunov function candidate can be expressed as,

$$V = \frac{1}{2}e^2 + \frac{B}{2\gamma}(\hat{\theta}_1 - \theta_1^*)^2 + \frac{B}{2\gamma}(\hat{\theta}_2 - \theta_2^*)^2 + \frac{B}{2\gamma}(\hat{\theta}_3 - \theta_3^*)^2 + \frac{B}{2\gamma}(\hat{\theta}_4 - \theta_4^*)^2 \tag{6.13}$$

It is important to note that the error goes to zero if the parameters of the controller are set to the initial values. This function is zero only when the error is zero and the controller parameters have the correct values. The derivative of V is given as

$$\frac{dV}{dt} = \frac{de}{dt}e + \frac{B}{\gamma}(\hat{\theta}_1 - \theta_1^*)\dot{\hat{\theta}}_1 + \frac{B}{\gamma}(\hat{\theta}_2 - \theta_2^*)\dot{\hat{\theta}}_2 + \frac{B}{\gamma}(\hat{\theta}_2 - \theta_2^*)\dot{\hat{\theta}}_3 + \frac{B}{\gamma}(\hat{\theta}_4 - \theta_4^*)\dot{\hat{\theta}}_4 \tag{6.14}$$

Substituting Eq. (6.12) into Eq. (6.14) with the values

$$\boldsymbol{a_m} = -C_1 + B\theta_2^*\,; \boldsymbol{b_m} = B(\theta_1^* + \theta_2^*); \boldsymbol{C_0} = -B\theta_3^*; \boldsymbol{C_2} = -B\theta_4^*;\ \boldsymbol{\Delta\theta_x} = \hat{\theta}_x - \theta_x^*$$

And the parameters are updated as

$$\dot{\hat{\boldsymbol{\theta}}}_1 = -\gamma e v_d;\ \dot{\hat{\boldsymbol{\theta}}}_2 = -\gamma e\,(v_d - v);\quad \dot{\hat{\boldsymbol{\theta}}}_3 = -\gamma e;\qquad \dot{\hat{\boldsymbol{\theta}}}_4 = -\gamma e\, v^2$$

Yields

$$\frac{dV}{dt} = e\left[C_1 v - B\hat{\theta}_2 v + B\hat{\theta}_1 v_d + B\hat{\theta}_2 v_d + B\hat{\theta}_3 + B\hat{\theta}_4\, v^2 - B\theta_3^* - B\theta_4^* v^2 + a_m v_m - B\theta_1^* v_d - B\theta_2^* v_d\right] + \frac{B}{\gamma}(\Delta\theta_1)(-\gamma e v_d) + \frac{B}{\gamma}(\Delta\theta_2)(-\gamma e\, v_d) - \frac{B}{\gamma}(\Delta\theta_2)(-\gamma e\, v) + \frac{B}{\gamma}(\Delta\theta_3)(-\gamma e) + \frac{B}{\gamma}(\Delta\theta_4)(-\gamma e\, v^2) \tag{6.15}$$

The resulting derivative of the Lyapunov candidate function can be expressed as,

$$\frac{dV}{dt} = -a_m(v - v_m)e \tag{6.16}$$

and

$$e = v - v_m$$

Therefore the final result is given as,

$$\boldsymbol{\frac{dV}{dt} = -a_m e^2} \tag{6.17}$$

Thus, the adaptive control system is globally stable, i.e., the signals e, $\hat{\theta}_1$, $\hat{\theta}_2$, $\hat{\theta}_3$ *and* $\hat{\theta}_4$ are bounded. Furthermore, the tracking error *e (t)* is guaranteed to be asymptotically convergent to zero because the boundedness of e, $\hat{\theta}_1$, $\hat{\theta}_2$, $\hat{\theta}_3$ *and* $\hat{\theta}_4$ implies the boundedness of *e (t)*, which implies the uniform continuity of V. As a result, the error function will converge to zero, for the adaptive control system is globally stable. A short analysis of Figure 26 reveals the powerful development of the control system and demonstrates its adjustability.

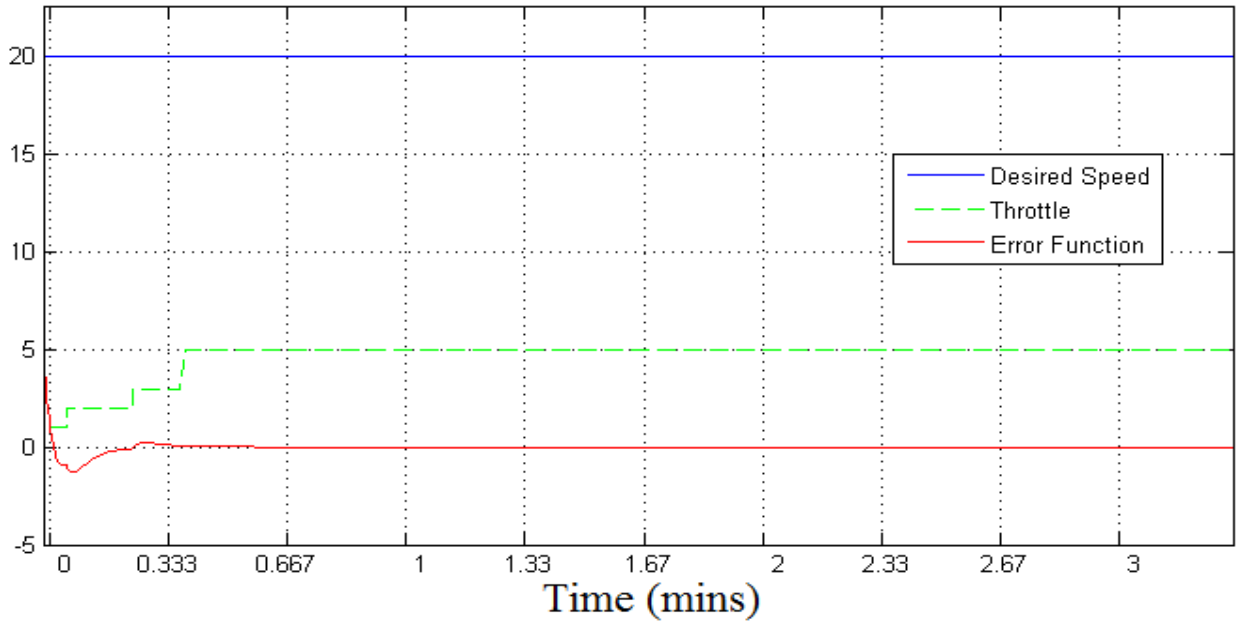

Figure 26: Error Function Converges to Zero

CHAPTER VII: Simulation Results

To demonstrate the effectiveness of the MRAC control under both tracking and regulatory conditions, the performance of the engine and DC motor were simulated under various operating conditions, such as varying the speed, varying the throttle and shifting the gears, for both the DCT and the traditional transmissions.

The experimental results show that the robustness is greatly enhanced by this adaptive scheme, and the results show excellent convergence to the desired speed under various conditions. In addition, the performance of the proposed controller was also evaluated for:

- Selection of desired driving mode.
- Sensitivity investigation of the response of the MRAC controller under the selection of various operating conditions.
- Interaction between various modes.
- Experimental validation of the MRAC used in an HDCT bus and a simulation study to compare the results of the proposed MRAC with the conventional controller.

Driving Selection Modes

Our first experiment has the following aims:

1) Comfortable Car: This mode has smooth shifting with no sense of any gear change; therefore, it takes longer to reach the desired value, as shown in Figure 27.

Desired Model: $\frac{dv}{dt} = -1(v_d - v)$

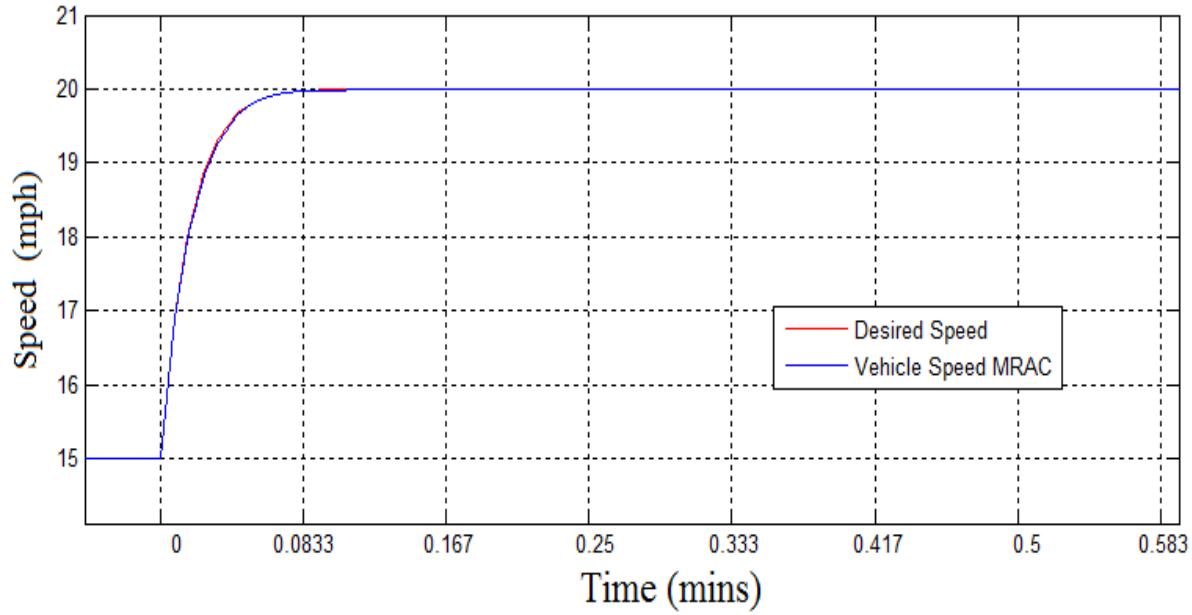

Figure 27: Response of the Comfortable Car

2) Sporty Shifting Car: This mode allows the driver to feel the shifting of the transmission and have the manual transmission experience; it takes less time to reach the desired value, as shown in Figure 28.

Desired Model: $\frac{dv}{dt} = -10(v_d - v)$

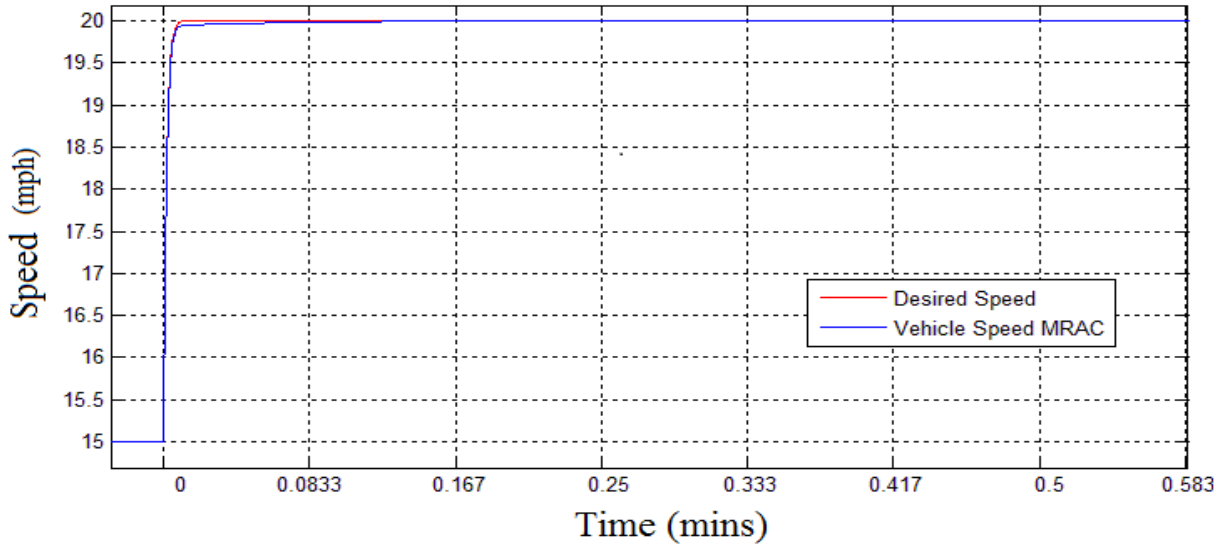

Figure 28: Response of the Sporty Car

Sensitivity Analysis of the MRAC Controller

To demonstrate the effectiveness of the MRAC control under both tracking and regulatory conditions, the performance of engine and DC motor has been simulated under various operating conditions such as speed and throttle varying, shifting gear. Simulation results show that the robustness is greatly enhanced by this adaptive scheme, and the results show excellent convergence to desired speed under various conditions.

- **Case 1: Speed is constant and throttle is varying:**

Increasing the engine throttle angle will cause the engine torque to increase, as shown between time 200 s thru 250 s in Figure 29, for example. The vehicle acceleration changes and the engine torques respond proportionally to the throttle; the engine accelerates to produce more torque and the controller reduces the motor torque by the same amount to maintain a balance. Similarly, reducing the engine throttle angle will cause the engine torque to decrease, as shown between time 50 s to 100 s in Figure 29. Thus, the electric motor will turn on to assist, and the MRAC controller will supply more voltage to the motor to compensate for the torque lost.

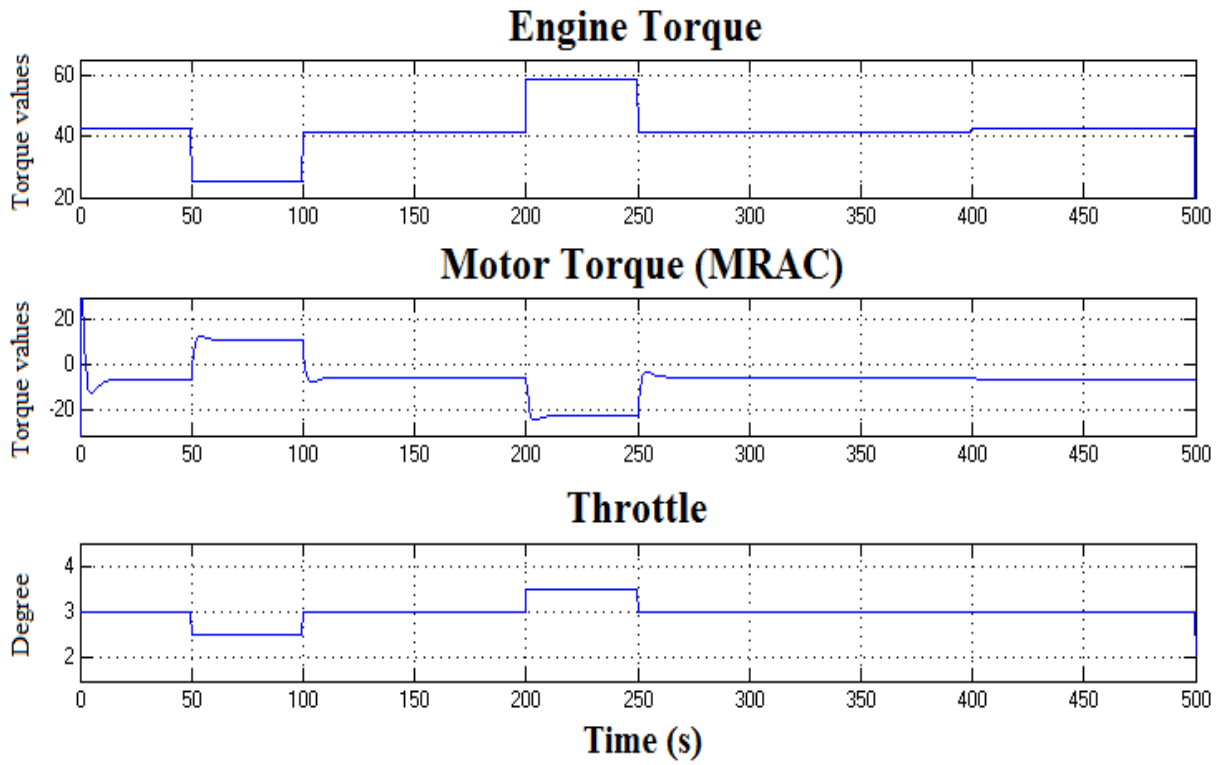

Figure 29: Throttle is Variable

- **Case 2: Throttle is constant and speed is variable:**

At higher speeds, the gasoline engine provides the primary power for the hybrid system, and the electric motor assists when extra acceleration is needed for passing, and provides the required torque during starting or stopping. Meanwhile, to meet the HEV's fast torque response, the MRAC supplies more voltage and an additional acceleration is imposed on the motor torque (see Figure 30). Both the engine and motor torque are changing simultaneously to accommodate the change of speed. However, when the speed is varying, the contributions of the engine and the motor are inversely proportional to each other.

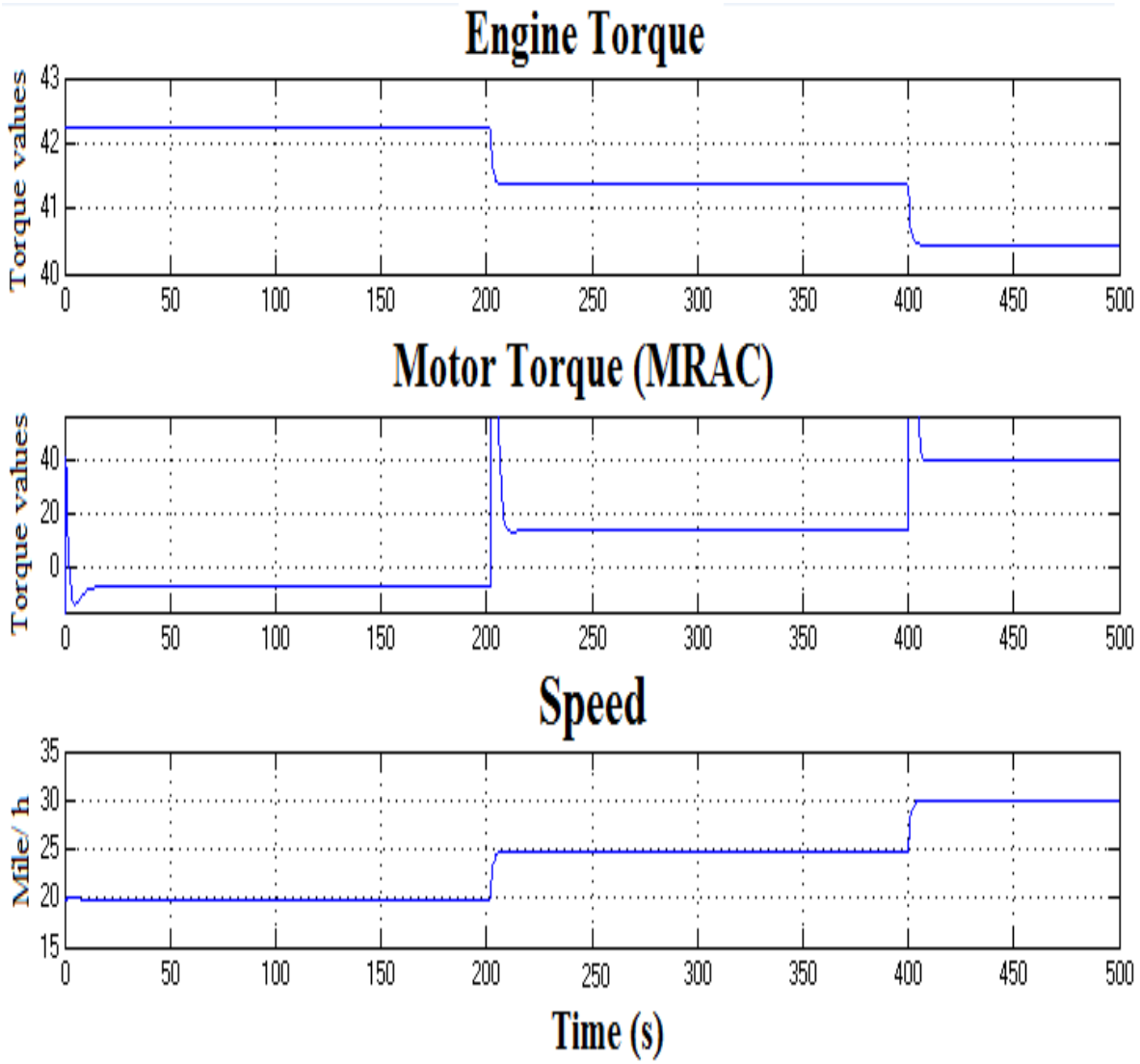

Figure 30: Speed is Variable

- **Case 3: Changing Gear:**

Shifting into a higher gear will result in an increase of engine power and can effectively reduce the required motor torque. In contrast, when the transmission shifts to a low gear, as seen at time 200 s in Figure 31, the MRAC will step up and supply more voltage to the motor to deliver higher torque in order to compensate for the power lost by the engine for smooth shifting and balancing.

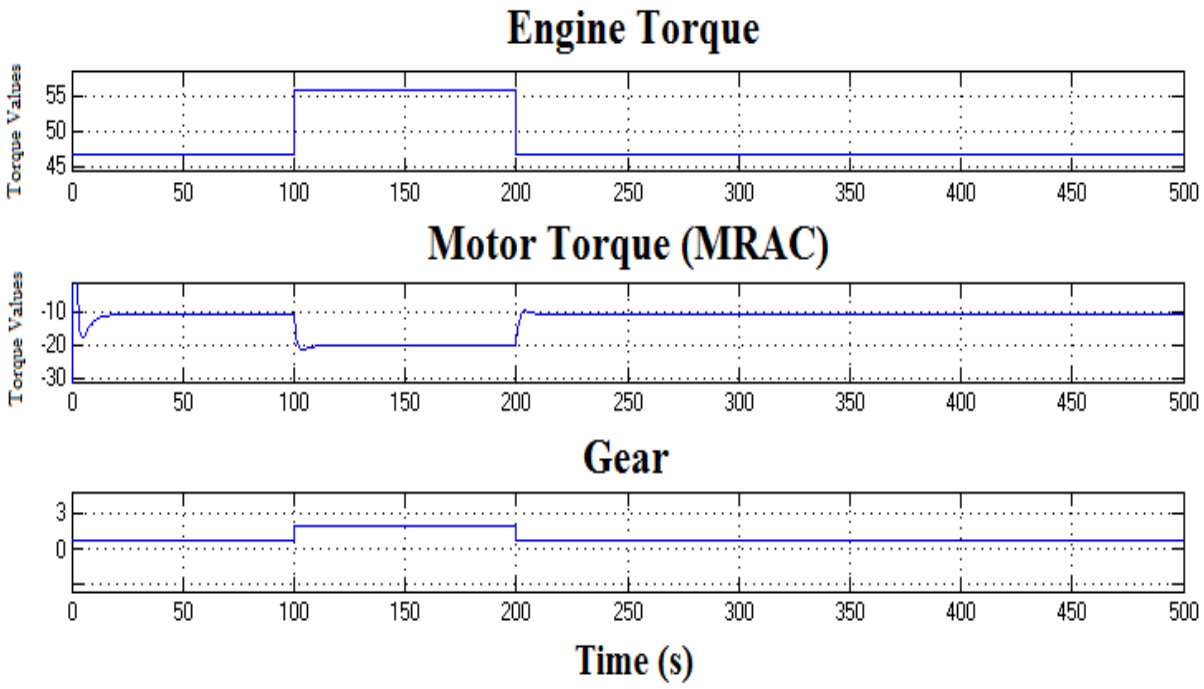

Figure 31: Changing Gears

- **Case 4: The Hybrid Dual Clutch Transmission**

The power loss during gear shifting is attributed only to clutch losses during its engagement. At this point, we will see power lost on the engine side. The MRAC-controlled motor will compensate for this power lost while changing gears or suddenly accelerating. During the driveline process, the speed will increase, so eventually more power is required by the HDCT design. The MRAC-controlled motor will produce more voltage to assist the engine in delivering the required torque to achieve the desired speed. As shown in Figure 32, the MRAC launches the

vehicle at time 20 s, after a few seconds the engine start assisting to bring the vehicle speed up to the proper value.

MRAC-comfortable is producing the torque slower than the sporty mode, for the sake of its smoother shifting. On the other hand, the MRAC-sporty mode reaches the desired value faster and produces more voltage than required. Shifting gears with the DCT will result in losing some engine power and can affect the motor torque. So the motor will deliver extra power to compensate for the power lost, as seen at times 29 s, 30 s and 40 s in Figure 32.

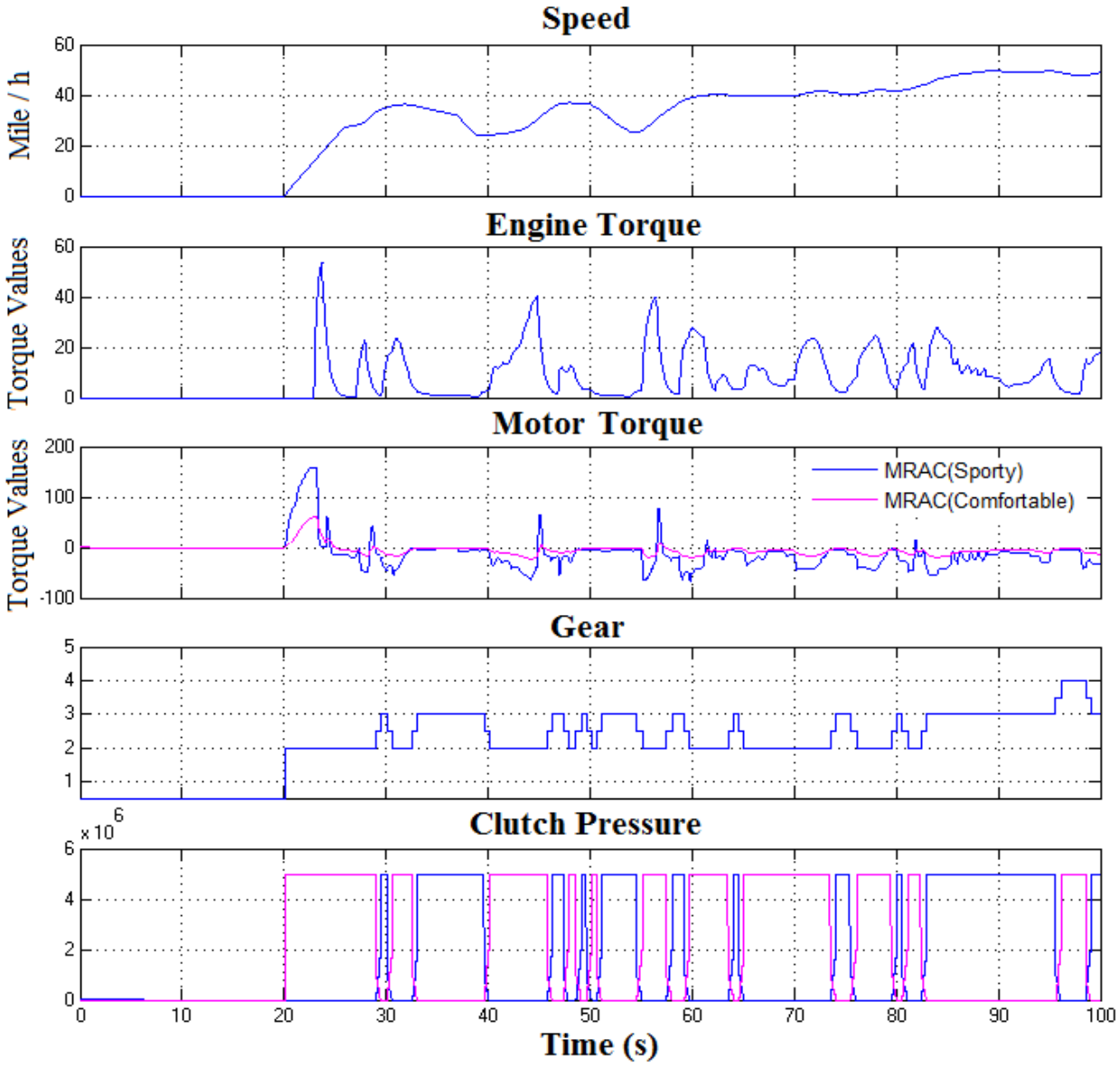

Figure 32: MRAC Controllers Response to Speed Changes

To look closely at the system when shifting gears, refer to the time from 28 s to 30 s in Figure 33, when the DCT is shifting from second to third gear. The engine is losing some torque when the DCT clutch pressure of the second gear is decreasing. However, when the third gear is engaged, the engine is gaining extra power and moving forward to drive the powertrain system. During this operation of gear shifting, the sporty mode controller is producing extra torque as a result of the fast response by the motor to compensate for the power lost by the engine: in this situation, the driver will feel the mode transition and more acceleration will result in vehicle jerk. On the other hand, the comfortable mode controller compensates with the correct amount that was lost, using a longer time, for the sake of smooth shifting and balancing.

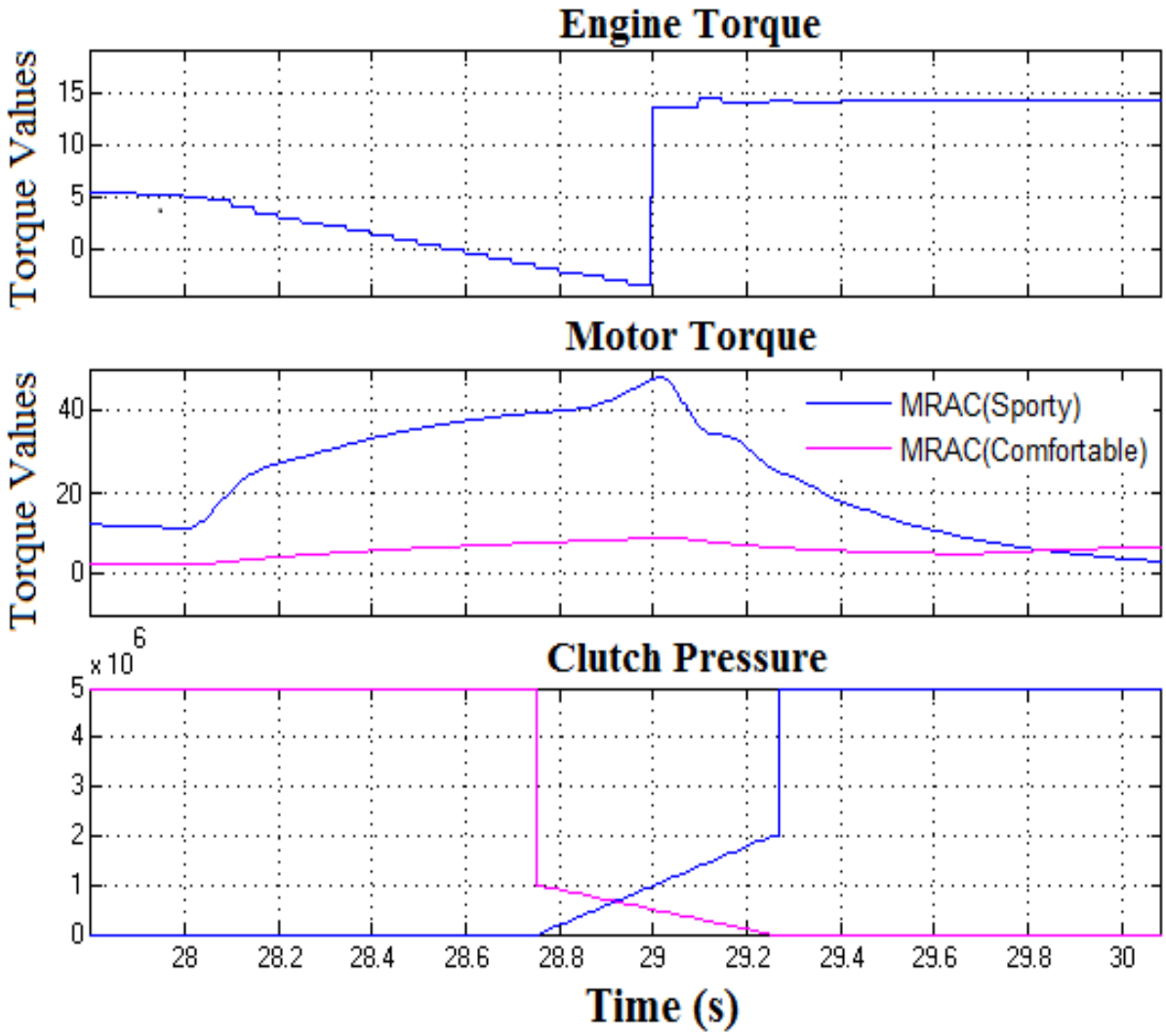

Figure 33: MRAC controllers During Gear Shifting

- **Case 5: Change the learning factor**

To further understand the design implications of the MRAC strategy, we considered the key factors that influence the mode transition performance, including three different values of the learning variable $\gamma_1, \gamma_2 \; and \; \gamma_3$ in Table II.

Table II: Gamma Value for the Control Law Signals

Parameters	Values
γ_1	$10e^{0}$
γ_2	$10e^{-1}$
γ_3	$10e^{-3}$

The selection of γ in the update rule will determine the behavior of the MRAC for motor torque response. One example of γ is given in Figure 34. The MRAC mode transition control yields good performance for the three different values. The results for different predefined values are not similar. Therefore, we conclude that the performance of the proposed MRAC is sensitive to different learning rate values.

The three different values of γ are used in simulation to assess the sensitivity of the performance to this design parameter.

- A larger value of γ (γ_1, γ_2or higher) leads to a torque disturbance; see the first stage (time 0-12 s) and the final stage (time 65–75 s) in the process of Figure 34.
- Choosing smaller γ is helpful for reducing the disturbance. Moreover, a small γ such as (γ_3) allows for shorter times for the MRAC to compensate for the torque losses. Consequently, a large γ in those cases causes an intensive vehicle jerk at mode transition.

Thus, a small γ is usually used in real applications to avoid this problem.

For this reason, most of the simulations presented in this paper use a small γ since the MRAC in this case prevents a disturbance or a sudden jerk, and provides shorter time responses.

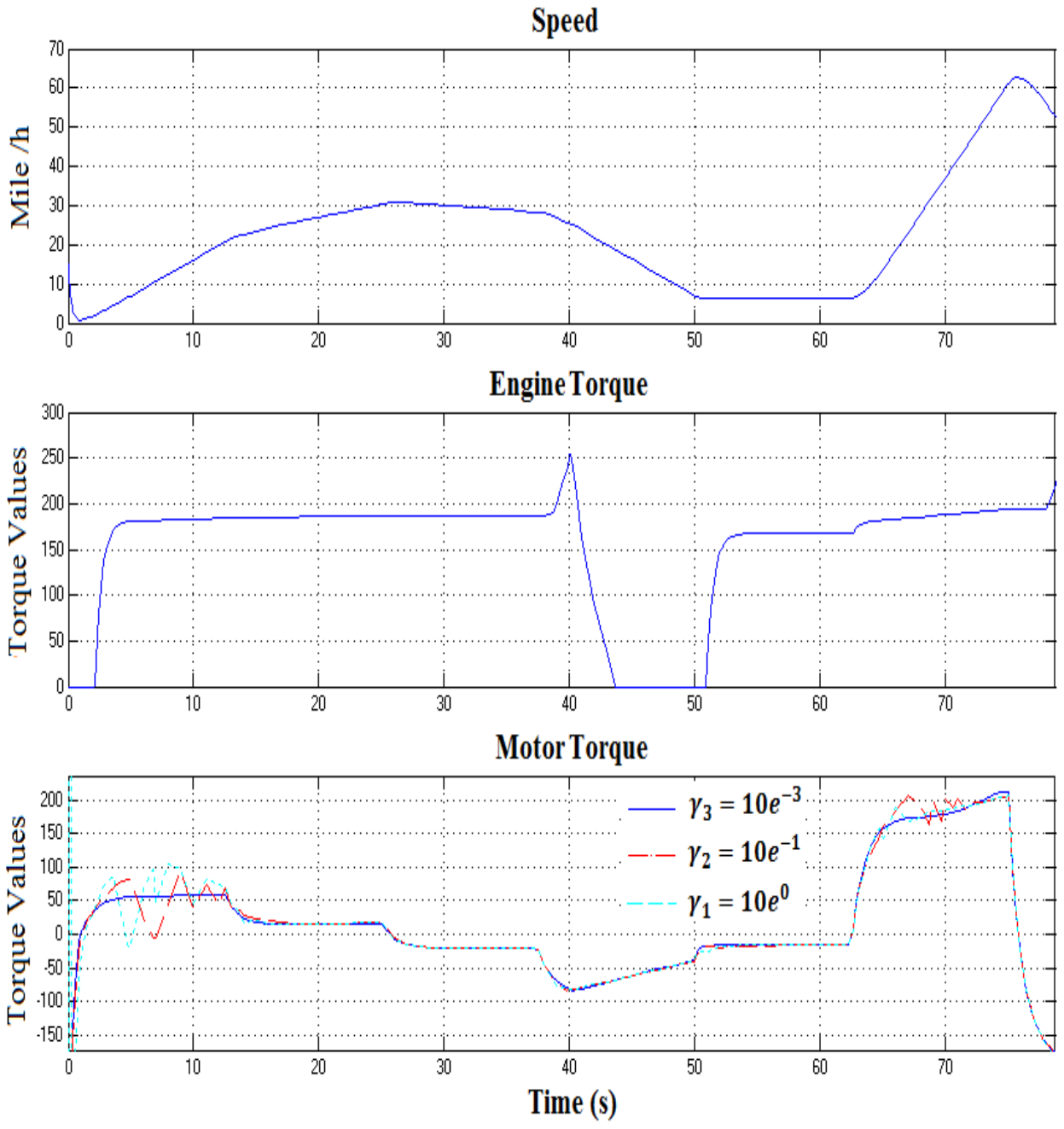

Figure 34: MRAC Responses to Different Learning Values

HDCT Operation Modes

Mode interactions are important elements of the control logic as they are the special conditions when the system goes from one mode directly to another mode. They are the factors that contribute to the response of the MRAC control system. The proposed system has five operating modes when the vehicle is in motion and one operating mode for standstill charging operation.

1. Motor Alone Mode

The vehicle is always launched in the motor only mode. The vehicle operates in this mode up to a maximum speed defined by the controller, provided that the SOC is greater than the minimum SOC for the battery (as per the system design). Since the engine does not operate in this mode, the dual clutches are disengaged to prevent any backlash to the engine.
This mode can be attained if all of the following conditions are satisfied:

$$(Spd > 0.01) \cap (Spd \leq Spd_{threshold}) \cap (SOC \geq SOC_{min}) \cap \left(T_{req} > 0\right) \cap (T_{req} \leq T_{maxmotor}) \quad (7.1)$$

Where,

- *SOC* is the battery state of charge.
- SOC_{min} is the minimum state of battery charge
- SOC_{max} is the maximum state of battery charge
- SOC_{eng_on} is the state of battery charge above which the engine power supply is turned off and the motor is turned on to avoid battery overcharge
- T_{req} is the required final drive torque of the vehicle
- $T_{maxmotor}$ is the maximum torque provided by the motor
- $T_{enginemax}$ is the maximum torque provided by the engine
- *Spd* is the required vehicle speed in the drive range
- $Spd_{threshold}$ is a specified low speed value below which the engine mode is turned off.
- $Spd_{highway}$ is the speed above which the vehicle enters highway driving condition
- *Acc:* vehicle acceleration

The motor torque and power are given by,

$$T_M = \frac{u}{i_M} T_O, \quad P_M = uP_O \tag{7.2}$$

Since the motor is the only power source in this mode: $P_O = P_M$

The power flow for the motor alone mode is shown in green in the Figure 35 below,

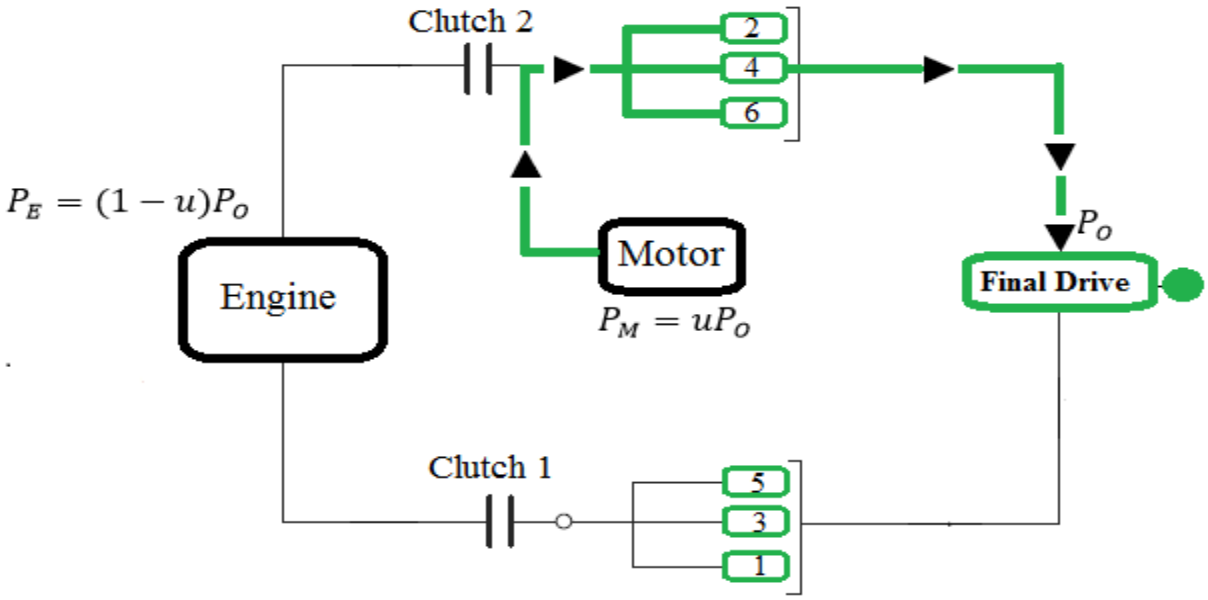

Figure 35: Power Flow for Motor Alone Mode

2. Combined Mode

This mode is selected when high torque is required for situations such as sudden acceleration or climbing a grade. This mode is also selected if the vehicle speed becomes greater than the maximum speed defined by the controller in the motor alone mode. Both the engine and the motor provide propulsive power to the drive shaft.

This mode can be attained if all the following conditions are satisfied:

$$(SOC \geq SOC_{min}) \cap (T_{req} \geq T_{maxmotor}) \cap (Spd > Spd_{threshold}) \tag{7.3}$$

The engine and motor torques and powers are given by,

$$T_i = \frac{(1-u)}{i_E} T_O, \;\; P_E = (1-u)P_O; \quad T_M = \frac{u}{i_M} T_O, \;\; P_M = uP_O \tag{7.4}$$

In this case, both sources are operating to satisfy the power requirements the vehicle: $P_O = P_M + P_E$
The power flow for the combined mode is shown in Figure 36 below,

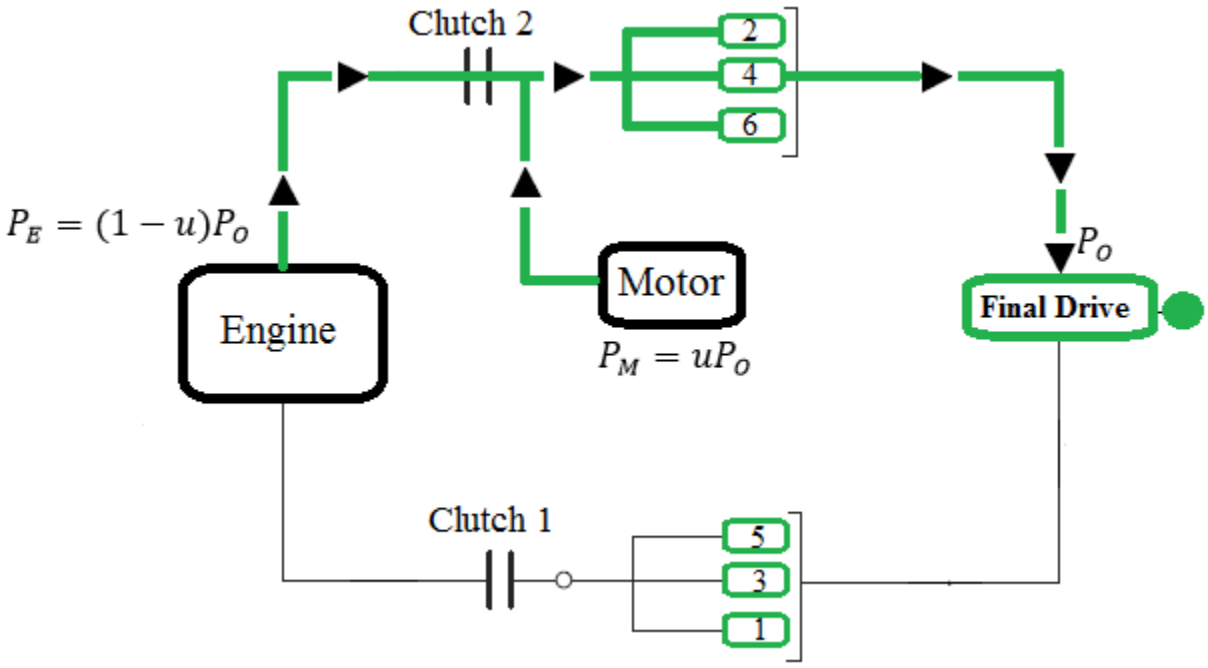

Figure 36: Power Flow for Combined Mode

3. Engine Alone Mode

This mode involves the engine as the only source of propulsion. The engine transmits power to the lowest possible gear ratio, such that the engine remains in the best efficiency window.
This mode can be attained if all the following conditions are satisfied:

$$\begin{gathered} \left(Spd > Spd_{highway}\right) \cap \left(Spd > Spd_{highway}\right) \cup \\ \left(SOC < SOC_{min}\right) \cap \left(T_{req} \geq T_{maxmotor}\right) \cup \\ \left(SOC > SOC_{max}\right) \cap \left(T_{req} < T_{maxmotor}\right) \end{gathered} \tag{7.5}$$

The engine torque and power are given by,

$$T_i = \frac{(1-u)}{i_E} T_O, \quad P_E = (1-u)P_O \tag{7.6}$$

Since the engine is the only power source in this mode: $P_O = P_E$

The power flow for the engine mode is shown in Figure 37 below,

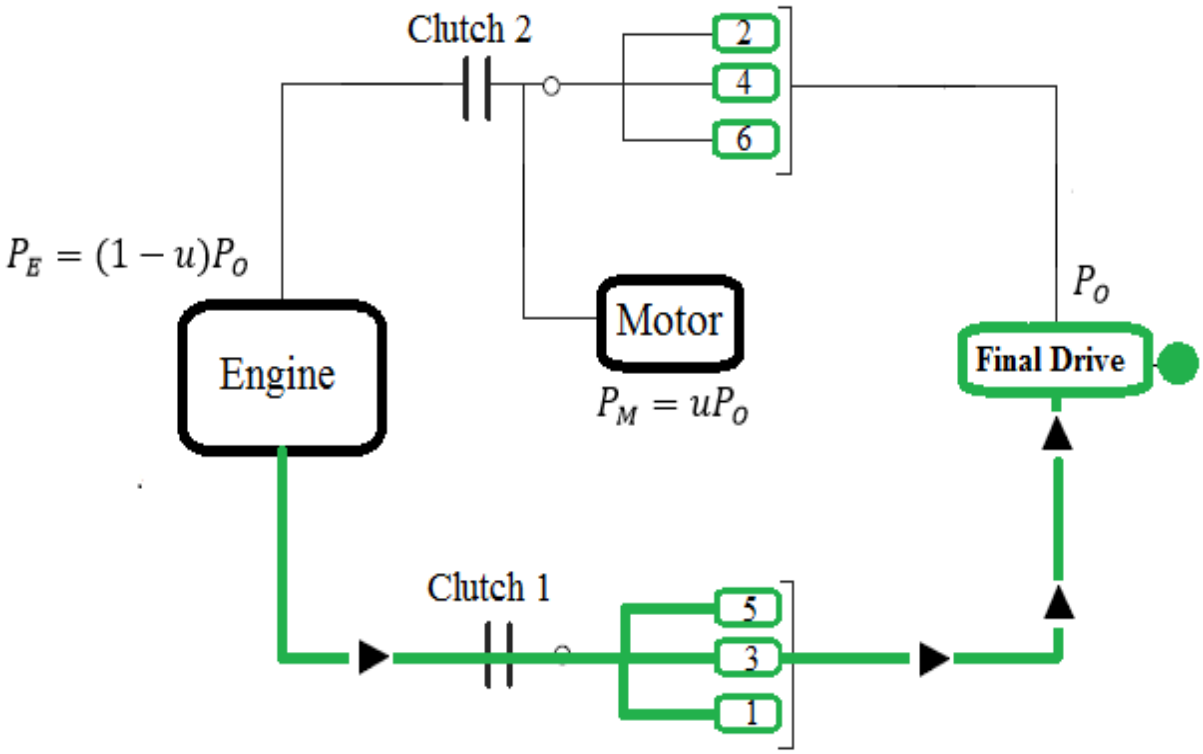

Figure 37: Power Flow for Engine Alone Mode

4. Regenerative Braking Mode

The motor is coupled to the output shaft through gears where it can function as a generator as well. This is used to recover the energy that is consumed in braking to charge the battery. In case the motor torque is not sufficient to break the vehicle, the hydraulic braking system is used as well.

This mode can be attained if the following condition is satisfied:

$$(T_{req} < -0.1) \cap (Acc < -0.01) \tag{7.7}$$

The power is reversed in this mode; the motors work like generator and start producing electricity instead of consuming: $P_O = -P_M$

The power flow for the regenerative braking mode is shown in Figure 38 below,

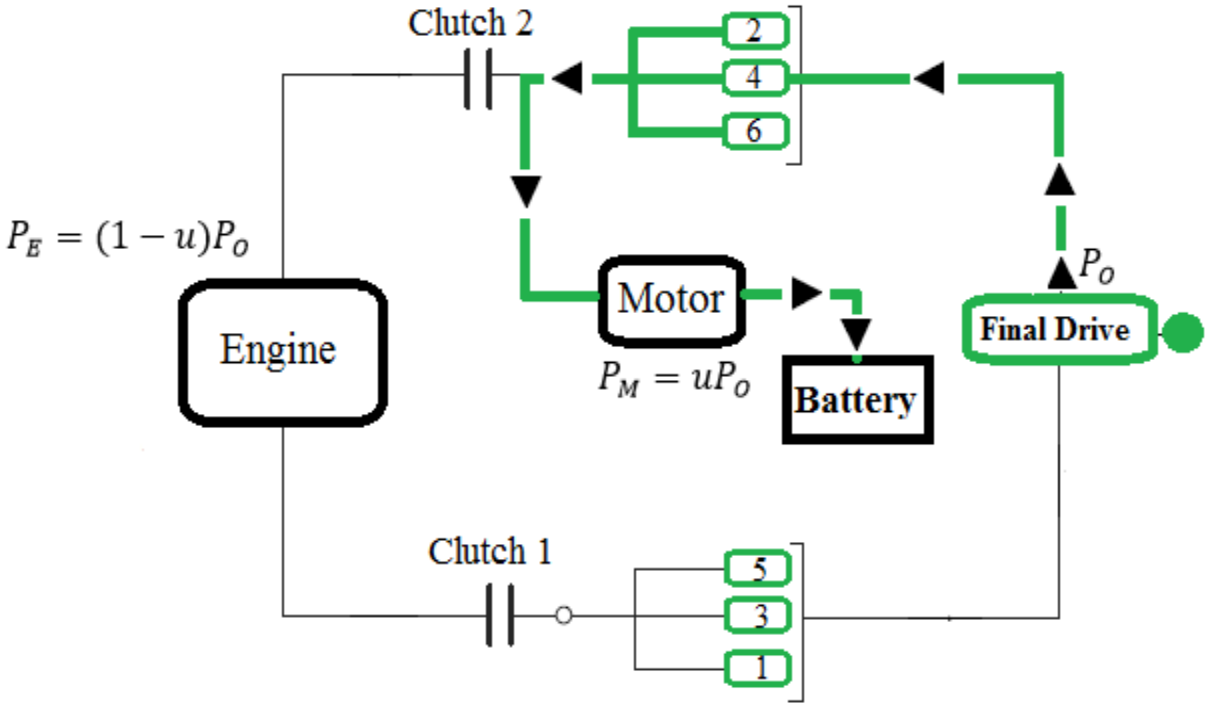

Figure 38: Power Flow for Regenerative Braking Mode

5. Brake Mode

This is a special operating condition when the battery SOC is more than the maximum SOC limit and a braking operation is required. The controller operates only the conventional brakes in this mode. No power is regenerated from the drive shaft.

6. Propelling Charging Mode

This mode is used to charge the battery when the vehicle is in motion. The controller selects this mode if the engine can supply the amount of power required to drive the vehicle. The excess power is then used to charge the battery. The motor on the same lay shaft that drives the output shaft is selected to act as generator to charge the battery.

This mode can be attained if all the following conditions are satisfied:

$$(Spd > 0.01) \cap (SOC \leq SOC_{min}) \cup (T_{req} > 0) \cap (Spd > 0.01) \cap (T_{req} < T_{maxmotor}) \quad (7.8)$$

The power in this mode can be written as: $P_O = P_E - P_M$

The power flow for the propelling charging mode is shown in Figure below,

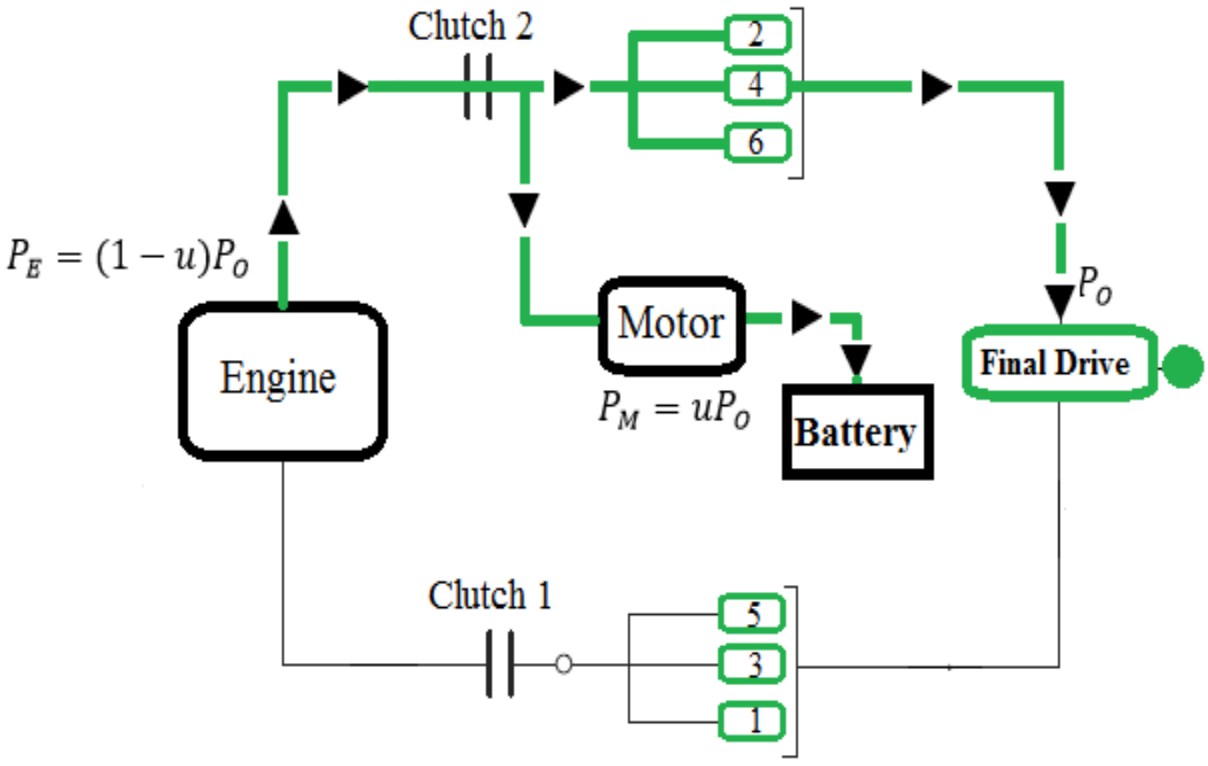

Figure 39: Power Flow for Propelling Charge Mode

Interaction between Various Modes

Selection of a mode is dependent on various parameters, such as SOC of the battery pack, current vehicle speed, torque required by the vehicle, minimum value of SOC of the battery pack, maximum permissible motor torque, maximum vehicle speed in motor only mode, etc. The parameters are checked for determining the correct operating mode of the vehicle. If the parameter condition is satisfied then the next parameter is checked until a particular mode is decided.

The controller intelligently selects the charge, engine and regenerative modes. The flowchart of how a decision is made for the mode selection is shown in Figures 40, 41 and 42.

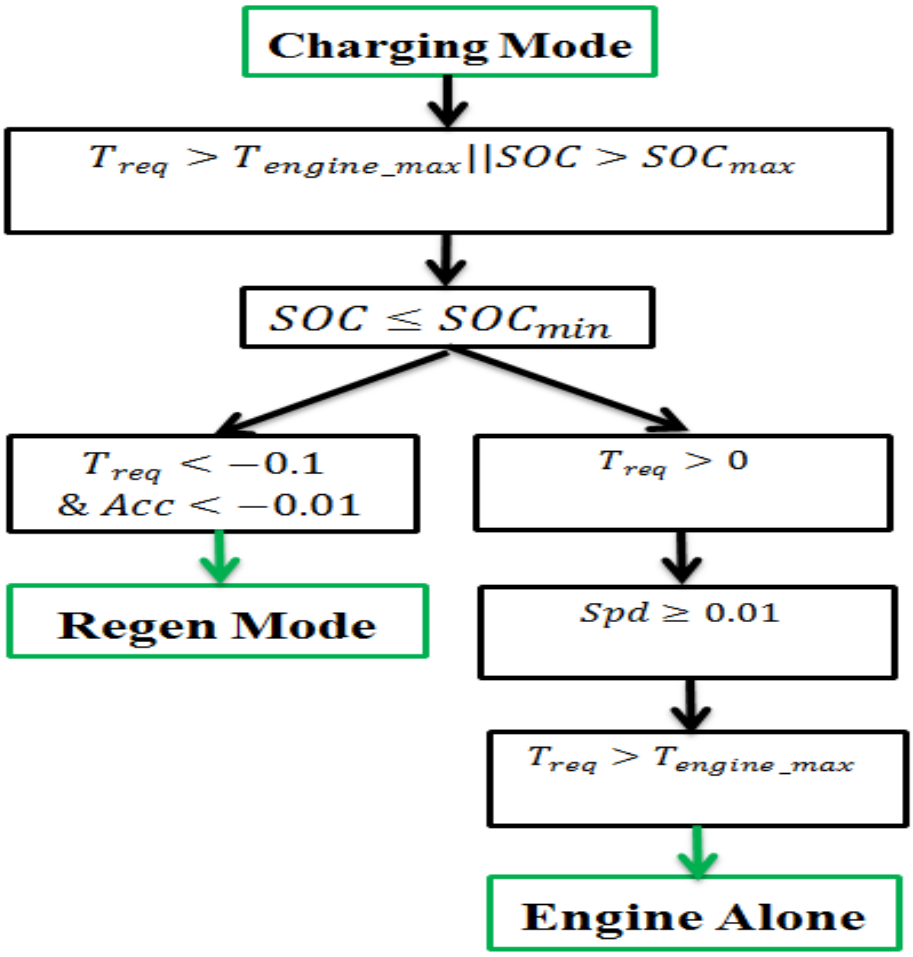

Figure 40: Interaction Between various Modes

For the example below, if the vehicle is in regenerative mode and if it still decelerates, but the SOC is already charged to the maximum, then the controller changes the mode to mechanical brake mode. Similarly, if the vehicle's required speed increases above the speed threshold of the motor, the mode changes from motor alone mode to combined mode. In this mode, the vehicle is driven by both the motor and the engine.

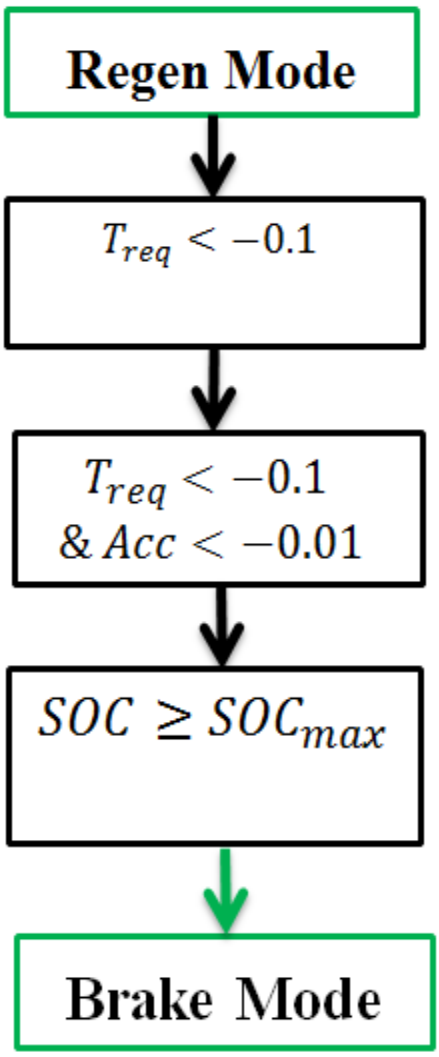

Figure 41: Interaction Regen and Brake Mode

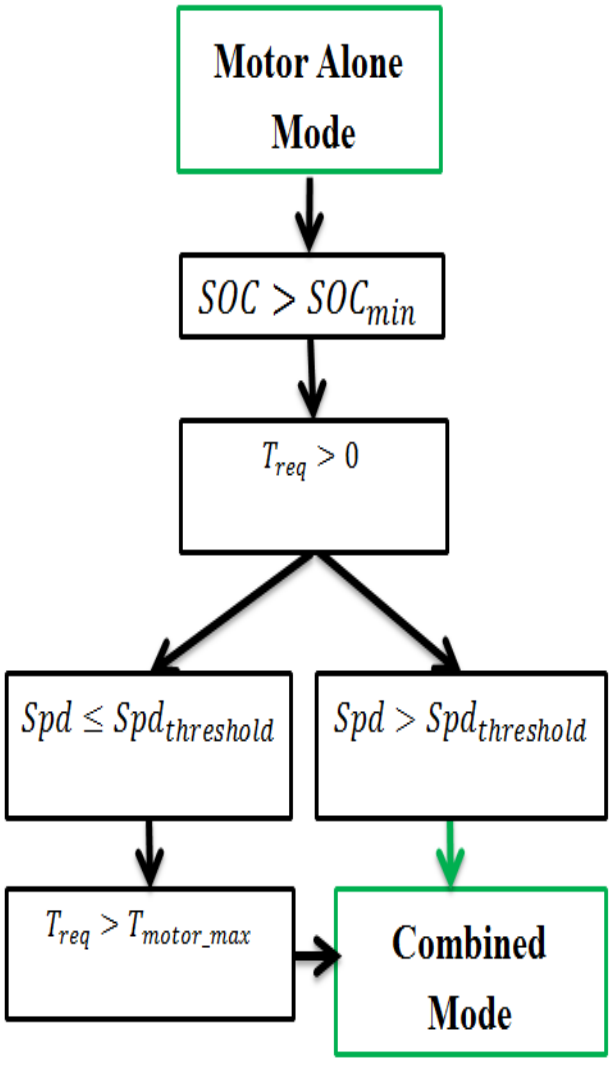

Figure 42: Interaction between Motor alone and Combined Mode

MRAC Mode Selections

The MRAC will step up and supply more voltage to the motor during mode changes to deliver higher torque in order to cover the power lost by the engine for smooth shifting and balancing.

- Figure 43 shows the graphs for various variables in the HDCT model. The graphs provide a correlation between the vehicle speed, controller mode, and vehicle torque. It can clearly be seen that since the torque demand of the startup of the drive cycle can be met by just the motor, the controller always selects the motor-only mode (1). The engine cranks in after the twenty eight seconds (28 s) when the controller mode changes from motor-alone mode (1) to combined mode (2) since the motor cannot provide the required torque and the MRAC compensates for the power lost in the system within that transition.

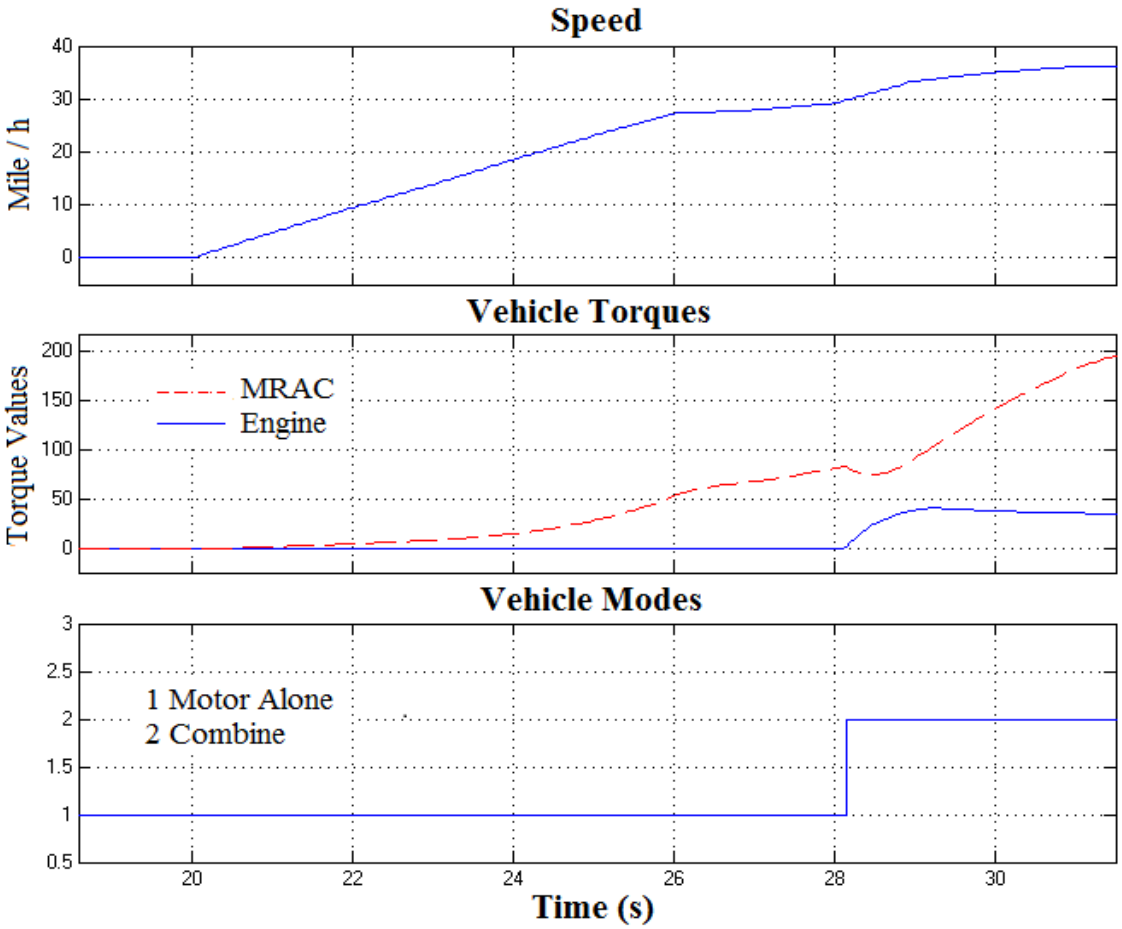

Figure 43: Changes from Motor-alone Mode to Combined Mode

- Similarly for Figure 44: the MRAC selects the motor-only mode (1) to drive the vehicle after a complete stop (time 27-30 s). The MRAC also switches from combined mode (2) to motor alone mode (1) when we have speed deceleration (time 22 s);

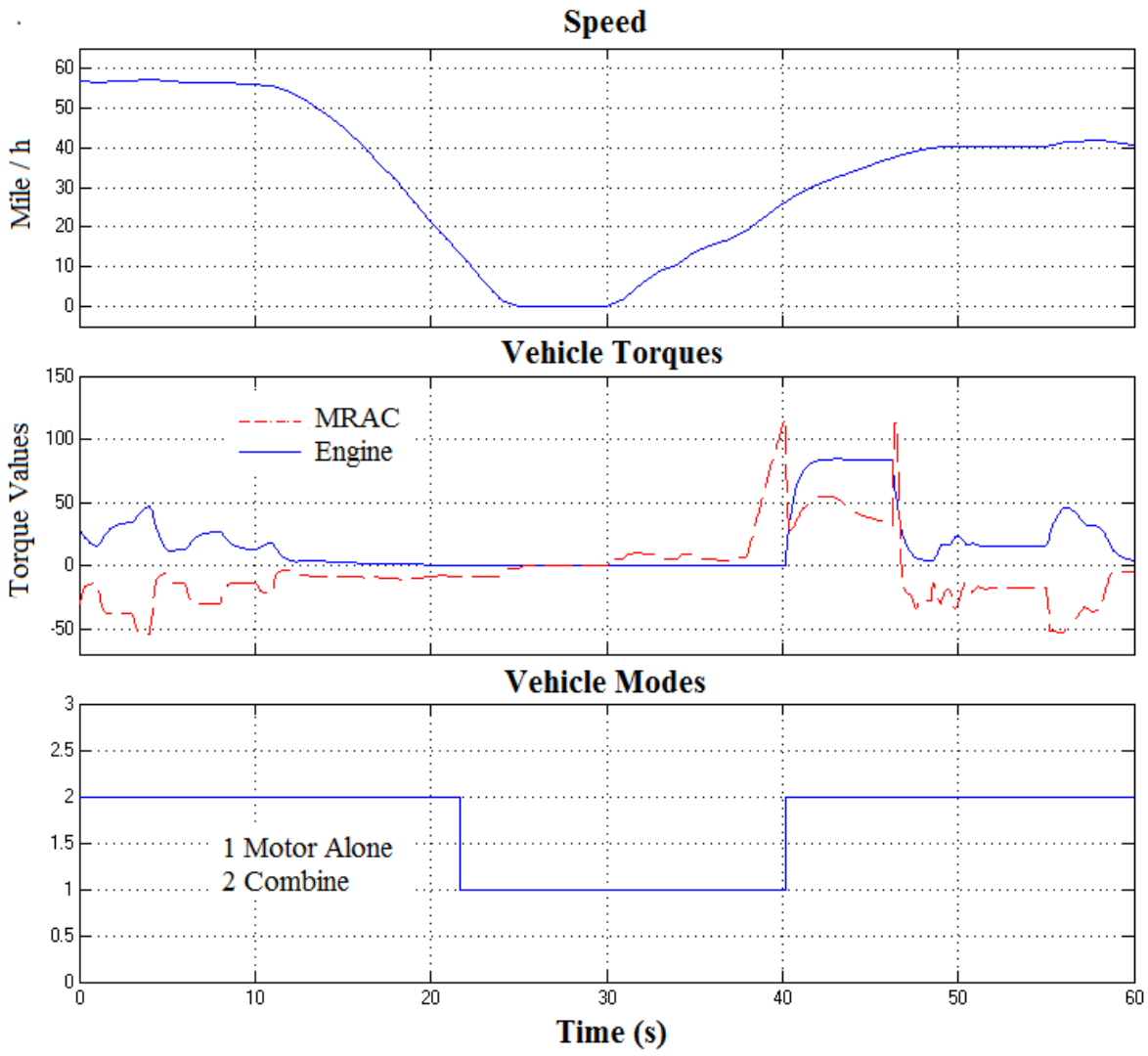

Figure 44: Changes from Combined Mode to Motor-alone Mode

- In other hand, when the driver is accelerating with a speed exceeding 50 mile/ h (HW driving cycle), the controller changes from motor-alone mode (1) to engine only mode (3) since the motor cannot provide the required torque as the battery SOC is low, as shown in Figure 45.

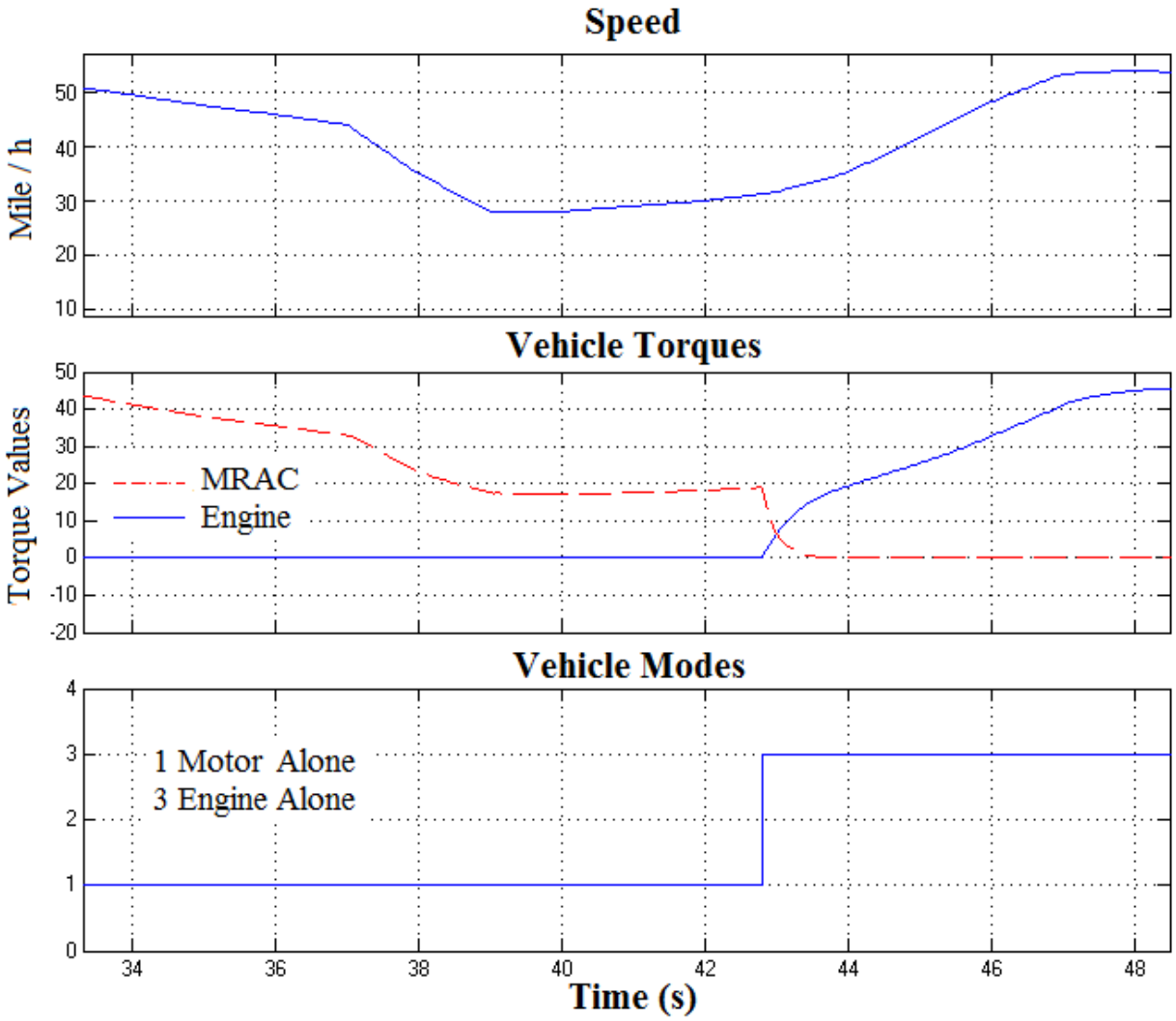

Figure 45: Changes from Motor-alone Mode to Engine Mode

- When the vehicle enters HWY driving condition, the engine alone drives the wheels; and in the case of deceleration, the controller selects mode 5 (regenerative mode) as can be seen from Figure 46. In general, most cars use friction brakes, which convert kinetic energy to heat. Regenerative braking allows some of the kinetic energy to be captured, turned into electricity, and stored in the batteries. This stored electricity can later be used to run the motor and accelerate the vehicle. It also exemplifies the control strategy that prevents the SOC from going below the minimum limit (0.4 in this test case).

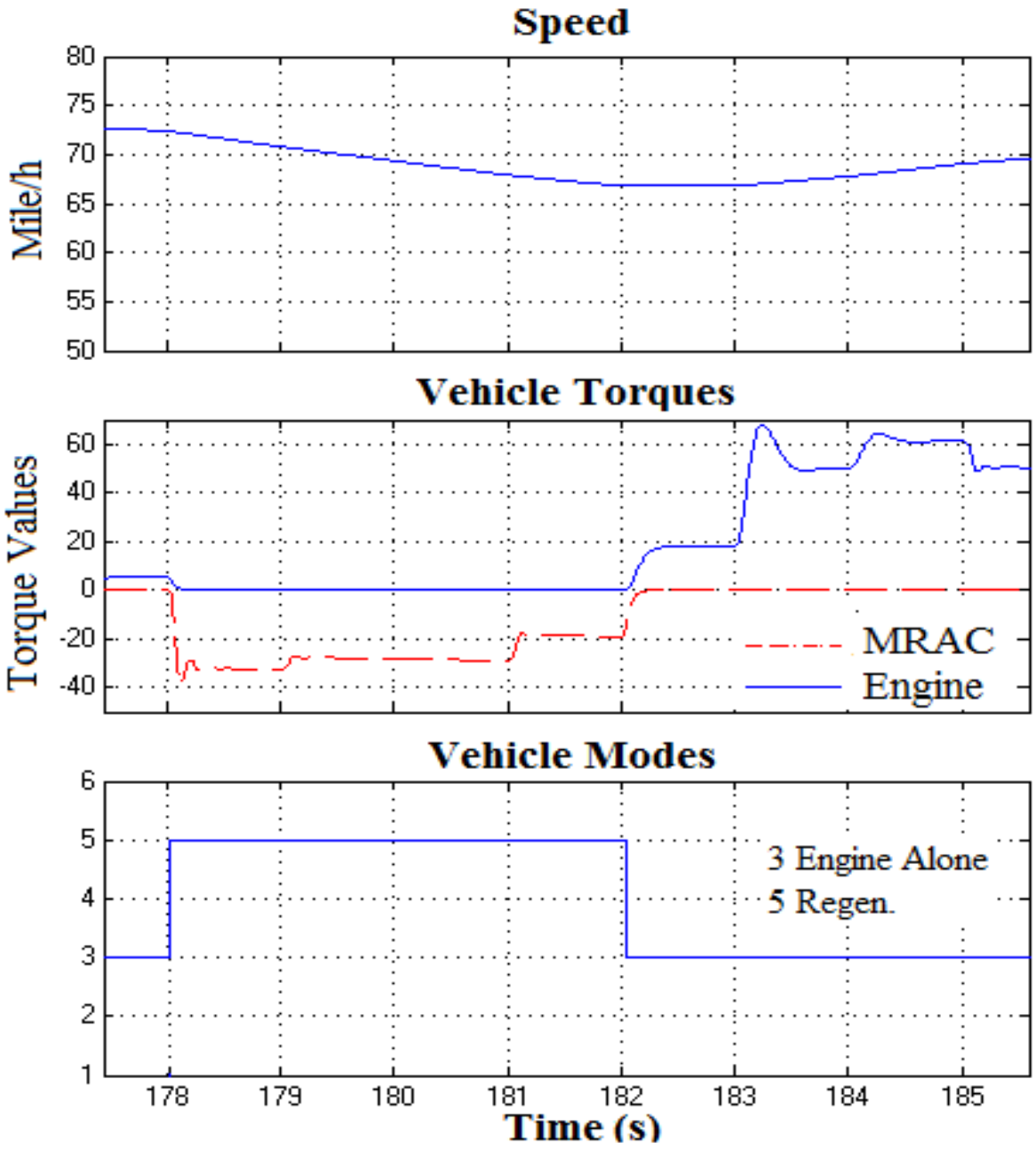

Figure 46: Changes from Engine Alone Mode to Regen.

- Another example for HWY drive cycle with the SOC being higher than the lower limit set by the design (0.4), the controller switches from regenerative mode (5) to brake mode in the event of continued vehicle deceleration and when the driver hits the brake pedal (time 292 s to 296 s), then it selects the engine alone mode (3) since the vehicle speeds up to the HWY driving speed (Figure 47).

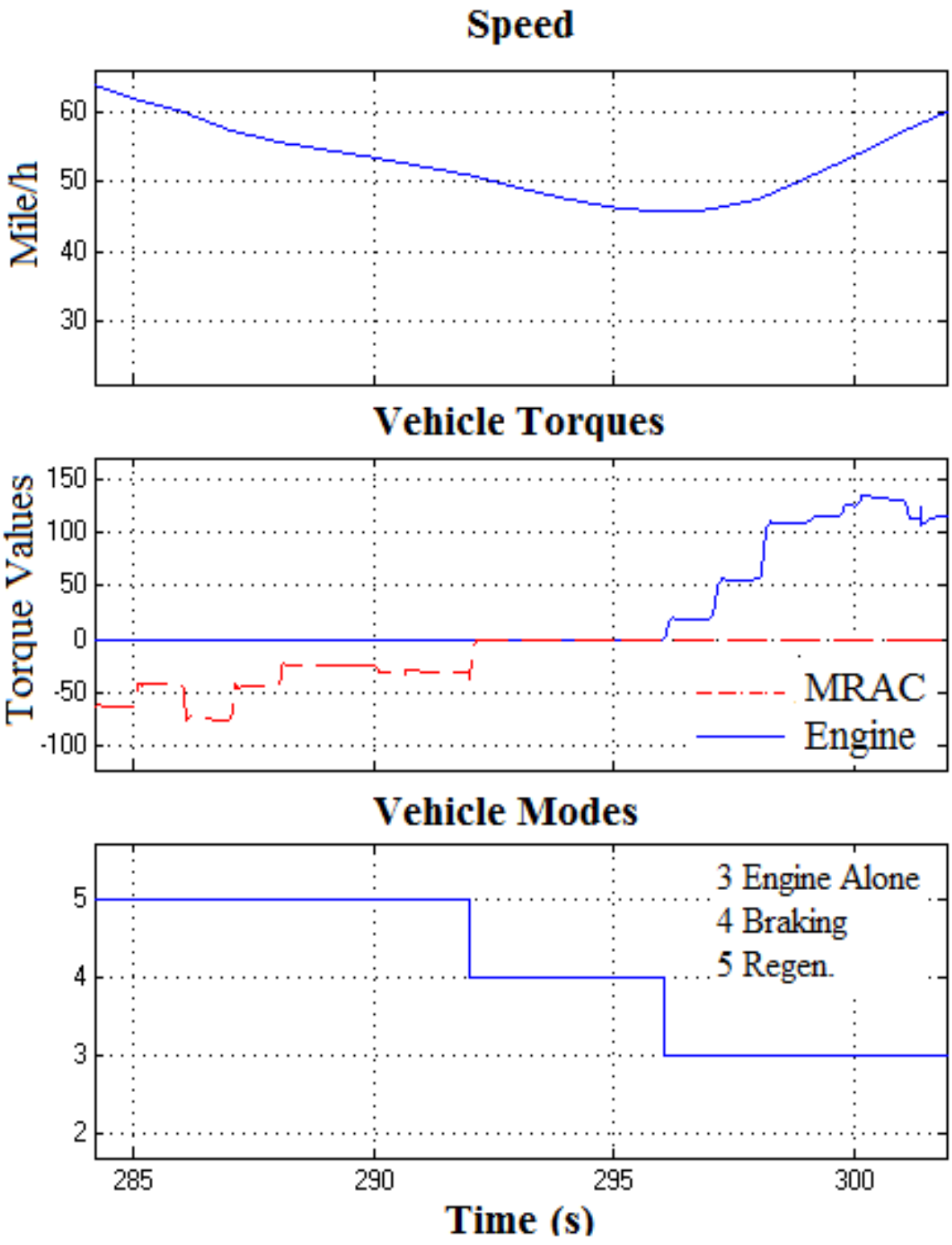

Figure 47: Changes from Braking to Engine Mode

Comparison with the Conventional Method

Desired Vehicle Input Changes

We consider the scenario of a typical drive-line process (the desired vehicle speed is changing) and compare the performance of the MRAC controller with the results of conventional operation (abbreviated by Conv.). The MRAC motor has provided more torque to start and drive the vehicle and has a fast torque response when the speed is changing to maintain balance, whereas that of Conv. falls by 70 points at the startup and does not respond quickly for all speed variations at time 30 s and 40 s, as shown in Figure 48.

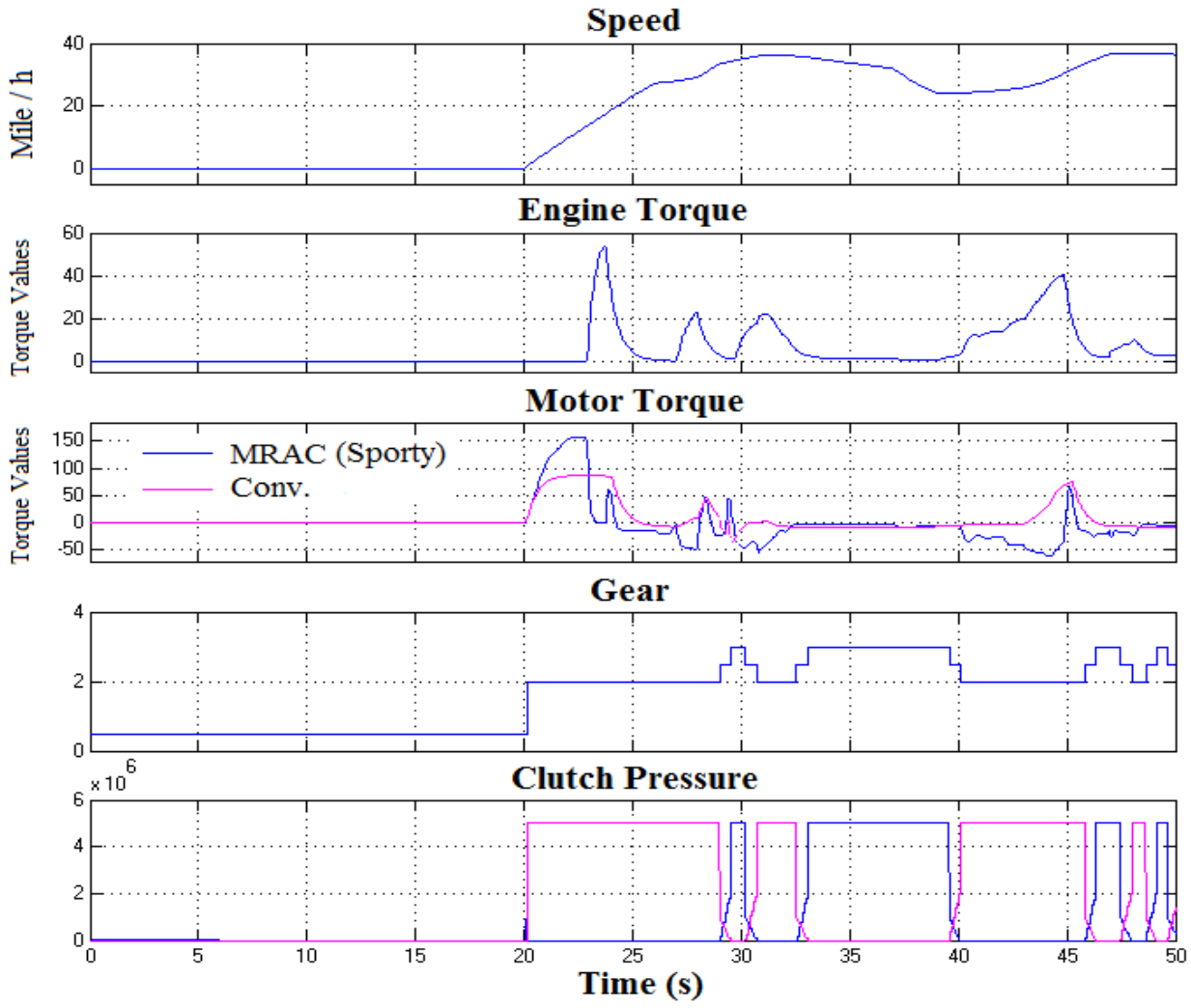

Figure 48: MRAC vs Conv. During Speed Changes

The MRAC motor has boosted more torque to compensate for torque deficits by the engine when the gear is changing to maintain balance, whereas that of Conv. falls by 45 points at the end of the third gear at time 29 s, as shown in Figure 49.

For conventional, the profile of the vehicle speed is similar, which implies that the clutch torque negatively affects the vehicle acceleration and causes the engine torque to decline. Moreover, the motor torque in the MRAC does not compensate for this negative effect.

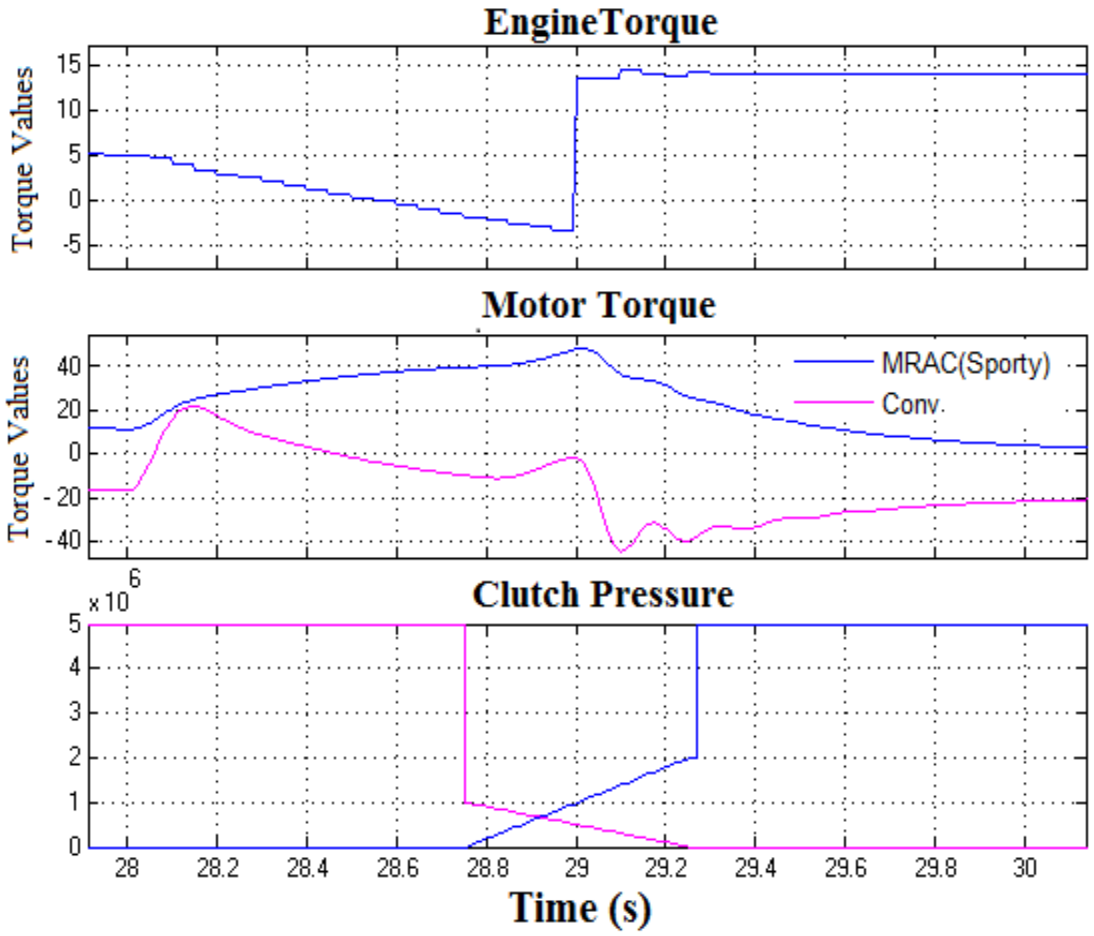

Figure 49: MRAC vs Conv. During Gear Shifting

Thus, the vehicle speed has to fall. However, the MRAC avoids this situation by increasing the traction motor torque to compensate for the negative effect. No substantial vehicle jerk occurs in the MRAC control simulation, even with a sudden change of the engine throttle. The MRAC scheme prevents the motor response from a large overshoot in the comfortable mode; it slowly compensates for the lost torque, and does this more quickly in the sporty mode. However, a

sudden vehicle jerk is found in the results from the conventional controller at time 40 s and 50 s, as shown in Figure 50. The reason for the sudden jerk is that Conv. cannot react quickly enough to the changes: the Conv.-controlled motor is clearly slower than the MRAC-controlled system. Finally, the performance of the Conv. controller quickly deteriorates, whereas the performance of the MRAC controller remains good and delivers smother response. Obviously, the MRAC controller can considerably improve the behavior of the motor in terms of this criterion.

It can be concluded that the HDCT design is more efficient than the conventional design in all conditions. Although the HDCT design improves the efficiency of the motor in compensating for all power lost in the system, it deteriorates the overall efficiency of the powertrain itself.

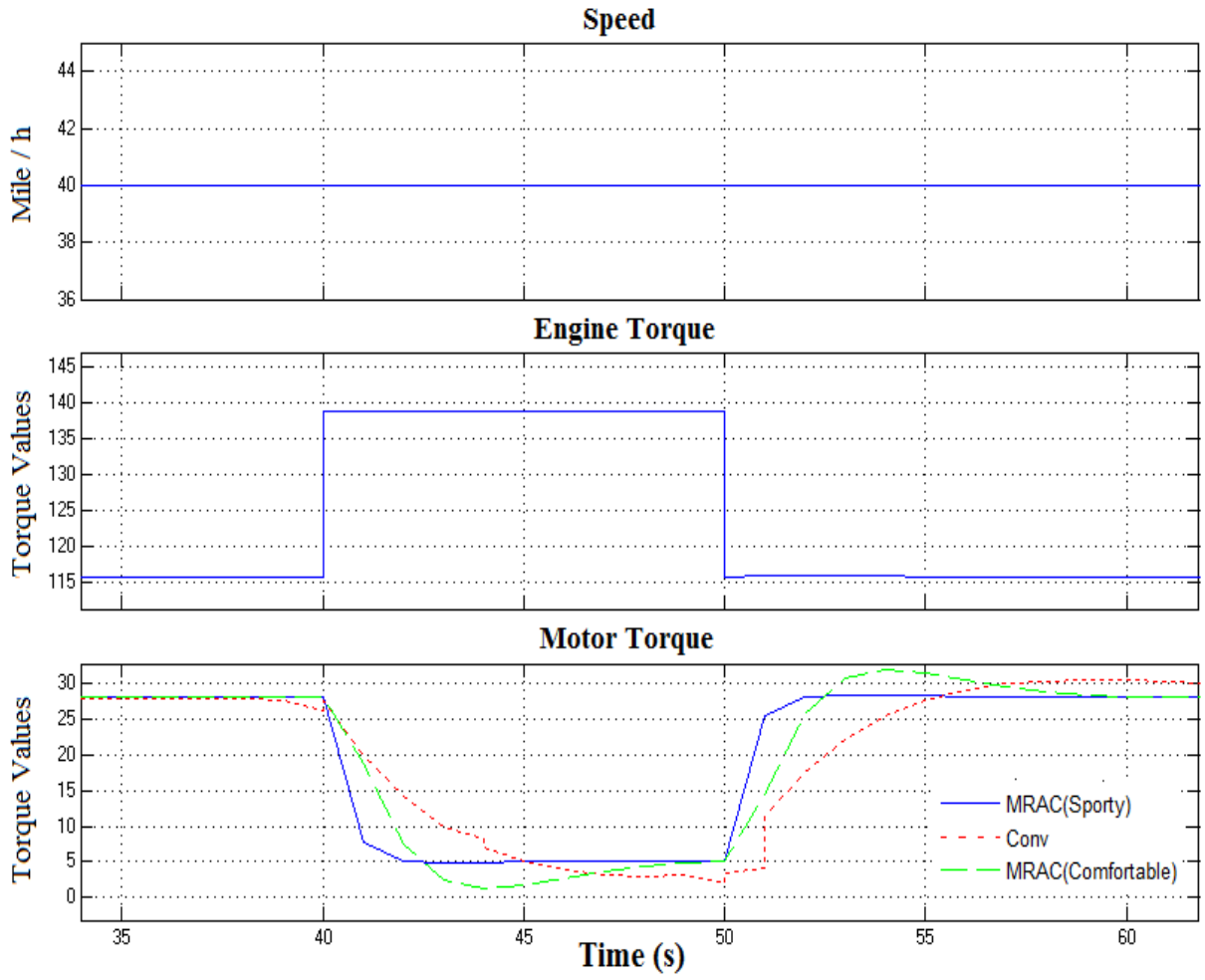

Figure 50: MRAC vs Conv. During Throttle Changes

Mode Transition Changes

The response of the MRAC is faster than that of the Conv., as shown in Figure 51. The MRAC controller is actuated earlier and with much higher intensity, so it quickly reacts to the startup and the MRAC controller will supply more voltage to the motor to run the vehicle. The mode transition begins at the 17th s when the mode changes from motor-alone (1) to combined mode (2). The MRAC motor has delivered less torque to the HDCT due to the extra power provided by the engine. However, the Conv. falls down before start responds slowly and stays in the low torque value.

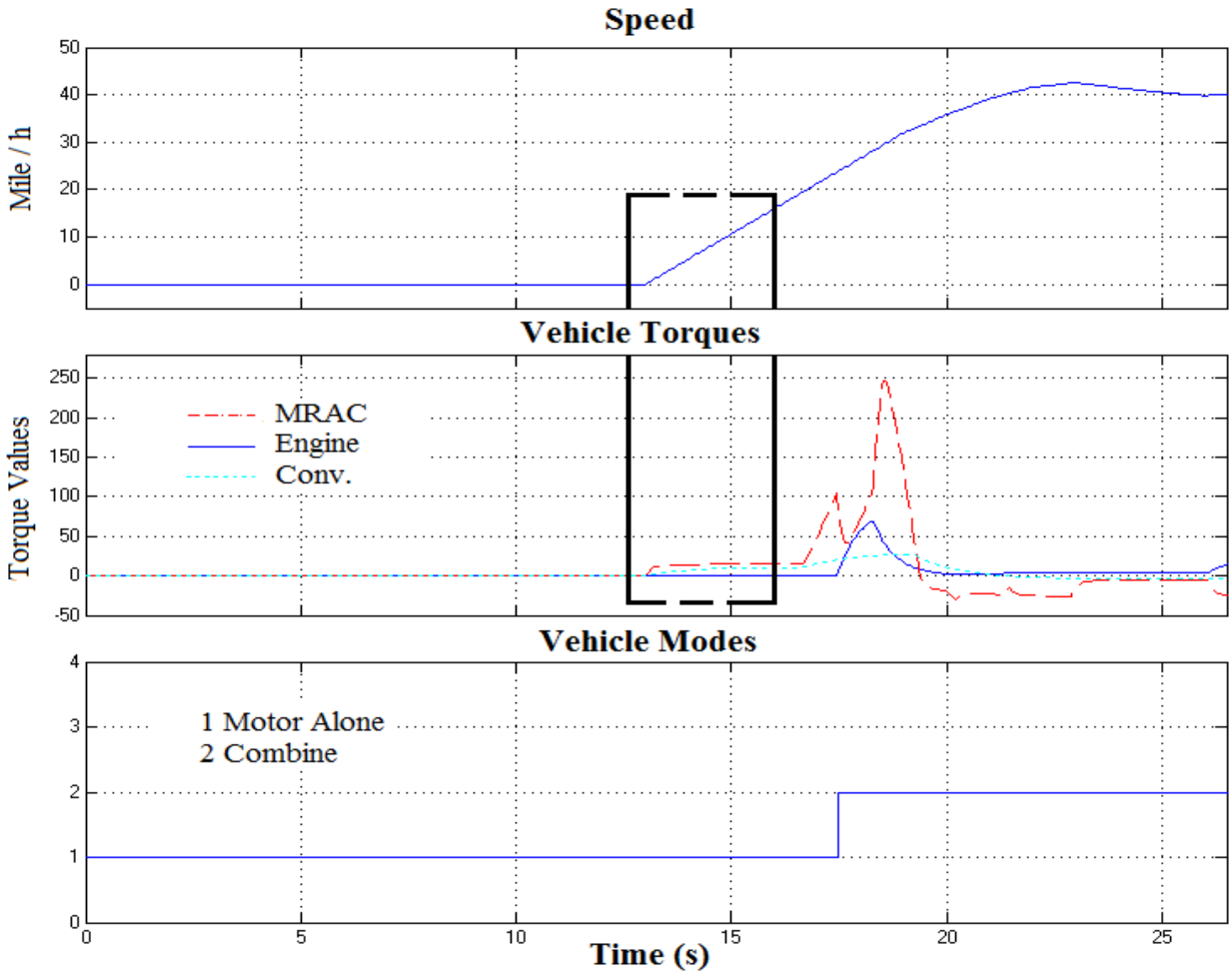

Figure 51: Conv. and MRAC Response during Startup

And as shown between times 18-20 s in Figure 51, the MRAC controller responds quickly to the transition and boosts more torque to compensate for torque deficits by the HDCT when the speed is changing as a result of the fast response by the motor to maintain balance. The vehicle acceleration of the MRAC is maintained in good balance around time 20 s, whereas that of the Conv. falls by 200 points at the end of the transition phase. For the Conv., the profile of the vehicle acceleration is similar to that of the MRAC, which implies that the both controllers respond correctly to the transitions. Moreover, the motor torque compensates for any torque changes in the system. However, the MRAC responds quickly.

Another mode transition example is shown in Figure 52; at low torque, (launch and Gentle acceleration) the HEV will operate in Electric vehicle mode “motor- alone (1)”, the motor drives the wheels. At higher requested torque (time 26 s) the engine will operate and the MRAC will switch to combined mode (2), ICE and motor are driving the wheels, this mode achieves higher fuel efficiency and low emission.

After the battery has reached its minimum (SOC) threshold, exhausting the vehicle's all electric power (time 29 s) the MRAC switches to engine-alone (3). Switching to this mode also after the HDCT enters HWY driving cycle, the engine will drive the vehicle by itself without the motor assistance, instantaneously, the MRAC controller responds to the transition and stops producing torques, while the Conv.-controller cannot react quickly enough to the changes and may produce negative torque. Finally, the performance of the Conv. controller quickly declines, whereas the performance of the MRAC controller remains good and stable, it provides smooth response and steadiness to the HDCT power train. It can be concluded that the MRAC design is more efficient than the conventional design in all conditions. Although the HDCT design improves the

efficiency of the motor in compensating for all power lost in the system, it deteriorates the overall efficiency of the powertrain itself. This is mainly because of the inherent losses in the engine's architectural design during gear changes, because no motor loss is encountered when the power demand at the wheel is met by an ICE alone via the mechanical path.

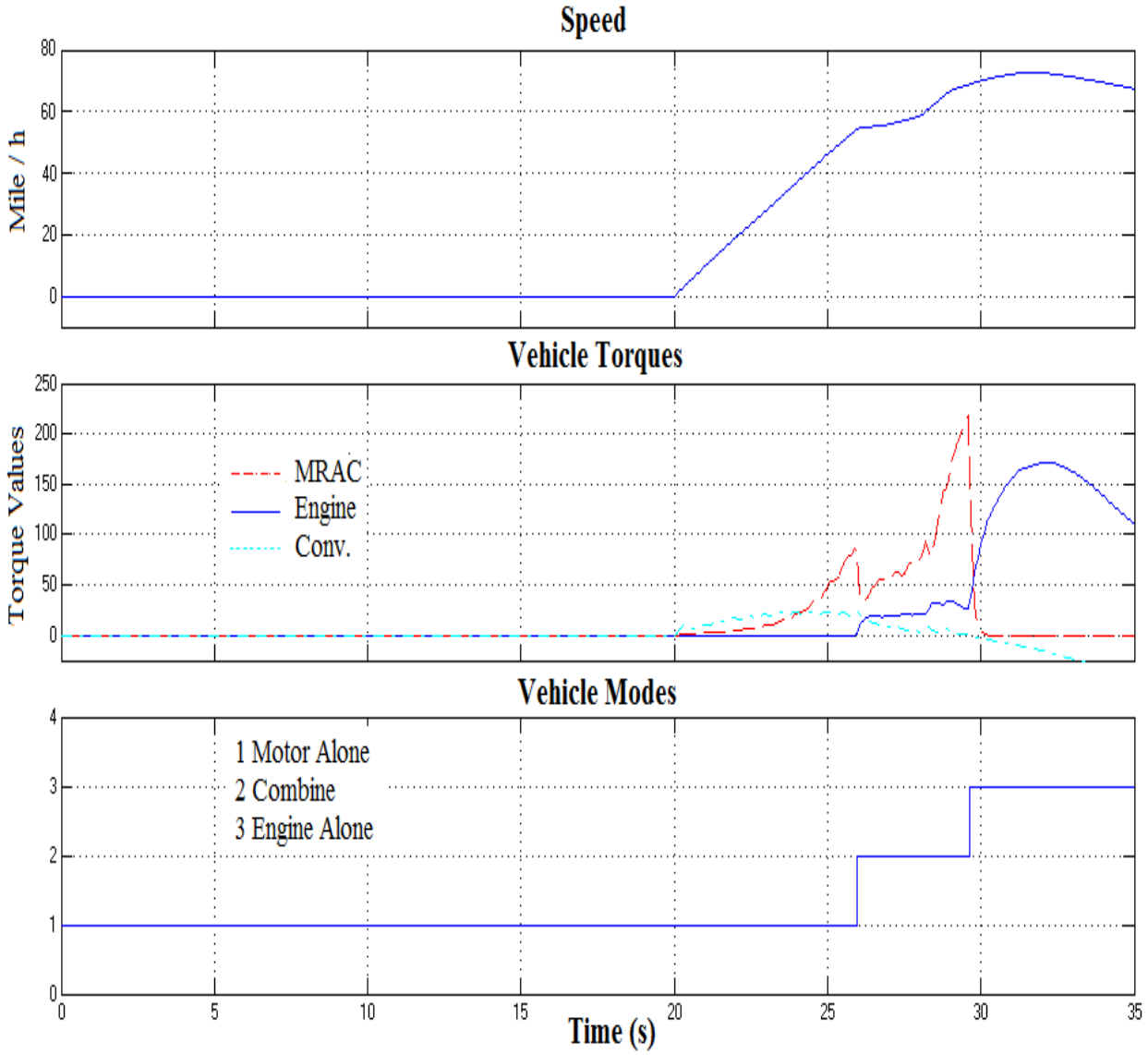

Figure 52: Conv. vs MRAC Responses during Mode Changes

CHAPTER VIII: Conclusions

A model reference adaptive control (MRAC) has been designed for the stability of a closed loop system using Lyapunov method. The MRAC takes the driving vehicle as the reference model, and the controller acts on the output errors between the reference model and the vehicle as the feedback signals to achieve smooth and efficient performance.

The proposed MRAC is applied to a hybrid electric vehicle with dual clutch transmission (HDCT), and has yielded good performance under different conditions, which implies that the MRAC is adaptive to different torque distribution strategies.

The current study, which was performed on the adaptive control applications, reveals that the Lyapunov method is working properly. The simulation results confirm that the MRAC outperforms the conventional operation method for an HDCT by reducing the vehicle jerk and the torque interruption for the driveline.

Several factors that can influence the performance of the MRAC mode transition were studied through simulations. The proposed MRAC yielded good performance for different values of the model learning parameter for the update rule, which implies that the MRAC is adaptive to different torque distribution strategies. The MRAC method is applied to the mode transition of an HDCT bus. The simulation results confirm that the MRAC outperforms the conventional operation method for an HDCT by reducing the vehicle jerk and the torque interruption for the driveline. Therefore, this thesis work shows that the MRAC is very promising for the control and HDCT vehicle. These promising results, particularly the model validation, have motivated us to further pursue the idea of MRAC and seek its robust and effective implementation to other mode transition control problems on other hybrid vehicle platforms.

APPENDICES

APPENDIX A

A. Model Integration and Simulation in Matlab

Using the kinematic equations of each of the component models, the integrated model for the system along with the controllers and the vehicle is developed.

The model is then subjected to various drive cycles and various parametric conditions such as low SOC at start, SOC greater than the maximum charging limit of the battery, desired speed and driver mode selection etc., to test for the model in various real life conditions.

The model integration involves signal conditioning for integrating the various subsystem models

Operation Modes: Simulink model

Figure 53 shown below is the block diagram of the operation modes design for HDCT system

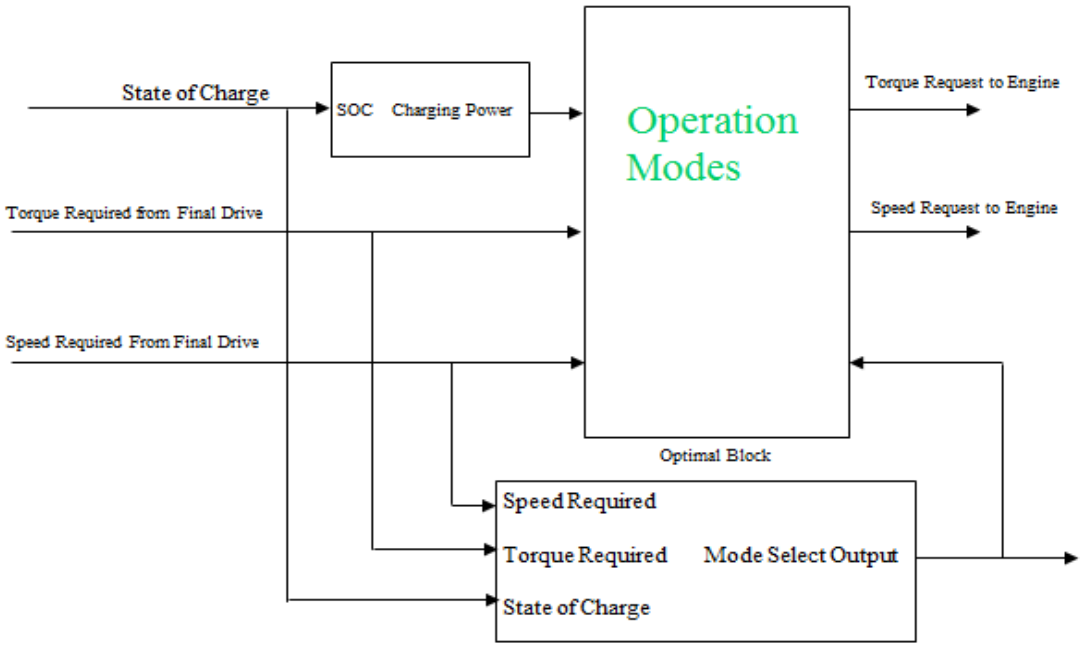

Figure 53: Operation Mode Simulink in Matlab

Platform: HEV Torque schematic

The simplified HEV model to demonstrate the proposed design is shown in Figure 54.

In this figure, the engine brake torque and the motor torque are feedback signals. However, for the sake of simplicity, we assume that the clutch is fully engaged and hence, i_M , i_E are the proportion of torques from the power sources contributed to the wheel. Also, the gear setting is disregarded in this simplified model. V ^{dem} is a command input to the control system, which represents the voltage delivered by the motor to achieve the desired motor torque (T_M), and U ^{dem} is the fuel of the engine. K represents the gain for the feedback regulator.

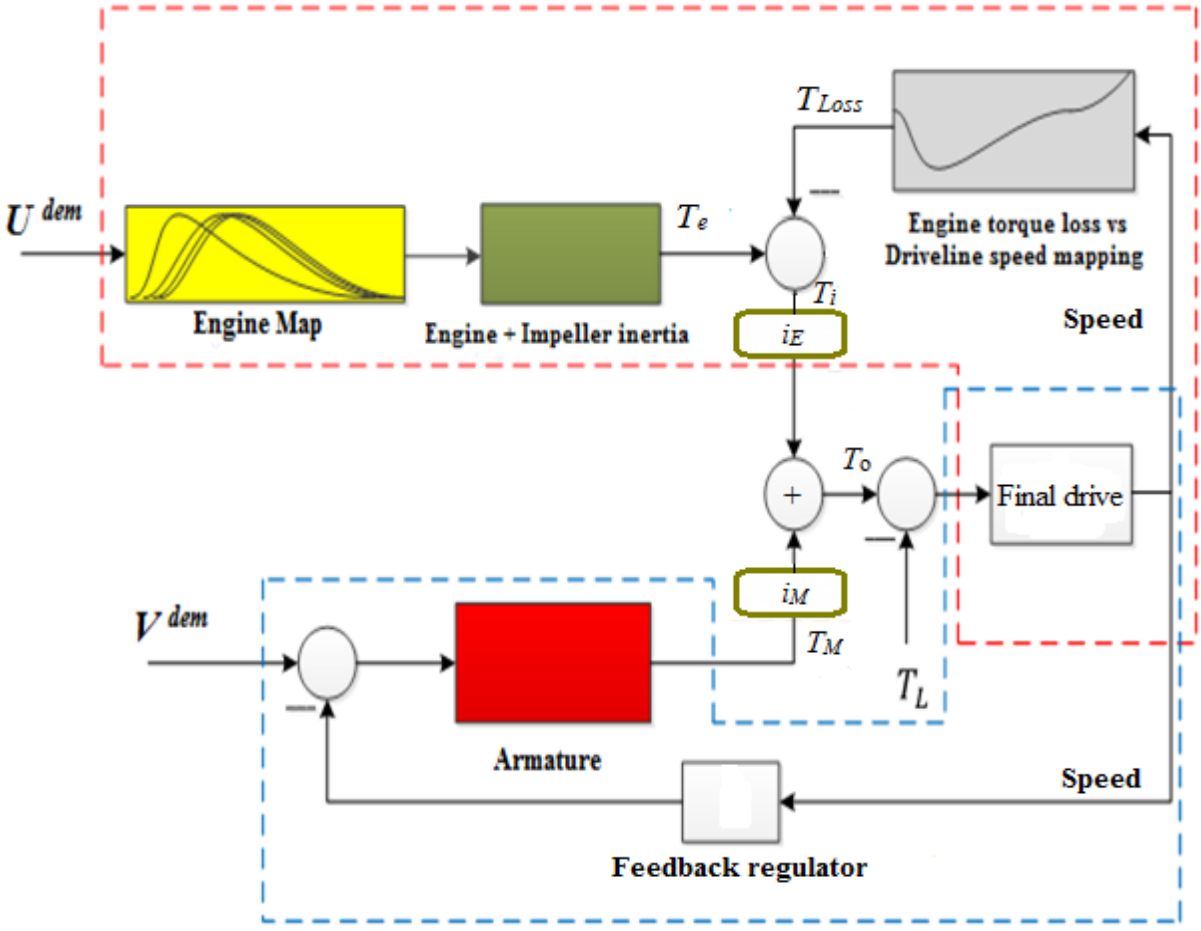

Figure 54: HEV Architecture

System Level Model: Simulink

Figure 55 shown below is the system level block diagram model of the hybrid dual clutch transmission model. It is similar to the typical control system model used for controlling a plant in a closed loop.

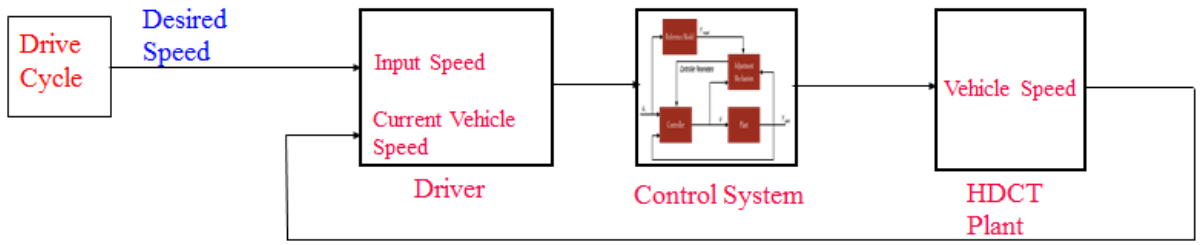

Figure 55: HDCT System Level Model

Dual Clutch Transmission subsystem

Two Disk Friction Clutch components from Simulink Driveline are connected in parallel, modeling the two clutches in a dual-clutch transmission [42]. Only one of these clutches is engaged at a time. Engaging and disengaging these clutches is how gear changes are made

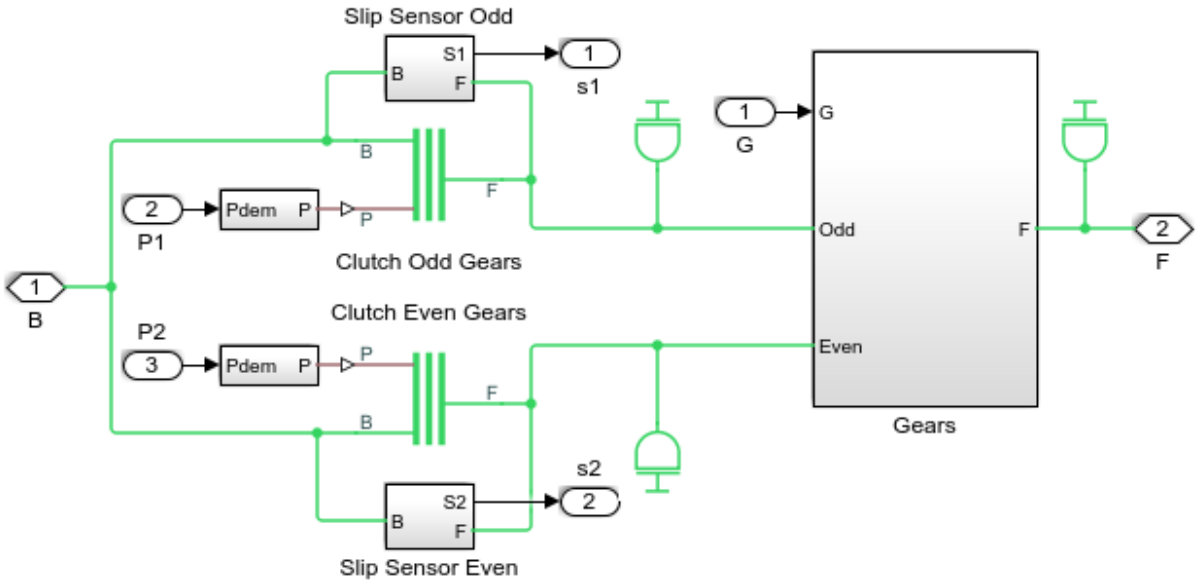

Figure 56: DCT Subsystem modeled in Matlab Toolbox

Gears Subsystem

Five Dog Clutch components from Simulink Driveline are connected between the follower shafts of each gear to the transmission output shaft. The controller preselects the next gear to which the transmission will shift by engaging the dog clutches. At any point, two of the dog clutches will be engaged, that for the current gear and that for the next gear to which the transmission will shift [42].

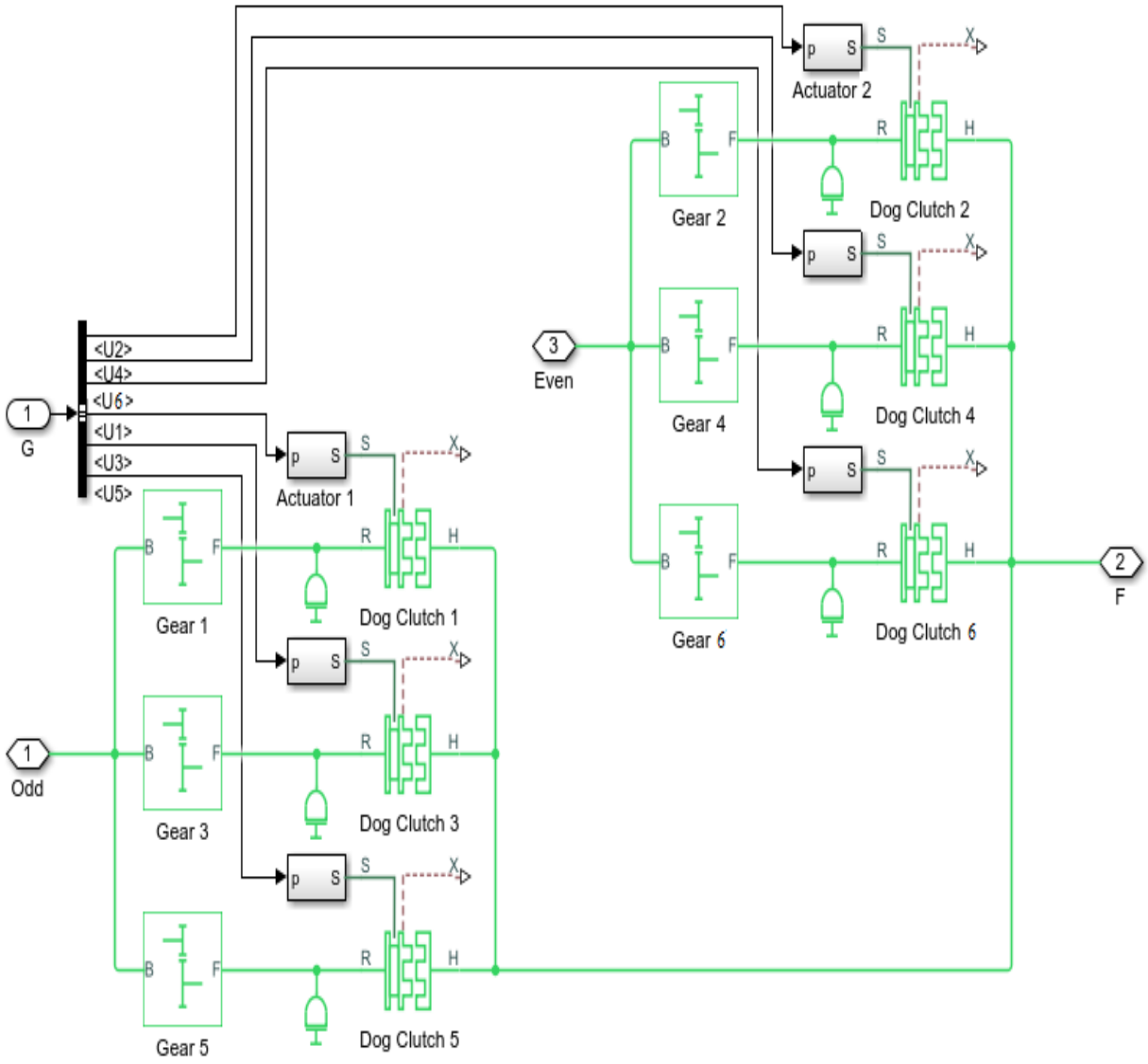

Figure 57: Gear subsystem modeled in Simulink Toolbox

Simulation Results from Simulink

The plots below show the engine and vehicle speed as it accelerates through the first three gears in the dual-clutch transmission. The half-gear states indicate gear shifts are taking place by engaging and disengaging the dual clutches [42].

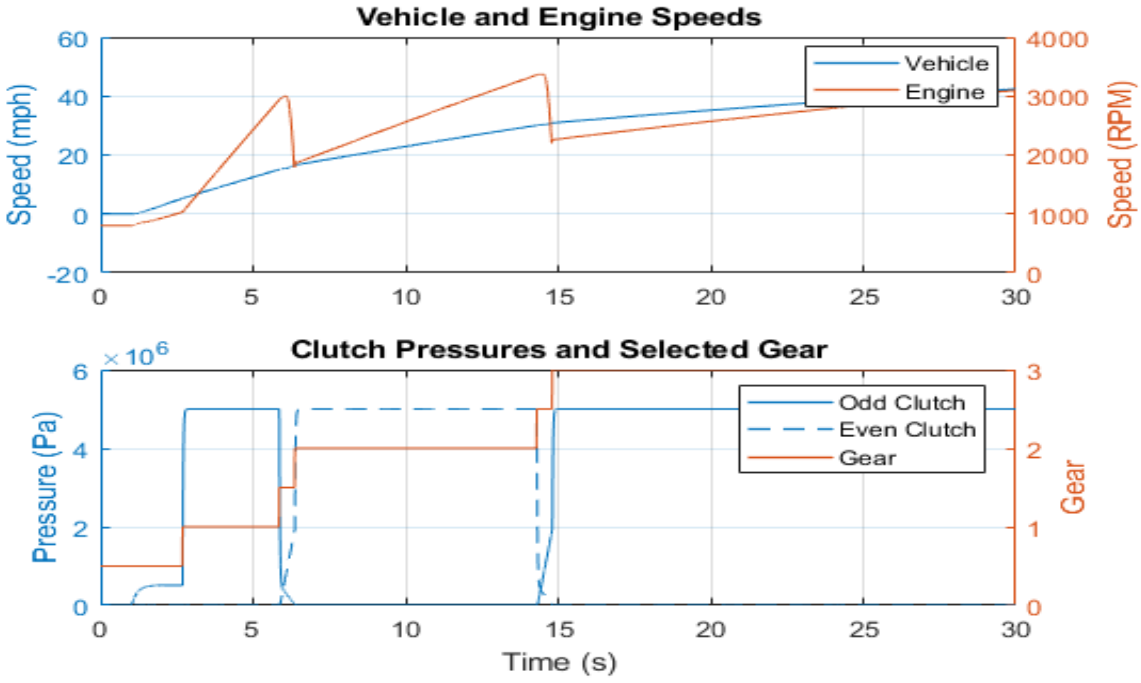

Figure 58: Simulation result for DCT Gear in Matlab Toolbox

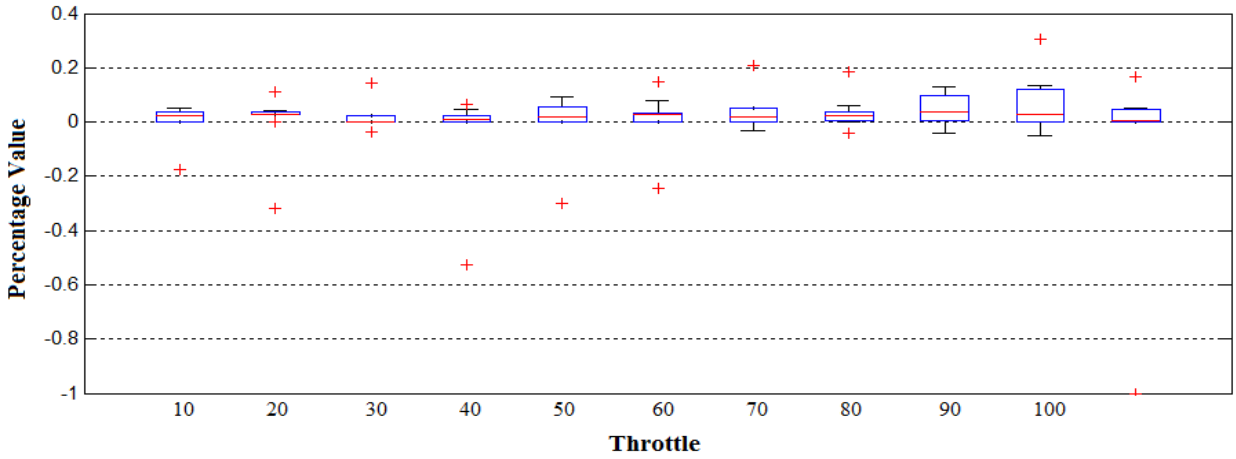

Figure 59: Percentage change for fuel engine map and its approximation quadratic function

APPENDIX B

B. Hybrid Production Models

Toyota Prius

Figure 60: Toyota Prius

- **Engine: 1.5 L 4-cylinders**
  76 HP / 82 lb-ft
- **Motor: DC Brushless; 500 V**
  50 kW / 400 Nm

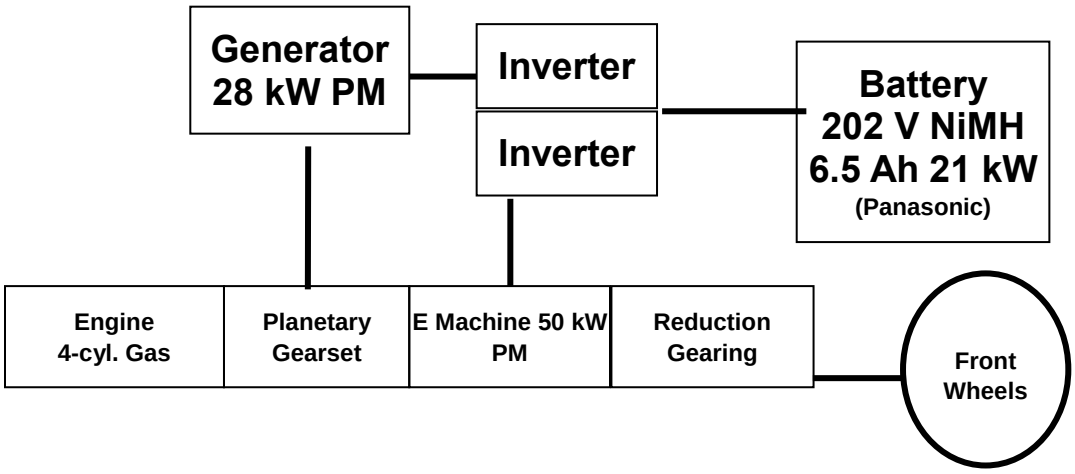

EPA MPG	1.8L AT Corolla	HEV	Gain (%)
City	30	60	100
Highway	**38**	**51**	**34**

Ford Escape

Figure 61: Ford Escape

- **Engine: 2.3 L Inline 4-Cylinder**
  133 hp / 129 lb-ft
- **Motor: PM, 330 V**
  70 kW / xx Nm

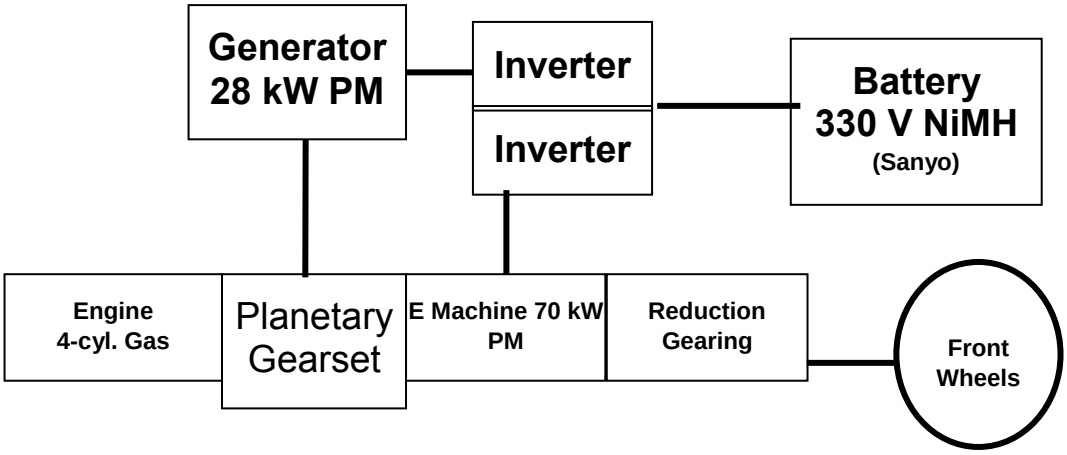

EPA MPG	3.0 L BL 1	AT HEV	Gain (%)
City	20	36	80
Highway	25	31	24

Honda Civic

Figure 62: Honda Civic

- **Engine: 1.34L 85 HP (63 kW) /119 Nm**
- **Motor: PM DC Brushless**
  10 kW / 62 Nm Assist
  12.6 kW / 108 Nm Regen

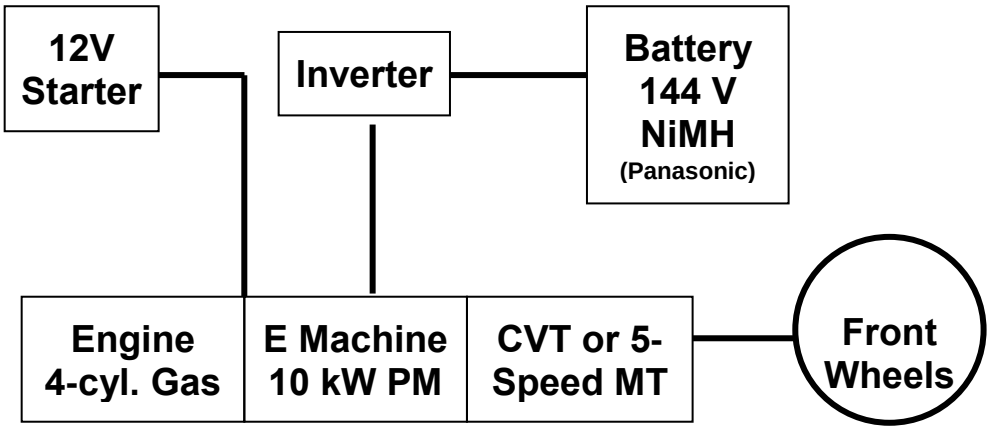

EPA MPG	AT BL	CVT HEV	Gain (%)
City	29	48	66
Highway	38	47	24

GM Hybrid Configuration with DCT

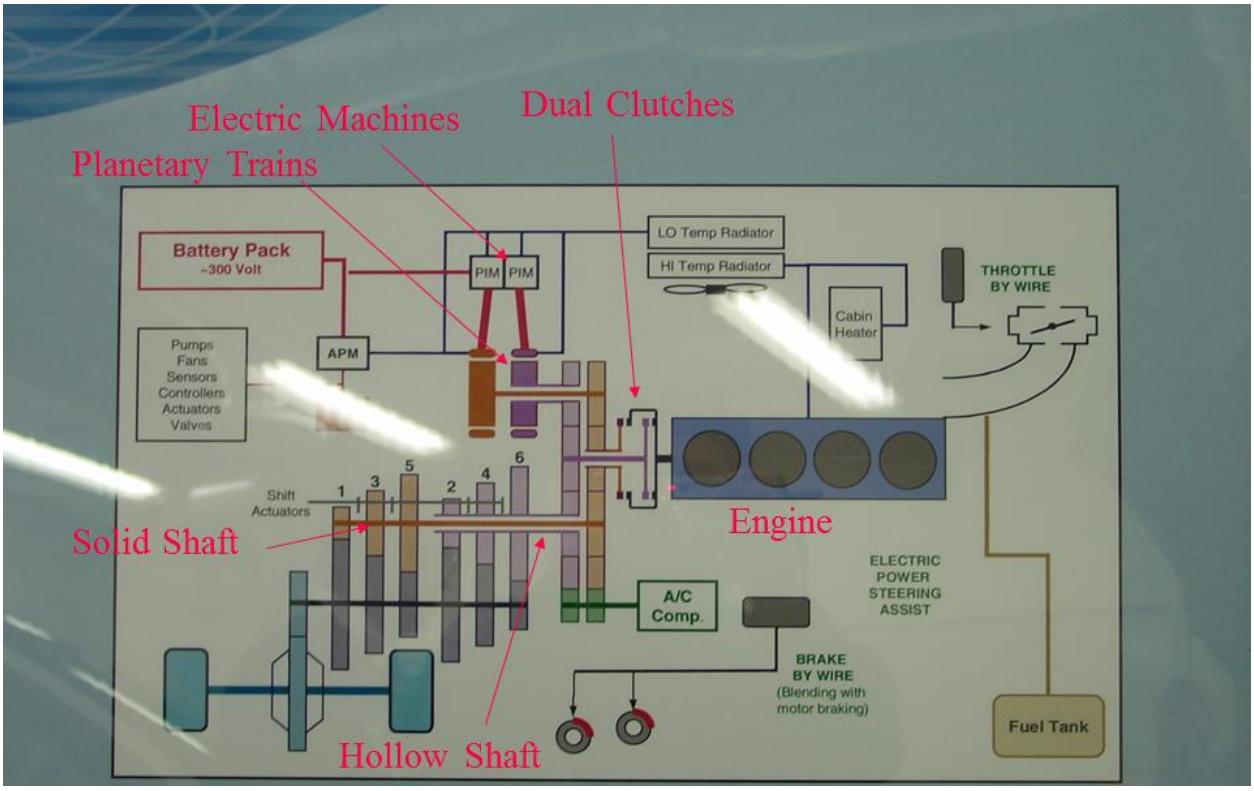

Figure 63: GM Hybrid with DCT

REFERENCES

[1] *IPCC Intergovernmental Panel on Climate Change fourth assessment report. . Available: http://www.ipcc.ch/ipccreports/assessments-reports.htm*

[2] *P. Ioannou and B. Fidan.“ Adaptive Control Tutorial. Volume 11 of Advances in Design and Control.” Philadelphia, PA: Society for Industrial and Applied Mathematics, 2006.*

[3] *M.P.R.V. Rao, “Non-quadratic Lyapunov Function and Adaptive Laws for MRAC,” IEE Electronics Letters, vol. 23, pp. 22782280, 1998.*

[4] *Waltermann, P., (1996), “Modeling and Control of the Longitudinal and Lateral Dynamics of a Series Hybrid Vehicle,” Proceedings of the 1996 IEEE International Conference.*

[5] *Michelena, N., Louca, L., Kokkolaras, M., Lin, C., Jugn, D., Filipi, Z., Assanis, D., Papalambros, P., Peng, H., Stein, J., Feury, M., (2001), “Design of an Advanced Heavy Tratical Truck: A Target Cascading Case Strudy,” SAE Paper 2001-01-2793.*

[6] *Brahma, A., Guezennec, Y., and Rizzoni, G., (2000), “Optimal Energy Management in Series Hybrid Electric Vehicles,” Proceedings of the American Control Conference, Chicago, Illinois, Jun. 2000.*

[7] *Jinming Liu,“Modeling, Configuration And Control Optimization Of Power-split Hybrid Vehicles”.dissertation,2007*

[8] *Conlon, B., (2005), “Comparative Analysis of Single and Combined Hybrid Electrically Variable Transmission Operating Modes,” SAE Paper 2005-01-1162*

[9] *Grewe T.M., Conlon, B.M., Holmes, A.G., (2007), “Defining the General Motor 2- Mode Hybrid Transmission,” SAE Paper 2007-01-0273.*

[10] *Zongxuan Sun and Kumar Hebbale , "Challenges and Opportunities in Automotive Transmission Control", GM Research and Development center.*

[11] *Bapi Surumpadi, "Automotive Manual Transmission Development, Vehicle system Research Department,SWRI*

[12] *Ricardo. 2006, September. Delivering value through technology, Available: http://www.ricardo.com/download/pdf/brochureweb.pdf.*

[13] *Ajinkya Joshi,Nirav P.Shah" Modeling and Simulation of a Dual Clutch Hybrid Vehicle Powertrain" Vehicle Power and Propulsion Conference, 2009. VPPC '09. IEEE.*

[14] *Gianluca Lucente,Marcello Montari and Carlo Rossi , "Modeling of automated manual transmissions", Department of Electronics and Computer Sciences, Bologna Italy ,November 2006*

[15] *PricewaterhouseCoopers. 2007 September, "The automotive industry and climate change ,Framework and Dynamics of CO2(r) evolution", A PricewaterhouseCoopers report, September 2007*

[16] *Engine Technology International, September 2007 edition.*

[17] *Markel,T.,Brooker, A., Hendricks, T., Johnson, V., Kelly, K., Kramer, B., O'keefe, M., Sprik, S., and Wipke, K., (2002), "ADVISOR: a Systems Analysis Tool for Advanced Vehicle Modeling," Journal of Power Source, Vol. 110, pp. 255-266.*

[18] *Rousseau, A., Sharer, P., and Pasquier, M., (2001b), "Validation Process of a HEV System Analysis Model: PSAT," SAE Paper 2001-01-0953.*

[19]*Hermance, D. and Abe, S., (2006), "Hybrid Vehicles Lessons Learned and Future Prospects," SAE Paper 2006-21-0027*

[20] *C. Ma, J. Kang, W. Choi, M. Song, J. Ji, H. Kim , "A comparative study on the power characteristics and control strategies for plug-in hybrid electric vehicles" International Journal of Automotive Technology, 2012, Volume 13, Number 3, Page 505*

[21]*Yu, Y.Wang, W.Zeng, X.Zhou, N.Wang, Q."The Research on Fuzzy Logic Control Strategy of Synergic Electric System of Hybrid Electric Vehicle" Technical Paper 2007-01-34812007*

[22] *Lianghui Yang; Hongwen He; Fengchun Sun; Shaoyou Shi; Yujun Li; Li Liu; , "Research of fuzzy logic control strategy for engine start/stop in dual-clutch hybrid electric vehicle," Fuzzy Systems and Knowledge Discovery (FSKD), 2010 Seventh International Conference on , vol.2, no., pp.912-917, 10-12 Aug. 2010.*

[23] *Won, J. S., Langari, R., and Ehsani, M., (2005), "An Energy Management and CharSustraining Strategy for a Parallel Hybrid Vehicle With CVT," IEEE Transactions on Control System Technology, Vol. 13*

[24]*Musardo, C., Rizzoni, G., and Staccia, B., (2005), "A-ECMS: An Adaptive Algorithm for Hybrid Electric Vehicle Energy Management" Proc. of IEEE Conference on Decision and Control, Seville, Spain.*

[25] *Li, X.Li, L.Sun, Y.Hu, Z.Deng, J. "Optimization of Control Strategy for Engine Start-stop in a Plug-in Series Hybrid Electric Vehicle" Technical Paper 2010-01-2214 2010*

[26] *Kim, M. and Peng, H., (2006), "Conbined Control/Plant Optimization of Fuel Cell Hybrid Vehicles," Proc. of the American Control Conference, Mineapolis, MN.*

[27] *Yi Zhang,Yonggang Liu, Datong Qin, Hong Jiang, Charles Liu, Zhenzhen Lei, ©2009 IEEE "Shift Schedule Optimization for Dual Clutch Transmissions"*

[28] *Yang Zhu; Zhiguo Zhao; Zhuoping Yu; Minglu Yin; , "Optimal Torque Based Fuzzy Logic Control Strategy of Parallel Hybrid Electric Vehicle," Intelligent Systems and Applications, 2009. ISA 2009. International Workshop on , vol., no., pp.1-5, 23-24 May 2009*

[29] *K. Upendra, "Dual Clutch Transmission for Plug-in hybrid electric vehicle Comparative analysis with Toyota hybrid system" Chalmers University Of Technology,Master's Thesis.2014.*

[30] *Jean-Jacques E. Slotine, Weiping Li; "Applied nonlinear control"*

[31] *Jeon,S I., Jo, S. T., Park, Y. I., Lee, J. M., (2002), "Multi-Mode Driving Control of a Parallel Hybrid Electric Vehicle Using Driving Pattern Recognition," ASME Journal of Dynamic Systems, Measurement, and Control, Vol. 124.*

[32] *Xuexun, G.Chang, F.Fei, C.Jun, Y.Zheng, Y."Modeling and Simulation Research of Dual Clutch Transmission Based On Fuzzy Control"Technical Paper 2007-01-3754 2007.*

[33] *K.S. Narendra and L.S. Valavani, "Stable Adaptive Controller Design Direct Control," IEEE Trans. Auto. Control, vol. 23, pp. 570583, Aug. 1978.*

[34] *K. K. Shyu, M. J. Yang, Y. M. Chen, and Y.-F. Lin, "Model reference adaptive control design for a shunt active-power-filter system," IEEE Trans. Ind. Electron., vol. 55, no. 1, pp. 97106, Jan. 2008.*

[35] *Y. T. Liu, K. M. Chang, and W. Z. Li, "Model reference adaptive control for a piezo-positioning system," Precision Eng., vol. 34, no. 1, pp. 6269, 2010.*

[36] *L. Yacoubi, K. Ai-Haddad, L.-A. Dessaint, and F. Fnaiech,"Linear and nonlinear control techniques for a three-phase three-level NPC boost rectifier," IEEE Trans. Ind. Electron., vol. 53, pp. 19081918,Dec. 2006.*

[37] *C. B. Kadu; B. J. Parvat;Narendra N.Parekar, "Modified MRAC for Controlling Water Level of Boiler System," 2015 International Conference on Computational Intelligence and Communication Networks (CICN).*

[38] *S. Coman and C. Boldisor, "Model Reference Adaptive Control for a DC Electric Drive," Bulletin of the Transilvania University of Braov Series I: Engineering Sciences, vol. 6, no. 2, 2013.*

[39] *Zhiguo Zhao, Haijun Chen, and Qi Wang," Control and Real-Time Optimization of Dry Dual Clutch Transmission during the Vehicle's Launch" Hindawi Publishing Corporation Volume 2014, Article ID 494731, 18 pages Published 2 February 2014.*

[40] *Li Chen, Gang Xi, and Jing Sun, "Torque Coordination Control During Mode Transition for a Series-Parallel Hybrid Electric Vehicle," IEEE Transactions on Vehicular Technology, VOL. 61, NO. 7, SEPTEMBER 2012.*

[41] *I. Landau, I. et al., "Adaptive Control: Algorithms, Analysis and Applications," London: Springer-Verlag, 2011.*

[42] *https://www.mathworks.com/help/physmod/sdl/examples*